Design of Automotive Joints Using Response Surface Polynomials and Neural Networks

by

Qi Ling

Thesis submitted to the faculty of the
Virginia Polytechnic Institute and State University
in partial fulfillment of the requirements for the degree of

MASTER OF SCIENCE

in

OCEAN ENGINEERING

APPROVED:

Dr. Efstratios Nikolaidis, Chairman

Dr. Rakesh Kapania

Dr. Eric Johnson

September 1998

Blacksburg, Virginia

Design of Automotive Joints Using Response Surface Polynomials and Neural Networks

by

Qi Ling

Committee Chairman: Efstratios Nikolaidis

Aerospace and Ocean Engineering

(ABSTRACT)

In the early design stages of a car body, a simplified model, which represents the constituent components of the car body by their performance characteristics, is used to optimize the overall car. The determined optimum performance characteristics of the components are used as performance targets to design these components. Since designers do not know the relation between the performance characteristics of the components and their dimensions and mass, this may lead to unreasonable performance targets for the components. Moreover, this process is inefficient because design engineers use empirical procedures to design the components that should meet these targets. To design the component more efficiently, design tools are needed to link the performance targets with the physical design variables of the components.

General methodologies for developing two design tools for the design of car joints are presented. These tools can be viewed as translators since they translate the performance characteristics of the joint into its dimensions and vice-versa. The first tool, called *translator A*, quickly predicts the stiffness and the mass of a given joint. The second tool, called *translator B,* finds the dimensions and mass of the most efficient joint design that meets given stiffness requirements, packaging, manufacturing and styling constraints.

Putting bulkheads in the joint structure is an efficient way to increase stiffness. This thesis investigates the effect of transverse bulkheads on the stiffness of an actual B-pillar to rocker joint. It also develops a translator A for the B-pillar to rocker joint with transverse bulkheads. The developed translator A can quickly predict the stiffness of the reinforced joint.

Translator B uses optimization to find the most efficient, feasible joint design that meets given targets. Sequential Linear Programming (SLP) and the Modified Feasible Direction (MFD) method are used for optimization. Both Response Surface Polynomial (RSP) translator B and Neural Network (NN) translator B are developed and validated. Translator A is implemented in an MS-Excel program. Translator B is implemented in a MATHEMATICA program.

The methodology for developing translator B is demonstrated on the B-pillar to rocker joint of an actual car. The convergence of the optimizer is checked by solving the optimization problem many times starting from different initial designs. The results from translator B are also checked against FEA results to ensure the feasibility of the optimum designs. By observing the optimum designs and by performing parametric studies for the effect of some important design variables on the joint mass we can establish guidelines for design of joints.

Acknowledgements

I would like to express my sincerest appreciation to Dr. Efstratios Nikolaidis, my advisor and mentor, for his guidance, support and encouragement during the completion of my graduate program and this thesis.

I would also like to thank Dr. Rakesh Kapania and Dr. Eric Johnson for their comments on this thesis and serving on my committee.

I would like to extend special thanks to Mr. LuoHui Long for his cooperation and helps throughout the research project.

Finally, I would especially like to thank my wife, YingHua Zhang, for all her support and patience while I pursue the higher education.

Contents

List of Tables

List of Figures

Nomenclature

α	weighting factor in objective function
β_i	*i*th regression coefficient
$\boldsymbol{\beta}$	vector of regression coefficients
γ	coefficient for confidence level
ε	error in the regression model
$\boldsymbol{\varepsilon}$	vector of errors in the regression model
μ_{Y_1} , μ_{Y_2}	mean values of data set Y_1, Y_2
σ	standard deviation
σ^2	variance of error $\boldsymbol{\varepsilon}$
$\hat{\sigma}^2$	unbiased estimator of σ^2
σ_{Y_1} , σ_{Y_2}	standard deviations of data set Y_1, Y_2
ρ_{Y_1,Y_2}	correlation coefficient of the two data sets Y_1, Y_2
AIC	Akaike's Information Criterion
$\mathbf{b}$	least square estimator of $\boldsymbol{\beta}$
b_i^k	bias of the *i*th neuron in *k*th layer in a neural network
$Cov(Y_1, Y_2)$	covariance of the two data sets Y_1, Y_2

CAD	computer aided design
CAM	computer aided manufacturing
C_N^i	combination of *i* number from total *N* numbers
C_P	statistics criterion
DOT	design optimization tools
est.std.	estimated standard deviation
F/A	forward/afterward
FEA	finite element analysis
f	general function
$\bar{f}$	mean value of f
$F, F(\mathbf{x})$	objective function
$f_i^k(z)$	transfer function for neurons in the *k*th layer
$g_j(\mathbf{x})$	*j*th inequality constraint
$h_k(\mathbf{x})$	*k*th equality constraint
I/O	inboard/outboard
$K_{F/A}$	predicted F/A stiffness
$\hat{K}_{F/A}$	target F/A stiffness
$\overline{K}_{F/A}$	value used to normalize F/A stiffness
$K_{I/O}$	predicted I/O stiffness
$\hat{K}_{I/O}$	target I/O stiffness
$\overline{K}_{I/O}$	value used to normalize I/O stiffness
K	stiffness of the B-pillar to rocker joint without transverse bulkheads
K_b	stiffness of the B-pillar to rocker joint with transverse bulkheads

K_{Tor}	predicted torsion stiffness
$\hat{K}_{Tor}$	target torsion stiffness
$\overline{K}_{Tor}$	value used to normalize torsion stiffness
l	number of equality constraints
m	number of inequality constraints
M	mass
MFD	modified feasible direction method
MSE	mean squared error
n	number of design variables
NLP	nonlinear problem
NN	neural network
NNs	neural networks
p	number of design variables in a linear polynomial
R^2	statistics criterion *R*-square
RSP	response surface polynomial
RSPs	response surface polynomials
std.	standard deviation
SLP	sequential linear programming
SQP	sequential quadratic programming
SSE	sum of square errors
Var	variance
$w_{i,j}^{k}$	weight of the *j*th input to the *i*th neuron in the *k*th layer of a neural network
$\mathbf{x}$	vector of design variables
$\mathbf{x}_0$	vector of design variables corresponding to a particular design
x_i	*i*th variable

x_i^L	lower limit of the *i*th design variable
x_i^U	upper limit of the *i*th design variable
$\mathbf{X}$	matrix of the regression variables
y	measured response
$\bar{y}$	average response
$\hat{y}$	prediction of response
$\mathbf{Y}$	vector of measured responses
z_i^k	total input for the *i*th neuron in the *k*th layer

Chapter 1
Introduction

1.1 Definition and Significance of the Problem

In the preliminary design of car bodies, a simplified model instead of a detailed model is used because the optimization of a detailed model involves too many design variables and is expensive. The simplified model uses *engineering parameters* that describe the performance characteristics of the components to represent the structural components of the overall car body. For example, beams are represented by their cross sectional properties, such as moments of inertia. Joints are represented by their static stiffnesses.

Figure 1.1 summarizes the design procedure of the overall car body. First, we find the optimum values of engineering parameters, such as joint stiffness, to maximize the overall performance characteristics (for example, the stiffness of the overall car structure) or to minimize the mass. Then, using the determined engineering parameters as performance targets, we optimize the components to find their physical design parameters (dimensions) so that the components meet these performance targets. This approach is more reasonable than an approach that tries to determine all the dimensions of the components simultaneously because it breaks down the design of car body structures into smaller tasks, which involve relatively few parameters (e.g. 10 ~ 50 parameters).

However, this approach has some drawbacks. For example, at the end of first step, the final optimum design of a component is defined using its engineering parameters (performance characteristics) rather than its dimensions. It is difficult to develop engineering drawings from these engineering parameters. Moreover, the final optimum design might not be feasible because the engineering parameters can not be directly linked to packaging, manufacturing and styling constraints.

To overcome these difficulties, we need design tools to link the engineering parameters to the physical dimensions of the components as well as the packaging, manufacturing and styling constraints. These tools can be viewed as translators because they translate engineering parameters into dimensions of the components and vice versa. Specifically, we need two design tools, called *Translator A* and *Translator B*: translator A predicts the performance characteristics of a given component while translator B determines the physical dimensions of a feasible design that meets given performance requirements. These tools should be very efficient so that they can be used in the early design stages. It is the common view among engineers and designers in various industries that such tools are extremely important because they will help build better products faster.

Joints are important components of the car overall body because their flexibility contributes remarkably to the flexibility of the overall car structure. Consequently, they can significantly affect the static and dynamic behavior of a car such as noise, vibration and harshness. It is important to develop design tools for car joints because:

- Using such design tools for car joints, designers will be able to quickly predict the performance of a given joint, and find the dimensions (e.g., width and height of a beam and thickness of a plate) of a feasible and efficient design that meets given performance targets.

- To the best of our knowledge, there are still no design tools for car joints to help designers to find a feasible design that satisfies given performance targets.
- We should be able to extend this methodology to other components of the overall car body because these components are usually simpler than joints.

In design of car structures, we use simplified models of joints, called *concept models*. Specifically, we assume that there are three rotational springs (inboard/outboard, forward/afterward and torsion) constraining the rotation of the flexible branch of a joint relative to the remaining branches. The performance of joints is characterized by the stiffnesses of these springs.

For car joints, translator A quickly predicts the stiffness and mass of a given joint (a joint with given dimensions). Translator B finds the dimensions and mass of a feasible and efficient joint according to given requirements on stiffness. The obtained joint must also satisfy given packaging, styling and manufacturing constraints.

Developing translator A includes parameterization of a actual car joint, identification of packaging, styling and manufacturing constraints, and establishment of a neural network and a response surface polynomial to quickly predict the stiffnesses (Inboard/outboard stiffness, forward/afterward stiffness, torsion stiffness) and mass of a given joint.

It is possible that there are many feasible designs satisfying given performance requirements. Translator B will use optimization to find the most efficient, feasible joint design (with lowest mass). An efficient design should have small mass and low cost. In this thesis, we try to minimize mass. Thus, translator B is an optimizer that minimizes

the mass or some measure of the difference between the stiffness of a design from given stiffness under given packaging, manufacturing and styling constraints.

1.2 Review of Previous Work

1.2.1 Characteristics and Modeling of Car Joints

Generally speaking, the car body has seven types of joints, which are *A-pillar to Roof Rail, A-pillar to Hinge Pillar to Shotgun, Hinge Pillar to Rocker, B-pillar to Roof Rail, B-pillar to Rocker, C-pillar to Roof Rail* and *Rocker to Rear Quarter* (Figure 1.2).

The geometry and construction of these joints are very complex. They are thin-wall structures consisting of intersecting beams fastened by spot welds. The adjacent beams can rotate relatively to each other. The flexible nature of car joints has been realized since an early time. Chang (1974) studied effects of the flexibility of car joints on the static response of body structures. He used a car body model with spring elements for the joint flexibility. He found that the body model with rigid joints would underestimate static deflection to a considerable degree. His analytical results of the car model considering joint flexibility correlated well with test results of an actual production body.

From a noise, vibration and harshness viewpoint, the joint flexibility (static stiffness in the direction of inboard/outboard, forward/afterward and torsion) is the most important characteristics of joints although there are many other performance characteristics (such as fatigue strength, static strength, etc.) that can be important for a joint.

In the design of a car, we typically idealize joints assuming that three rotational springs usually constrain the rotation of the most flexible branch relative to the remaining branches. The remaining branches are assumed rigidly connected. The performance of the joints is characterized by the (static) stiffness of three rotational springs (inboard/outboard, forward/afterward, and torsion), and performance targets are specified on the values of these stiffnesses.

Since 1970's researchers have tried to develop simplified models to model the behaviors of joints. Chang (1974) used torsional springs to account for the joint flexibility in analysis of the overall car body stiffness. Sunami and Yoshida (1987, 1990) studied the joint stiffness of T- and L-shaped joints, which are made of two box beams under in plane and out-of-plane bending. Their results agree with experiment and FEA results, but their model can't account for structural imperfections like service holes and spot welds. Nikolaidis and Lee (1991) developed procedures to determine the parameters of simplified joint models using a detailed FEA model and experimental measurements. Nikolaidis and Lee (1992) further developed a 3-D model considering the flexibility of joints. Nikolaidis and Zhu (1991) applied Valsov's theory in inboard/outboard bending of a T-shaped joint made of two box beams. Their results agreed well with FEA results and those obtained by Sunami (1990). Zhu (1994) developed a generic model for a B-pillar to rocker joint. His model can predict inboard/outboard stiffness accurately. The results from his model for forward/afterward and torsional stiffness are not satisfactory because he used flat plates for the blending areas of the joint.

Two types of joint models can be used for studying the car joint behavior: simplified models and detailed FEA models. A simplified joint model is a very simple finite element model consisting of springs, hinges and rigid elements. It is used for conceptual design. Unfortunately, it can not be used directly to get physical dimensions that define a joint.

A detailed finite element model can include many aspects of an actual car joint such as flanges, spot welds and access holes. It is used to predict the static and dynamic response of a given joint with considerable accuracy (error is less than 10%). By studying the detailed FEA model, we can better understand the deformation mechanisms of joints (Zhu 1994).

To develop design tools (translator A and B) for car joints, it is important to parameterize a joint and develop a generic model, which is defined by its values of design parameters. Long (1998) developed a generic model for the B-pillar to rocker joint of an actual car (Figure 1.3) based on the original one created by Murphy (1995). To create the model, physical design parameters that define the joint were first selected and determined after examining many joints of different cars and interacting with engineers in the automotive industry. *Pro/E* (*Pro/Engineer*, a parametric modeling CAD software developed by *Parametric Technology Corporation*) was used to build this generic joint model. FEA models of given designs could be developed automatically by using this generic model. The inboard/outboard (I/O) stiffness, forward/afterward (F/A) stiffness and torsional stiffness were defined in the following equation (Figure 1.4), which is in accordance with the practice in automotive industry (i.e. off-diagonal terms of the stiffness matrix are unimportant to the design performance, and are neglected):

$$Stiffness = \frac{Moment\ in\ the\ given\ direction}{resulting\ rotation\ in\ the\ same\ direction} \tag{1.1}$$

The joint stiffnesses predicted by the model agreed with the experimental results well, and the errors were within the range in which measurements can vary due to hardware variability and experimental errors (Long 1998).

In our study, we use this generic joint model and the resulting FEA models to analyze many alternative designs for the B-pillar to rocker joint. The physical design

parameters of the joint are the inputs of the generic model, and a data deck for FEA of the joint is the output. We use *MSC/NASTRAN* to do finite element analysis and obtain the joint's structural response quantities.

1.2.2 Neural Networks and Response Surface Polynomials in Structural Design

Shape optimization is used to design a component that meets given targets (Belegundu 1993, Ali 1994). However, in many structural optimization problems, the evaluation of the objective function and constraints will require the execution of costly finite element analysis (FEA) programs for predicting structural response. The optimization may require hundreds, even thousands, evaluations of the objective function and constraints. The cost of repeating the finite element analysis so many times is usually prohibitive. An alternative approach is to use approximate methods to establish mapping relations between design parameters of the structure and the performance characteristics obtained from a FEA package. In many problems, it is better to simulate a time consuming finite element analysis program using a *Response surface polynomial* and *artificial neural network* (Guyot and Nikolaidis 1997).

1.2.2.1 Response Surface Polynomial

Using *response surface polynomials* (RSP) is a common global approximation method. With this method, a function such as joint stiffness or mass is sampled at a number of design points, and then a polynomial (usually a linear or quadratic polynomial) is fitted to the data. The process begins with the assumption of the analytical form of the response polynomial, which can be a linear, quadratic or of higher degree, and then adjusts the unknown polynomial coefficients to match the approximated function by using least-square regression (Myers 1971, Draper and Smith 1981). An additional

benefit of using response surface polynomial is that the least-square regression process tends to smooth out noise due to numerical or other errors in the function values. When using RSP, we make the following fundamental assumptions:

- The assumed form of the polynomial is exact, that is the differences between the response polynomial and the fitting designs (also called experiments) are due to the noise.
- The noise is assumed normally distributed, with zero means and zero correlation between experiments.

Response surface polynomials have been widely used in the structural design. Zhu (1994) developed a translator for a car joint using RSP technique. He used a complete second degree polynomial, which might include some unimportant terms and reduce the generalization performance (i.e. the capability of the polynomial to predict the stiffness and mass of designs it has not seen in fitting). Giunta (1997) and Balabanov (1997) used RSP in the analysis and design of the aircraft. The stepwise regression technique was used in their studies to get the best regression model.

When using RSPs, a proper analytical form of the polynomial is important for the approximation. The design points, or *experiments* in terms of standard terminology, should be carefully selected because the model parameters (polynomial coefficients) can be estimated more efficiently if proper experiments are used to collect the data. There are many methods that can be used to create experiments. Rogers (1994) compared the results of 4 different methods: *Hypercube, Linear, PROSSS, and Random.*

The hypercube method needs to build a hypercube around the midpoint of the design space, which is the set of initial design variables. The best choices of points for the hypercube are points at each corner, the midpoint for each face, and the midpoint of

the design space. The Linear method creates the fitting experiments, which start from the lower bound of each design variable and step through the design space until reaching the upper bound. PROSSS (Programming System for Structural Synthesis) is a structural synthesis software that can also be used to create fitting experiments. The Random method uses a random number generator to create experiments, and all values must be inside the lower and upper bounds of the design variables.

The Taguchi method is another design of experiment method, which is very popular in industry. In this method, simple charts are used to describe how to design an experiment, and how to obtain the information from the experimental results. Users don't need to know the statistics theory and details behind this method.

In our study, when using Hypercube, Taguchi method or some other methods for design of experiments, we need to find the stiffness and mass of joints for many predetermined combinations of joint dimensions that correspond to infeasible designs. Most of these designs can not be modeled using a parametric model. Therefore we used the random method to create the fitting experiments. Each design that corresponds to an experiment should be checked against the constraints, and will be thrown away if constraints are violated.

1.2.2.2 Artificial Neural Networks

Artificial neural networks (NN) are computational paradigms motivated by biological neural networks of human brains. An artificial NN can have layers of inter-linked processing elements, which are called neurons. Links, which are called synapses, connect the neurons. Signals passing through the links are scaled by the corresponding weights. Each neuron receives input signals and outputs the sum of the scaled inputs. Thus, a NN maps an input vector to an output vector like a RSP.

To train the network to map a set of input values to another set of output values, weights of the neural network must be set up by a interactive process. One approach to training is to present the network with patterns of typical input data (exemplars) and adjust the weights to minimize the difference between the output patterns and the exemplars. This adjustment is performed repeatedly, and for many input patterns, until the network operates satisfactorily. Some of the major benefits of NN (Anderson 1995, Hagan *et al* 1996) are:

- No programming is needed if an existing computer code is used for training.
- They can deal with noisy and uncertain data.
- In principle, a neural net can simulate any computable function.
- They can operate quickly once they have been trained.

Using NNs in structural design is a quite new concept. Since they can simulate very complicated and highly nonlinear systems, NNs have received considerable attention in their applications to structural analysis and design (Hajela and Berke 1990, Carpenter 1992, Rogers 1994).

Applications of NN to structural mechanics problems have been studied by several investigators. Swift and Batill (1991) used NNs in preliminary structural design. They used a 5-bar truss, a 10-bar truss and a light-aircraft wing box as examples to illustrate the use of NN as a fast, inexpensive structural analysis tool in the structural optimization. Berke and Hajela (1992) used a 5-bar truss and a 10-bar truss to demonstrate the application of NNs in structural mechanics. Rogers (1994) applied NNs to find the optimal shape of a beam. Zhu (1994) used NNs to develop a translator for a car joint. The NN is used to map design variables of the joint to its stiffness and trained using FEA results of different joint designs. Botkin and Lust (1995) considered the

application of NN to shape optimization of automotive components. They used some optimal design pairs to train the NN directly. The trained NNs can predict the values of optimal mass, performance measures and design variables with small error (about 3.5%).

This study applies NNs to simulate the FEA analysis process of a car joint. Specifically, NNs are used to approximate the relation between a set of parameters defining the dimensions of a car joint and its stiffness and mass. The examples in this study are real life problems, involving complex geometry and a large number of constraints, whereas the examples in most previous studies tended to be considerably simpler.

1.3 Objectives of the Study Presented in This Thesis

Long (1998) has developed translator A for the B-pillar to rocker joint of an actual car, which will be simply referred to as the B-pillar to rocker joint in this thesis (Figure 1.3). Chapter 2 briefly describes the methodology for developing translator A.

As an application of the methodology developed for translator A, this thesis studies the effect of bulkheads on stiffnesses of joints. Bulkheads have the advantage of increasing the stiffness significantly without considerable penalty on the mass.

The objectives of this thesis are:

- Demonstrate how to use the methodology for constructing translator A to predict effect of bulkheads on the stiffness of an actual car joint, which in this study is a B-pillar to rocker joint.
- Develop a methodology for constructing translator B that finds the most efficient, feasible joint design that meets given targets on stiffness. A

methodology for translator B is described and demonstrated on the B-Pillar to rocker joint of an actual car.

The B-pillar to rocker joint is a typical but comparatively simple joint. In design of car structures, it is important to make the B-pillar to rocker joint stiff enough in the inboard/outboard direction because the behavior of the joint under inboard/outboard bending significantly affects the torsional rigidity and the vibration characteristics of the overall car structure. Thus, the B-pillar to rocker joint is selected as the first car joint to demonstrate the developed methodologies for translator A and translator B.

As an application of translator B, a parametric study was performed in this thesis for the effect of stiffness requirements and the effect of relaxing or tightening the constraints on the mass of an optimum joint obtained using translator B. For example, we studie the change in the optimum mass as a function of the minimum required stiffness. It also studies the effect of important dimensions, such as the thickness of the rocker outer cell and length of pillar base on the joint stiffness and mass.

1.4 Outline

The contents of this thesis are organized in the following order:

Chapter 2 describes briefly the methodology for developing translator A for rapid prediction of the performance and mass of a given design.

Chapter 3 describes the methodology for developing translator B for finding the best design that meets given performance targets. It starts with the formulation of the general structural optimization problem, which includes selecting design variables and establishing the objective function and constraints. Then several optimization algorithms

are investigated, which were used in this study. Finally, we describe how to validate the results.

Chapter 4 investigates the effect of transverse bulkheads on the B-pillar to rocker joint. A translator for predicting the effect of transverse bulkheads on inboard/outboard stiffness ($K_{I/O}$), forward/afterward stiffness ($K_{F/A}$) of the B-pillar to rocker joint with bulkhead is developed. To study the confidence in the predicted values, we developed a method to calculate the confidence interval for the predicted stiffness of the B-pillar joint with bulkheads.

Chapter 5 demonstrates the methodology for developing translator B on the B-pillar to rocker joint of an actual car. The objective function and the constraints used in the translator B for the B-pillar to rocker joint are explained in detail. The developed translator B is validated using several methods. By using translator B, parametric studies are performed to study the change of optimum mass when stiffness requirements change and when upper and lower limits on some important dimensions change. Several observations are obtained based on the optimum designs and the parametric study. Finally, the results are discussed.

Chapter 6 presents the conclusions of this study and recommendations for future work.

Chapter 2

Methodology For Developing Translator A For Rapid Prediction Of Performance And Mass Of A Given Design

For car joints, translator A rapidly predicts the stiffness and mass of a given joint from its physical design parameters. It needs to be developed first since it is needed to develop translator B for finding the dimensions and mass of the most efficient and feasible joint meeting given requirements on stiffness. Long (1998) developed the translator A for the B-pillar to rocker joint of an actual car. This chapter briefly presents the methodology used in developing the translator A.

Several steps are involved in the development of translator A. First, a generic model must be created using a parametric modeling CAD package such as CATIA, I-DEAS or Pro/Engineer. Using its physical design parameters, this model can quickly create the FEA model, which keeps the major performance properties of the joint such as the stiffness. Then a database including many feasible designs and their corresponding FEA results is developed. Response surface polynomials and neural networks are used to simulate the relation between the design parameters of the joint and the performance (stiffness) characteristics and mass of the joint obtained from a FEA package. This approach enables translator A to rapidly predict the performance of any given joint.

This chapter starts with the description of the parametric (generic) model in Section 2.1. Then, the database for developing translator A is explained in Section 2.2. The development and validation of response surface polynomial and response neural network are described in Sections 2.3 and 2.4.

2.1 Parametric Model

To develop the parametric (generic) model, parameterization of an actual car joint is determined first. This includes identification of the construction types of the joints by examining actual joints, simplifying the joint geometry, classifying different types based on the internal joint construction and selecting important physical design parameters to represent the joint. The parameterization is organized in different levels. The overall shape of the joint is defined by the design parameters of higher levels, and the more details of the joint are defined by the design parameters of lower levels. This study uses six levels of design parameters to define the joint as follows (Murphy 1995):

- Level 1: Number and position of branches
- Level 2: Cross section of branches
- Level 3: Blending Area
- Level 4: Internal Reinforcements
- Level 5: Connections
- Level 6: Openings

The definition and selection of physical design parameters of the joints are very important for developing effective translators. These parameters must make sense to designers and can be controlled by designers. A well-chosen set of physical design

parameters will contain a small number of important dimensions and joint topology, which define the geometry of the joints and account for the major properties of the joint.

Then, the packaging, manufacturing and styling constraints are identified and expressed in terms of physical design parameters. The development of constraints starts with a review of design manuals and discussion with engineers in automotive industry. Different types of constraints such as packaging, manufacturing and styling constraints are identified. They are expressed in mathematical equations in terms of the physical design parameters of a joint.

Using a parametric modeling package such as CATIA, I-DEAS or Pro/Engineer, the parametric (generic) model is developed. In this study, we chose Pro/Engineer to build the parametric model for developing translator A because only I-DEAS and Pro/Engineer are available to us and the parametric modeling capability in Pro/Engineer is better than that in I-DEAS, especially for its assembly capabilities.

In the parametric model, *Control parameters* are used to specify the construction type of a joint. They use "Yes" and "No" as their values to control the construction type. Other design parameters use numerical values to describe (or control) the geometry and FEA features of the model. In our study, the construction type of the joint is fixed as the most common type for translator A. Thus, the control parameters are fixed at the beginning and only those design parameters that control the geometry and FEA features of the joint can change their values.

2.2 Database of Designs for Developing Translators A

For different feasible designs, we can use the generic model to obtain the corresponding FEA results. A database that stores the input design parameters of each feasible design and its FEA results is needed for establishment of the response surface.

As described in Section 1.2.2.1, many methods can be used to create the input-output pairs including Hypercube, Linear, PROSSS and Random method (Rogers 1994). It is important to select a suitable method because the model parameters can be estimated more efficiently if the input-output pairs are properly collected. In our study, the random method is selected to create the pairs because the stiffness and mass of joints for many predetermined combinations of joint dimensions that correspond to infeasible designs are required when using Hypercube and other methods.

Developing the database is a very time-consuming task. Each design is checked against the constraints. In this study, about 16% ~ 20% of the designs (several thousands) are found to be feasible designs, for which no constraints are violated. A database storing the values of the design parameters of these feasible designs and their FEA results is then created. Developing polynomial translator A and neural network translator A will use this database.

2.3 Developing and Validating a Response Surface Polynomial

Linear polynomials, quadratic (second degree) polynomials and double regression models can be used as a response surface. Specifically, a linear polynomial is used to simulate a linear relation between the input (design variable) and the output (stiffness and mass). Quadratic or higher degree polynomials can be used to simulate the complicated input-output relations with more flexibility. However, with increase of the degree of the

polynomial, the number of the regression model parameters increases exponentially, and accordingly, they need a very large database for fitting. The prediction of those designs out of the fitting database can be poor if the database is not large enough. In our study, linear polynomial and quadratic polynomial are used as response surfaces to develop translator A. A double regression model is also used in our study because of the need for some simulations of the A-pillar to roof rail joint (Long 1998).

2.3.1 Determining the Most Important Design Parameters

Among all the design parameters of the joint, some have big effects but some only have small or even no effects on the stiffness and mass of the joint. To create an efficient regression model, we only need those design parameters that have big effects on the stiffness and mass of the joint. Therefore, we need to rank the design parameters in terms of importance and use the most important design parameters, which have significant effects on stiffness and mass of the joint, in the regression model. In our study, we use a linear polynomial and *Stepwise Linear Regression* (McCUEN 1985) to find the most important design parameters and the statistically best linear polynomial model. The procedure is explained in the following paragraphs.

First, the design parameter having the biggest effect on the error between the predicted results and the FEA results is determined and included in the model. Next, from the remaining design parameters, the one that reduces the error most significantly when included in the model is added in the regression model, and so on. *Significance probability*, which is the probability that the actual effect of a term on the fitting error is zero, is used to measure the improvement in the overall fitting resulted from adding a design parameter. A *hypothesis test* (the actual effect of a variable on the overall fitting is zero) is performed at every step to decide when to stop. A design parameter is added into the model if the reduction in the overall error is statistically significant, and the

procedure continues until there are no important design parameter that can be added into the regression model.

The *F – ratio* is used as a criterion to determine the importance of the design parameters. During each step of linear stepwise regression, the F – ratio of each design parameter is calculated. Its value is equal to the reduction of *sum of squared error* of the results when a design parameter is added into the regression model divided by *the mean squared error*. The design parameter with bigger value of the F – ratio has bigger effect on the output and thus is more important.

2.3.2 Choosing Polynomial Regression Models

A linear polynomial is used to simulate the linear relations between the input variables and the output. Since it has a relatively small number of regression parameters compared to a higher degree polynomial, and thus can take all the design parameters of the joint into account, it can be used to determine the important design parameters. The drawback of using linear polynomials is that the fitting and testing results can not be satisfactory for complicated input-output relations.

A quadratic polynomial regression model needs more parameters than linear polynomial regression model. If we consider all the design variables, all the cross-product terms and the square terms of all the design variables, the regression model needs at least $C_N^0 + 2C_N^1 + C_N^2$ (N is the number of design variables) designs for fitting. This requires a very large database. Actually, a complete quadratic regression model may include many terms that have very small effects on the output. Including these terms can lead to larger errors in estimating the model parameters. To solve this problem, we can gradually increase the number of design variables. Based on the most important design

variables from linear stepwise regression, we do the stepwise regression by using these design variables and their cross-product terms, and square terms to find the terms that should be included in the regression model. Then, we gradually add more design variables in terms of the importance. The process continues until all the important design variables, their cross-product terms and square terms are included in the regression model. By comparing the results from different quadratic polynomial models, the one with the smallest *standard deviation* in the results is selected.

For the A-pillar to roof rail joint in our study (Long 1998), we use a double regression model to improve the simulation because the results from the linear regression model are not linearly related to the FEA results. From the scatter plots of FEA results versus the predictions from the linear regression model, it is found that the predicted results are almost evenly distributed along the two sides of a quadratic/cubic polynomial. Therefore, a second regression using a quadratic/cubic is used to simulate the relation between the predicted results from the linear regression model and the FEA results. This improves the prediction significantly.

2.3.3 Criteria for Validating and Testing the Regression Models

Four criteria are used to validate and test the regression model in our study. They are *Significance Probability*, R^2, C_p *criterion* and the *AIC* criterion (Akaike's Information Criterion). Long (1998) gives the detailed explanations to these criteria.

Among these criteria, the Significance Probability is used to determine how important a term should be in order to be included in the regression model. In our study, its value is 5% while many applications use a value between 1 ~10%. The determination factor is denoted as R^2, which express the percent of the variation in the response of the

designs from the mean response. The higher the value of R^2 is, the bigger the proportion in fitting that can be explained by the regression model will be, and the better the fitting results will be. The C_p criterion is an alternative statistic to determine the quality of a polynomial regression model. The AIC criterion is similar to the definition of the sum of squared error. The model with the smallest AIC value is considered as the best one.

To test the generalization performance of polynomial, the database is divided into two sets with one set for fitting and the other for testing the generalization performance. The standard deviation of the prediction over the observation (actual value) is calculated. The polynomial with the smallest standard deviation for testing has the best generalization performance.

2.4 Developing and Validating a Response Neural Network

To build a neural network, the network architecture, the transfer function of the neurons and the training algorithm must be first selected. Since the *Multilayer Perceptron* is the most widely used static network model, it is selected in our study. The *Backpropagation* training algorithm is selected because it is the most popular algorithm for function approximation.

As to the network architecture, the number of hidden layers and the numer of neurons in each hidden layer must be decided. Most applications use neural networks with one or two hidden layers to approximate input-output relations. It has been shown that a neural network with one hidden layer is able to approximate almost any continuous function theoretically. A neural network with two hidden layers needs less neurons, but it might need much more time to train. Thus, a neural network with one hidden layer is selected in our study.

2.4.1 Transfer Function

The transfer function for the hidden layer is the *sigmoid function*, and the transfer function for the output layer is the *linear function*. The sigmoid function has the following form:

$$f_i^k(z_i^k) = \frac{1}{1+e^{-z_i^k}}$$
$$z_i^k = \sum_{j=1}^{N^k} w_{i,j}^k x_j^{k-1} + b_i^k \tag{2.1}$$

The *linear transfer function* has a very simple form:

$$f_i^k(z_i^k) = z_i^k = \sum_{j=1}^{N^k} w_{i,j}^k x_j^{k-1} + b_i^k; \tag{2.2}$$

In the above forms, k identifies the k th layer. z_i^k is the sum of the inputs from the proceeding layer for the i th neuron in the k th layer. f_i^k is the output of the i th neuron in the k th layer. N^k is the number of inputs for the neurons in the k th layer. $x_{i,j}^{k-1}$ is the j th input from the $k-1$ th layer to the ith neuron in the k th layer. The quantities $w_{i,j}^k$ are the weights of the ith neuron corresponding to the j th input in the k th layer, and b_i^k is the bias of the i th neuron in the k th layer.

2.4.2 Normalization of Parameters

It is necessary to normalize the input and output parameters because the range of each parameter varies greatly. For example, the plate thickness can vary in less than 1 mm while the width of the joint (for the B-pillar to rocker joint) can vary in a range of 32 mm. Generally speaking, the order of the input parameters varies from 10^0 to 10^2. The order of output parameters varies from 10^7 to 10^8. In this study, two normalization methods are considered and tested:

- Normalization through dividing their mean value.
- Normalization to the range [-1,1], of which the formula is:

$$P_{Normalized} = \frac{2 \times P_{UnNormalized} - (P_{Max} + P_{Min})}{(P_{Max} - P_{Min})} \tag{2.3}$$

where, $P_{Normalized}$ is the normalized parameter, $P_{UnNormalized}$ is the parameter without normalization. P_{Max} is the maximum value of the parameter and P_{Min} is the minimum value of the parameter.

The second method, which normalizes the parameters to the range [-1,1], is selected because it generally converges faster than the first method. Since we use the sigmoid function as the transfer function (equation 2.1), the convergence speed is related to the derivative of the function $f_i^k(z_i^k)$ with respect to z_i^k, and the derivative will be bigger when z_i^k is within the range [-1,1] than it is outside the range.

2.4.3 Determining the Number of Neurons Needed in the Hidden Layer

For the three layer network used in our study, the number of the neurons in the input layer is determined by the number of parameters considered. The number of the neurons in the output layer is fixed as one for each neural network predicting I/O, F/A, the torsional stiffness and the mass. The number of the neurons in the hidden layer can be changed and has effects on the generalization performance of the network. A neural network with too many neurons in the hidden layer will memorize the training data and can not generalize relations from the training data. A neural network with too few neurons in the hidden layer will neither learn nor be able to generalize relations from the training data.

It is a widely accepted criterion that the number of neurons in the hidden layer should be selected so that the total number of unknowns is less than the total number of the input-output pairs used in the training. In this case, the network is determined. In our study, the number of neurons in the hidden layer is chosen according to this criterion. For the mapping relations that are relatively simple, the number of design parameters is changed from 1 to the maximum value. The number of neurons in the hidden layer is chosen to make the total number of unknowns approximately equal to 80-90% of the total number of designs for training. For the complicated mapping relations, not only the number of design variables, but also the number of neurons are changed from the 1 to maximum allowable value. From all the neural networks, the neural network with smallest testing error is selected as the translator.

2.4.4 Method of Determining When to Stop Training and Testing the Generalization Performance of the Trained Neural Network

Using the training set (input-output pairs for fitting), we can train the neural network to match the examples (output) in the training set as closely as possible. We need to decide when to stop the iterative training process.

There are several stopping criteria. According to the first criterion, the training process is stopped when the magnitude of the gradient of the total error in training with respect to the parameters (weights and biases of the network) is small enough since the gradient will be zero at the minimum by definition. According to the second criterion, the training process is terminated when the sum of square error falls below a small fixed value. This criterion requires some knowledge of the minimum value of the sum of square error, which is not always available. According to the third one, the training process is stopped when a fixed number of iterations have been performed, but it is not guaranteed that the training is stopped at a minimum.

The fourth criterion is the method of *cross-validation*, which is used in our study. This method can be used to achieve better generalization performance in trained networks and keep the networks from overfitting on the training set. The idea of this method is to separate the data set into two parts: the training set, and the testing set. The training set is used to compute the gradient and to update the weights. The testing set is used to monitor the general performance of the network. During the training process, the performance of the network on the training set will continue to improve, but the improvement of its performance on the testing set will stop at a point. Beyond this point, the network will start to overfit the training set and the performance of the network will begin to degrade. The training process is terminated at this point.

The database is divided into three sets: training set and two testing sets. The training set and the first testing set are used for training and determining when to stop the training with cross validation method. The second testing set is used to test the trained neural network. The standard deviation of the ratio of the predicted results over the FEA results is used to compare the results from neural networks with different architectures. In our study, the neural network translator uses the neural network with the smallest value of the standard deviation for the testing results.

Chapter 3

Methodology For Developing Translator B For Finding The Best Design That Meets Given Performance Targets

To optimize the overall car body at the early design stage, we need design tools (Translator A and Translator B) to link the performance characteristics of the components with their physical design parameters (dimensions) as well as their packaging, manufacturing and styling constraints. For car joints, translator A allows designers to derive the stiffness and mass of a given joint from its physical design parameters. Chapter 2 has described the methodology for developing translator A, which involves following steps:

- Parameterization of actual car joints using a few, important physical design parameters, which are controllable in the early design stages of a car.
- Identification of packaging, manufacturing and styling constraints, which can be expressed in terms of physical design parameters.
- Development of a generic joint model that predicts the performance (stiffness) and mass of a given joint. For this purpose, the methodology uses a parametric modeling CAD software, such as CATIA, I-DEAS or Pro/Engineer and a FEA package, such as MSC/NASTRAN.
- Development of the database that stores many feasible designs and their corresponding FEA results.

- Development of an algorithm to predict the performance of any given joint very rapidly using artificial neural networks and/or response surface polynomials.

Unlike translator A, which gives the stiffness and mass of a given joint, translator B for car joints solves the inverse problem. It finds the dimensions and mass of the most efficient, feasible joint meeting given targets on stiffness. Here, a feasible joint is a joint that satisfies given stiffness requirements and packaging, manufacturing and styling constraints. An efficient joint is the joint with the lowest mass whose stiffness is as close as possible to a given target. In this thesis, we refer the most efficient, feasible joint design as the optimal (or best) joint design.

Translator B finds the optimal design using optimization methods. The objective function to minimize can be the mass of a joint or the sum of mass and some measure of the difference of the performance (stiffness). Design variables are the physical design parameters of a joint. There are constraints on the performance characteristics, the values of the design variables, packaging, manufacturing and styling requirements as well as mathematical requirements for a joint with a reasonable shape.

This chapter describes the general methodology for developing translator B for car joints. The outline for this Chapter is listed as follows:

- Section 3.1 describes the formulation of the optimization problem for car joints.
- Section 3.2 explains and compares several different algorithms for the optimization of the car joints in this study.
- Section 3.3 studies how to validate the results of the optimization problem.

3.1 Formulation of Optimization Problem

A general optimization problem is formally stated in the following mathematical form:

Minimize: $F(\mathbf{x})$ Objective Function (3.1a)

Subject to:

$g_j(\mathbf{x}) \le 0, \quad j = 1, m$ inequality constraints (3.1b)

$h_k(\mathbf{x}) = 0, \quad k = 1, l$ equality constraints (3.1c)

$x_i^l \le x_i \le x_i^u, \quad i = 1, n$ side constraints

Here, $\mathbf{x} = \{x_1, x_2, \cdots, x_n\}^T$, is the vector of design variables, and component x_i is the *i*th design variable. x_i^l and x_i^u are the lower and upper limits of *i*th design variable. m is the number of inequality constraints. l is the number of equality constraints. n is the number of design variables.

3.1.1 Selection of Design Parameters

According to Long (1998), in general, 50-200 design parameters are needed to completely describe the geometry and FEA information about a joint.

Among all the physical design parameters of a joint, as Chapter 2 has discussed, only few design parameters affect stiffness and mass, and thus are considered as design variables. Including design parameters that do not significantly affect the objective function will cause numerical problems because the gradients of the objective function

and constraints with respect to these parameters can be zero. Those design parameters that do not effect the stiffness and mass must be fixed in the optimization program.

Some design parameters are fixed by the program because of design rules and conventions. Designers can not change their values. For example the *rocker_length* of the B-pillar to rocker joint is fixed (Figure 5.22) because the member lengths of the joint should be fixed so that the different joints can be compared fairly.

Some design parameters are often fixed by the designers because of manufacturing, packaging or styling considerations. For example, because of packaging and manufacturing considerations, designers often fix design parameters such as the *pillar_angle* , *pillar_io_angle, length_of_flange* and *spot_weld_spacing* at some values in design of the B-pillar to rocker joint (See Figures 5.16, 5.22 for definitions).

Some design parameters are dependent on others. For example, the outer blending radii of the B-pillar to rocker joint are dependent on the corresponding inner blending radii because they are equal to each other (Figure 5.18).

Accordingly, we can divide the physical design parameters into four sets:

1. those fixed by the program because of design rules and conventions.
2. those fixed by designers because of manufacturing, packaging and styling considerations and conventional rules.
3. those determined from other independent parameters.
4. those changed by the optimizer

For a particular car joint, the number of first set and third set of design parameters are fixed while the number of the second set of design parameters (fixed by designers) can be changed for different designs. By fixing more or less design parameters,

designers can decide the number of design parameters to be considered in the optimization. Translator B in our study accounts for different number of design parameters. To fix a design parameter, designers only need to modify the input data file instead of modifying the program. This feature of translator B has following benefits:

- First, it can handle some design variables with discrete values. This is very useful for the design of car joints because the thicknesses of metal plates used in joints can only take discrete values, and from our study, their values have significant effects on the performance characteristics (stiffness and mass) of the joints. Specifically, designers can first assume that the thickness has the continuous value and find the optimum design. Then, designers can select the value (one of the discrete values of the thickness) that is closest to the optimum value, fix the thickness at this value and exclude the thickness out of the optimization process. The optimum design can be obtained by solving the optimization problem again with the reduced number of design variables.
- Designers can only change those design variables that have significant effects and exclude the rest that are comparatively less important out of the optimization design.
- Designers do not have the freedom to change some design variables, whose values come from the styling or other requirements and are fixed at the beginning. The best way to handle them is to exclude them from the optimization process. It simplifies the optimization problem and avoids potential divergence problem.

In the process of optimization, only independent design parameters are considered, and the first three sets of design parameters (those fixed by the optimization program and users and those determined from others) are excluded out of the optimization process.

3.1.2 Objective Function

The objective function is a target that the user wants to achieve through optimization. To find the best joint design with lowest mass, we need to minimize the joint mass. Thus, the objective function can be the joint mass. The obtained optimal design satisfies stiffness requirements (i.e. the stiffnesses are larger than their required minimum values) as well as manufacturing, packaging and styling constraints.

However, in the practical design of car joints, there can be additional objectives required for the optimal design than just the lowest mass. Design engineers sometimes need to design a joint with not only lower mass but also its performance (stiffness) must be close to some performance targets. These targets are determined from the optimization of the overall car body using a concept model or they can be derived from experience. To consider this situation, the objective function is more generally defined as the combination of mass and performance (stiffness). Specifically, it is the sum of mass and some measure of difference between the performance (stiffness) of a design from given performance (stiffness) targets. It can be expressed in the following form:

$$\mathrm{F} = \alpha\, M + (1-\alpha)\; f((K_1 - \hat{K}_1),(K_2 - \hat{K}_2),\ldots,(K_i - \hat{K}_i),\ldots) \tag{3.2}$$

Here, M is the mass of a given joint. α is a weighting factor used to include the effects of the performance (stiffness) on objective function. K_i $(i = 1,2,\ldots)$ is the *i*th performance (stiffness), $\hat{K}_i$ $(i = 1,2,\ldots)$ is the target values of the *i*th performance (stiffness).

3.1.3 Constraints

Design of car joints should consider the requirement that the joint is compatible with other components of the overall car structure. For example, it needs to consider the interaction between the joints and other components such as doors and seats. Also, the joint must be practically manufacturable and should meet some styling requirements. From these considerations, constraints on the joint construction can be used to ensure feasible designs.

In the optimization, there are several types of constraints addressed, namely, packaging constraints, manufacturing constraints, styling constraints, mathematical constraints, performance target constraints, and side constraints for the range of design variables. They are elucidated in the following list:

- Packaging constraints are the constraints that are related to the arrangement of the car components in limited space. They constrain the joint to be compatible with the nearby components, and ensure that there is enough space for driver and passengers. For example, the width of inner rocker cell of the B-pillar to rocker joint should be constrained to be smaller than a specified upper limit so as to leave enough space for the seat mechanism. The *door_edge_height* and *door_edge_width* of the B-pillar to rocker joint should be large enough to accommodate the sealant and the door edge (Figure 5.21).

- Manufacturing constraints are the constraints induced from manufacturing limitations. They are used to ensure that the pieces of the joint can be formed from a piece of sheet metal. One example of these constraints is: For the B-pillar to rocker joint, the angle of the upper and lower edge of rocker cells (inner and outer cells) should be able to avoid die lock (Figures 5.33, 5.34).

- Styling constraints are constraints expressing the styling requirements. An example is the constraint dictating that the bottom flange of the rocker cross section should not be visible to a person standing at the side of the car (Figure 5.37).

- Mathematical constraints are the requirements that some dimensions should meet to ensure that a joint has a reasonable shape. An example is the constraint dictating that the *outboard_cell_width* of the rocker cross section should be less than the overall width of the rocker section (Figure 5.21).

- Performance constraints are the target stiffnesses that the designer wants to achieve through optimization.

- Constraints on the range of design variables are used to ensure that translator A does not extrapolate during the optimization process. Translator A and translator B use neural networks or polynomials to simulate the relations between the design variables and stiffness and mass of joint. A database was first created in order to create translator A, which was used to train the neural network and/or fit the polynomials. The accuracy of both translator A and translator B are closely related to this database. To maintain the accuracy of the optimization results, limits on the ranges of the dimensions should be imposed as side constraints (can not be changed) in the optimization program to prevent the dimensions from assuming values that are out of the ranges that were used to create the database.

To avoid extrapolation of translator A in the optimization, stiffness ($K_{I/O}$, $K_{F/A}$, K_{Tor}) targets can not be too large or too small also. They must be within the range of the

stiffnesses of the designs in the database. Since the stiffness $K_{I/O}$, $K_{F/A}$ and K_{Tor} are interrelated to each other, the database can be further divided into several zones according to the combination of $K_{I/O}$, $K_{F/A}$ and K_{Tor}, and the combination of stiffness ($K_{I/O}$, $K_{F/A}$, K_{Tor}) targets should be within these zones.

It should be noted that the differences among the categories of constraints are not so distinctive for some constraints. They can be classified as different types of constraints if we consider them from different starting point. For example, constraints dictating that the blending radii can not be too large or too small can be classified as either packaging constraints or styling constraints. They can be classified as packaging constraints because they ensure the joint to be compatible with other components like doors. They also can be classified as styling constraints because the styling considerations require the blending radii can not be too large or too small. Actually, they are from both packaging and styling considerations. Based on discussion with some design engineers, we classify the types of constraints using the most widely used type.

3.2 Solution of the Optimization Problem

The optimization of car joints is a constrained nonlinear optimization problem since its objective function (general form) and some of the packaging and manufacturing constraints are nonlinear.

Design Optimization Tools (DOT) is an optimization package developed by Vanderplaats Research & Development, Inc. It is written in standard Fortran 77. Several people in the department (Giunta 1997, Balabanov 1997) have used DOT in their research. It is selected in our study because it was available for this research project and its algorithms for constrained nonlinear problem fit our optimization problem.

For constrained optimization problems, DOT implements *a Modified Feasible Direction* algorithm, *Sequential Linear Programming* algorithm, and *Sequential Quadratic Programming* algorithm (DOT manual 1995). Gradients can either be supplied by the user or estimated by the program using finite difference method. In our study, the Modified Feasible Direction (MFD) and Sequential Linear Programming (SLP) algorithms are used to solve the optimization problem.

As the developer of DOT stated, MFD is a powerful, general method that can be applied to most constrained nonlinear problems. It is a method that attempts to deal directly with the nonlinearity of the problem. It tries to find a usable-feasible searching direction, which will reduce the objective function without violating the active constraint for some finite move. The searching direction in MFD method is determined by using the *Fletcher-Reeves Conjugate Direction* method when there is no active or violated constraints. If there are active and violated constraints, a more complicated method for searching direction is used. Detailed explanations are provided in DOT manual and are not described here. Using the conjugate search direction method is just a simple modification to the *Steepest Descent* method. It accounts for not only the steepest descent direction but also the previous search direction. It provides more efficiency of the convergence to the optimum.

SLP is a method that tries to solve the nonlinear problem using linear programming methods repeatedly (Vanderplaats 1984). First, it linearizes the nonlinear problem (including the objective function and the constraints) and obtains the solution to this linear approximation using the linear programming method. Having this approximate solution, it then linearizes about this point and solves the new linear programming problem. It repeatedly linearizes and solves the resulting problems until it converges. This method is also powerful for nonlinear problems (NLP), especially for those NLPs with behaviors close to linear problems.

Sequential Quadratic Programming (*SQP*) method is also a powerful NLP method. It is not used in this study because some constraints of the optimization problem of the car joints are linearly related to design variables, and it is not efficient to use SQP to solve the problem. We also found that, when using SQP, the optimization program can not find a feasible design in the few cases when the initial design is in infeasible domain (for designs not satisfying stiffness requirements).

For the optimization problem of car joints, there are many constraints, and the feasible design space is, therefore, very limited. Specifically, the design variables can only vary in narrow ranges. The nonlinear problem then behaves like a linear problem. We expect SLP to be well suitable for this problem.

We decided to use DOT with both SLP method and MFD method to find the optimum design of car joints. We will check the results obtained using the two methods to see if the optimization program can find the global optimum design, and decide if both methods will be used or if we have to select a better one for the translator B.

In addition to the DOT program, a *Mathematica* program is developed using the SLP package from the course tutorials of AOE/ESM 4084, "*Engineering Design Optimization*". We use this program to solve the same optimization problem. The results can be used to verify that obtained using DOT program.

3.3 Validation of the Results

There might be some possible problems in the large, complicated optimization process. First, the optimization may not converge or converge to a local optimum instead of the global optimum. Second, the optimization can find a design that appears to meet

performance requirements but is actually infeasible because translator A overestimated stiffness. Third, users may specify performance (stiffness) targets that actually can not be achieved. For example, users might set a too high stiffness requirement for a joint design.

A reasonable approach to solve a large problem is to start with a simplified version of the problem that has fewer design variables and fewer constraints than the original design problem. We can build such problem by fixing more design variables and excluding nonlinear constraints. After we solve the simplified problem, we can then solve a more complicated version of the problem by adding more design variables and constraints. Finally, we can solve the real problem with more confidence.

In general, nonlinear optimization problems are computationally difficult to solve and suffer from the fact that it is difficult to know if the global optimum has been found or if the optimizer found a local optimum. One way to find whether we have the global optimum is to solve the problem starting from a different initial point and compare the solutions. If the solutions are the same, then the optimum is likely to be the global one.

Although our problem behaves like a linear problem because there are many constraints limiting the feasible design space, we still need to check the results to see if the optimizer finds a global optimum solution. We can do this as follows:

- Solve the problem from different starting points to see if the optimizer converges to the same solution.
- Solve the problem again using the optimum design as initial guess to see if the optimum design changes.

If possible, we should also solve the same problem using different optimization method or code. In this study, we use a Sequential Linear Programming package in *Mathematica* environment, and developed a *Mathematica* program to solve the problem.

The above checks help ensure that the optimizer does converge to the global optimum solution. We also need to check if the optimum is actually feasible. This is important because in many design problems, the optimizer tends to take advantage of weaknesses (errors) in predictive models (translator A in our study), and yields a design that actually has low cost or weight but also unacceptable performance. For this purpose, we modify the parametric generic model by setting its dimensions to the optimum ones and visually examine the CAD model of the optimum design in Pro/engineer. The stiffness and mass of the optimum design are checked using FEA. A large difference between FEA and translator B results (say the error is larger than 25%) indicates that the optimum design may be close to the boundary of the region corresponding to the values of the parameters in the database. In such cases, one may have to narrow the ranges in which the design variables are allowed to vary.

We should compare the optimum designs obtained by using the stiffness of several actual car joints as the performance targets with the FEA results to ensure that the final designs are meaningful. We should also ask experts in automotive joint design to critique the characteristics of the final optimum designs.

The above checks ensure that translator B (the optimizer) translates the performance (stiffness) targets into a feasible and reliable joint design.

Chapter 4

Application Of Methodology For Developing Translator A: Effect Of Transverse Bulkheads On The B-Pillar To Rocker Joint

In design of car structures, joint stiffnesses (static stiffness for inboard/outboard, forward/afterward and torsion) are very important to the behavior of the overall car body structure, and are used as performance targets for joints. An efficient joint is a joint with small mass but high stiffness. Bulkheads in the joint structure are effective reinforcements because they increase stiffness without a significant penalty on mass.

Long (1998) has developed a translator A for the B-pillar to rocker joint of an actual car, but this translator does not account for bulkheads in the rocker. In this chapter, we study the effect of transverse bulkheads on the stiffness of the B-pillar to rocker joint and further develop the translator A so that it can predict the stiffness of the strengthened joints. Moreover, A method to calculate a confidence interval for the predicted stiffness of the B-pillar to rocker joint with transverse bulkheads is also developed in this chapter. Following is the outline of this chapter:

- Section 4.1 describes briefly the parametric model of the B-pillar to rocker joint and translator A for the joint without bulkhead. Long (1998) described this model in more detail.

- Section 4.2 describes the parametric model of the B-pillar to rocker joint with transverse bulkheads in the rocker.
- Section 4.3 presents the approach for developing the translator to predict effect of transverse bulkheads on the B-pillar to rocker joint.
- Section 4.4 presents the results and discussions.

4.1 Parametric Model of the B-pillar to Rocker Joint and Translator A for the Joint without Bulkhead

Long (1998) developed a parametric model (built in Pro/Engineer) for the B-pillar to rocker joint of an actual car based on the original one created by Murphy (1995). Table 4.1 shows the design parameters used in the model. Figures 5.16 – 5.22 shows the definitions of these design parameters. In this thesis, we use the same names for these design parameters as in the Pro/Engineer model of the B-pillar to rocker joint.

In the parametric model, there are some flags (i.e. control parameters) to determine the type of the joint and reinforcements. For example, *frontrock_generic_type* is a flag used to determine the type of rocker cross section. *Pillar_reinf_extended* is a flag used to determine which type of pillar reinforcement is present (regular or extended). For transverse bulkheads, two flags, *outboard_rocker_bulkheads* and *inboard_rocker_bulkheads* are used to determine whether there are transverse bulkheads in outboard/inboard rocker cells or not.

To study the B-pillar to rocker joint without bulkheads, the flags, *outboard_rocker_bulkheads* and *inboard_rocker_bulkheads* were set as "No". Using this parametric model, Long (1998) developed translator A for the B-pillar to rocker joint without bulkheads. One common type of construction was considered for the joint,

which had an extended pillar reinforcement and centerplate with the generic type of rocker cross section (Figures 1.3, 5.23 and 5.24). This translator A was implemented in a Fortran program and in spreadsheet format (MS Excel). It can quickly predict the stiffness ($K_{I/O}$, $K_{F/A}$, K_{Tor}) and mass of the joint for a given design of the B-pillar to rocker joint without bulkheads.

4.2 Adding Transverse Bulkheads in the B-pillar to Rocker Joint

Transverse bulkheads are flat plates placed in the cross section of joint members. They have proven to be effective in increasing the stiffness of the joint because they can reduce shear deformation of the cross-sections of members (Zhu 1994). For the B-pillar to rocker joint, we can put transverse bulkheads in the rocker cells and the B-pillar. Since bulkheads in the rocker cell are more effective than in the B-pillar, we put bulkheads in the rocker cells in this study. The transverse bulkheads in the rocker cells fill the cell portion of the cross section from the center plate to the sides of the rocker (Figure 4.8).

To study the effect of transverse bulkheads on the stiffness of the B-pillar to rocker joint, we set rocker-bulkheads flags as "Yes" in the parametric model. Except for the flags, the thickness of bulkhead and the position of bulkheads along the rocker must be provided in the parametric model. Design parameters of the B-pillar to rocker joint with transverse bulkheads are shown in Table 4.1. The same construction type was used in this study.

Adding transverse bulkheads is an effective reinforcement to strengthen the B-pillar to rocker joint. It improves the joint stiffness significantly while only increasing the joint mass slightly. It is important to investigate the effect of transverse bulkheads on

the B-pillar to rocker joint and develop the translator A that can rapidly predict the effect of bulkheads on the stiffness.

4.3 Development of Translator A to Predict Effect of Bulkheads

Long (1998) developed a database of 600 designs to establish translator A for the B-pillar to rocker joint (without bulkheads). This database consists of the dimensions of each design and its stiffnesses and mass calculated using FEA. We used a subset of the designs, added inboard rocker cell bulkheads at the defined best positions and analyzed them by FEA to calculate their stiffness. We chose a linear polynomial to do regression of K_b / K (the ratio of the stiffness with bulkhead to the stiffness without bulkhead). Stepwise regression was used to determine the most important design variables and then to obtain the best regression model. Finally, based on the developed translator A for the stiffness of the B-pillar joint without bulkheads, we obtained the translator A for the I/O and F/A stiffnesse ($K_{I/O}$ and $K_{F/A}$) of the B-pillar joint with bulkhead which yields both the predicted stiffnesses and confidence intervals for the stiffness. We only considered $K_{I/O}$ and $K_{F/A}$ in developing the translator because the effect of bulkheads on torsional stiffness (K_{Tor}) is small compared to the effect on other directions (Table 4.5). Moreover, the effect of bulkheads on mass is negligible (increase in mass is small). Therefore, we did not develop the translator for predicting the increase of mass.

4.3.1 Putting Bulkheads in Inboard Rocker Cell vs. in Outboard Rocker Cell

We put two transverse bulkheads near the two ends of the rocker. We first studied the effects of transverse bulkheads in inboard rocker cell vs. that in outboard

rocker cell. To compare the two cases, we put the transverse bulkheads at such positions that the distances between the bulkheads and ends of the rocker in the inboard rocker cell are the same as the corresponding distances of the bulkheads in the outboard rocker cell.

From the results (Table 4.2), it is observed that bulkheads has the smallest effect on the K_{Tor} while they increase the $K_{I/O}$ considerably. They also increase $K_{F/A}$ although the increase is not as large as that of $K_{I/O}$. When the bulkheads are close to the ends of the rocker, transverse bulkheads in outboard rocker cell generally increases the stiffnesses only slightly compared to transverse bulkheads in inboard rocker cell. Because of the blending areas at outboard rocker cell, it is impractical to move the bulkheads in the outer cell toward the center of the rocker. However, putting transverse bulkheads in the inboard rocker cell can improve the stiffness considerably when bulkheads move close to the center of the rocker (Figures 4.1 to 4.4).

Figure 4.1 and 4.2 show the effect of bulkheads in the inner cell of the rocker on the inboard/outboard stiffness for two joint designs as a function of the distance between the bulkhead and the end of the rocker, L1 (See Figure 4.8 for the definition of L1). In this study, L1 takes the same value for the bulkheads at both ends of the rocker. From the figures, it is observed that:

- The stiffness increases considerably when the bulkhead is near the center of the joint.
- The location of the bulkhead has a big effect on the increase in stiffness.
- The effect of the bulkhead changes from one joint design to another.

On the basis of the above observations, we chose to put bulkheads in inboard rocker cell.

4.3.2 Study of the Effect of Bulkhead Location along the Rocker on Stiffness

We then studied the effect of transverse bulkheads on the stiffness with respect to the locations along the rocker. We tried to determine the optimum location of the bulkheads along the rocker to maximize the joint stiffness.

Our calculations show that the stiffness, in general, increases when the distance between the transverse bulkheads and ends of the rocker increases. However, the increase is nonlinear (Figures 4.1 to 4.4). The rate of increase in stiffness is significant when the bulkheads are close to the ends of the rocker, that is, when L1 is small. Figure 4.1 and 4.2 show that when the transverse bulkheads move toward the center of rocker, stiffness $K_{I/O}$ can be improved only slightly. Figure 4.3 and 4.4 show that there is a maximum $K_{F/A}$ when putting transverse bulkheads at a position between the end and the center of rocker.

The best location of the transverse bulkheads varies from one joint design to another. However, we can define the best location of the transverse bulkheads along the rocker as midpoints of forward horizontal blending radii and afterward horizontal blending radii (Figure 4.5). The stiffness improvements resulting from putting transverse bulkheads at these locations are over 90% of the largest stiffness improvements that can be obtained by putting bulkheads in the inboard rocker cell (Table 4.3).

4.3.3 Effect of Bulkhead Thickness on Stiffness

Our study shows that increasing the thickness of transverse bulkheads will not have a significant effect on the joint stiffness though it will slightly increase the stiffness

(Table 4.4). We calculated the stiffness for several designs with the increase of bulkhead thickness, and found that the improvements of stiffness are small with comparison to the improvements resulting from moving bulkheads toward the center of rocker. Thus, in this study, we neglect the effect of bulkhead thickness on stiffness and assume the bulkhead thickness as a constant equal to1.2 mm.

4.3.4 Response Surface Polynomial for the Stiffness of a Joint with Bulkheads

Our objective is to develop a translator to predict the stiffness of the B-pillar to rocker joint with transverse bulkheads, K_b. Since we already have a translator to predict stiffness of the B-pillar to rocker joint without bulkhead, K, we now need to predict K_b / K (the ratio of stiffness with transverse bulkhead to stiffness without bulkhead). Both response surface polynomial (RSP) and neural network (NN) can be used for the prediction. We used a RSP to predict the stiffness ratio, K_b / K, because RSP and NN do not have significant difference in terms of accuracy (Long 1998) and it is relative simple to use RSP. In this thesis, we use symbols K_b and K for the I/O and F/A stiffnesses of a joint with transverse bulkheads and without transverse bulkheads respectively.

The stiffness of joints with bulkheads (K_b) can be calculated as:

$$K_b = (K_b / K) \times K \tag{4.1}$$

Choosing a subset of designs from the database that was created by Long (1998) to develop translator A for joints without bulkheads, we added bulkheads at the defined

best positions in the inboard rocker cell. Using MSC/NASTRAN, we obtained the stiffness and mass that are used for fitting and testing.

Because of the high cost of finite element analysis, we can't afford to perform FEA for hundreds of designs to obtain a large sample of designs for the regression of K_b / K. Practically, we first analyzed a small number of designs, and then added more designs until the RSP has a satisfactory accuracy of prediction. Totally 66 designs were analyzed by FEA, and the first 48 designs were used for fitting and the rest18 designs were used for testing.

4.3.5 Choosing the Degree of a Polynomial

Based on the comparison between the linear polynomial regression model and the quadratic polynomial regression model, we decided to use linear polynomials to do regression of K_b / K.

Confidence interval can be used as a measure of accuracy of the regression model. It is defined as an interval (range) which contains the actual value (to be predicted) with a confidence level (possibility). With a fixed confidence level, the smaller the confidence interval, the better the regression model. The method for calculating confidence intervals for a linear polynomial model is presented in Section 4.3.7.

Results from stepwise regression using quadratic polynomials show that the predicted confidence interval will not improve (reduce) significantly by using quadratic polynomial regression model relative to a linear model (Figures 4.6, 4.7). Figure 4.6 shows that the ratio of the confidence interval of the quadratic model to that of linear

model is between about 0.95 to 1.05 for the fitting designs. Figure 4.7 shows the similar situation for the testing designs. We could conclude that the quadratic model does not significantly reduce the confidence intervals, and thus decided to choose linear polynomials to predict K_b / K.

4.3.6 Method of Determining the Most Important Design Variables

As mentioned in Section 4.2, the B-pillar to rocker joint with transverse bulkheads has about 50 design variables (Table 4.1). Among all these design variables, only a few affect significantly the total stiffness and mass of the joint. To obtain the relations between the design variables (input) and the stiffness (output), we need only those important design variables.

One method to rank design variables in terms of importance would be to consider all possible polynomials with all possible combinations of input variables and compare the errors. Obviously, this method is impractical. Instead, stepwise linear regression method is much faster than fitting all possible polynomials. In our study, we used stepwise linear regression to find the most important design variables. The computer program *JMP* (JMP Guide 1995) was used for this purpose.

In each step of linear stepwise regression, we computed the F-ratio of each design variable. To obtain F-ratio of a design variable at a particular step of regression, we computed the decrease in sum of squared error (*SSE*) when we included the new design variable in the regression model. Dividing this reduction by the mean squared error (*MSE*) of the improved model obtained at the previous step, which includes the new design variable, we obtained the F-ratio. We used the F-ratio as a criterion to determine

the importance of the design variables. The variable with bigger F-ratio was considered more important.

Tables 4.6 to Table 4.7 rank the important design variables for I/O and F/A stiffness ratios when using a linear polynomial. It is observed that when the transverse bulkheads are put in the inner rocker cell, the *outboard_cell_width*, the *rocker_width* and *A5* (Figure 5.21) have significant effects on both I/O and F/A stiffnesses. When increasing *rocker_width* and decreasing *outboard_cell_width*, transverse bulkheads in the inner rocker cell tend to increase both I/O and F/A stiffness. This can be explained by the fact that increase of *rocker_width* and decrease of *outboard_cell_width* tend to increase the area of the bulkhead in the inner rocker cell (Figure 5.21), and thus strengthen the joint. Both I/O and F/A stiffness are increased when *A5* is increased, which makes the upper side plate of the inner rocker cell tend to be vertical.

4.3.7 Determine a Linear Polynomial for K_b / K

In this section, the linear regression model is studied and the vector of regression coefficients is derived. The estimated standard deviation of the predicted mean value of the observation and that of the actual value of an individual observation are derived. Finally, the confidence interval for an individual observation is obtained.

A linear regression model can be written in the following general form (Draper and Smith 1981, Edwards 1984, Montgomery and Peck 1992):

$$y = \beta_0 + \beta_1 x_1 + \beta_2 x_2 + \cdots\cdots + \beta_p x_p + \varepsilon \qquad (4.2a)$$

Where: $x_1, x_2, \cdots\cdots, x_p$ are p regression variables,

$\beta_0, \beta_1, \cdots\cdots, \beta_p$ are regression coefficients, and

ε represents the error.

Denote $\hat{y} = \beta_0 + \beta_1 x_1 + \beta_2 x_2 + \cdots\cdots + \beta_p x_p$. (4.2b)

Then, $y = \hat{y} + \varepsilon$ (4.2c)

Where, $\hat{y}$ represents the approximation of y.

In this model, we have two assumptions. First the assumed analytical form, $\hat{y}$, is exact, and the error ε (differences between the response surface and the fitted values) are due to noise. The second is that the noise (error) is assumed normally distributed, with zero mean. Moreover, the noise is independent from one measurement to another.

It is more convenient to express the model in matrix notation. This allows a very compact display of the model, data and results. Thus, the model can be written as:

$$\mathbf{Y} = \mathbf{X}\boldsymbol{\beta} + \boldsymbol{\varepsilon} \tag{4.3}$$

Where:

$$\mathbf{Y} = \begin{Bmatrix} y_1 \\ y_2 \\ \vdots \\ y_n \end{Bmatrix}, \qquad \mathbf{X} = \begin{bmatrix} 1 & x_{11} & x_{12} & \cdots x_{1p} \\ 1 & x_{21} & x_{22} & \cdots x_{2p} \\ \vdots & \vdots & \vdots & \vdots \ \vdots \\ 1 & x_{n1} & x_{n2} & \cdots x_{np} \end{bmatrix}$$

$$\boldsymbol{\beta} = \begin{Bmatrix} \beta_0 \\ \beta_1 \\ \vdots \\ \beta_p \end{Bmatrix}, \qquad \boldsymbol{\varepsilon} = \begin{Bmatrix} \varepsilon_1 \\ \varepsilon_2 \\ \vdots \\ \varepsilon_n \end{Bmatrix}$$

In general, **Y** is an $n \times 1$ vector of the observations, **X** is an $n \times (p+1)$ matrix of the levels of the regression variables, $\boldsymbol{\beta}$ is a $(p+1) \times 1$ vector of the regression coefficients, and $\boldsymbol{\varepsilon}$ is an $n \times 1$ vector of errors.

The least square estimator of $\boldsymbol{\beta}$, that minimizes the error sum of squares $\varepsilon^T \boldsymbol{\varepsilon}$ for the given n observations is:

$$\mathbf{b} = (\mathbf{X}^T \mathbf{X})^{-1} \mathbf{X}^T \mathbf{Y} \tag{4.4}$$

Then the fitted values are obtained from

$$\hat{y}_0 = \mathbf{x}_0{}^T \mathbf{b} \tag{4.5}$$

Where, $\mathbf{x}_0{}^T = (1,\ x_{10}, x_{20}, x_{30}, ..., x_{p0})$, and $x_{10}, x_{20}, x_{30}, ..., x_{p0}$ are the values of the regression variables corresponding to a particular design.

Let σ^2 to be the variance of error ε. An unbiased estimator (model dependent) of σ^2 is:

$$\hat{\sigma}^2 = MSE = \frac{SSE}{n-(p+1)} = \frac{\mathbf{Y}^{\mathrm{T}}\mathbf{Y} - \mathbf{b}^{\mathrm{T}}\mathbf{X}^{\mathrm{T}}\mathbf{Y}}{n-(p+1)} \tag{4.6}$$

The variance of the predicted mean value of y, $\hat{y}_0$ at a specific value $\mathbf{x}_0$, of $\mathbf{x}$ is:

$$\text{Var}(\hat{y}_0) = \sigma^2 \, \mathbf{x}_0{}^T (\mathbf{X}^T \mathbf{X})^{-1} \mathbf{x}_0 \tag{4.7}$$

The estimated variance of $\hat{y}_0$ is obtained by replacing σ^2 in equation 4.7 with its estimated value $\hat{\sigma}^2$. The estimated standard deviation of $\hat{y}_0$ is obtained by taking the square root of the estimated variance of $\hat{y}_0$:

$$\text{est.std.}(\hat{y}_0) = \hat{\sigma} \sqrt{\mathbf{x}_0{}^T (\mathbf{X}^T \mathbf{X})^{-1} \mathbf{x}_0} \tag{4.8}$$

Since the actual observed value of y varies about the mean value with variance σ^2, a predicted value of an individual observation will still be given by $\hat{y}$ but will have variance

$$\sigma^2 (1 + \mathbf{x}_0{}^T (\mathbf{X}^T \mathbf{X})^{-1} \mathbf{x}_0) \tag{4.9}$$

with corresponding estimated standard deviation :

$$\hat{\sigma} \sqrt{1 + \mathbf{x}_0{}^T (\mathbf{X}^T \mathbf{X})^{-1} \mathbf{x}_0} \tag{4.10}$$

Therefore, a 100 (1- γ) percent confidence interval for an individual observation at the point $\mathbf{x}_0$ is:

$$\hat{y}_0 - t_{1-\gamma/2,n-(p+1)}\ \hat{\sigma}\ \sqrt{1+\mathbf{x}_0{}^T(\mathbf{X}^T\mathbf{X})^{-1}\mathbf{x}_0}\ \le\ y_0\ \le\ \hat{y}_0 + t_{1-\gamma/2,n-(p+1)}\ \hat{\sigma}\ \sqrt{1+\mathbf{x}_0{}^T(\mathbf{X}^T\mathbf{X})^{-1}\mathbf{x}_0} \quad (4.11)$$

For 95% confidence (γ = 0.05), $t_{1-\gamma/2,n-(p+1)} \approx 2.0$

The confidence interval becomes:

$$\hat{y}_0 - 2\hat{\sigma}\ \sqrt{1+\mathbf{x}_0{}^T(\mathbf{X}^T\mathbf{X})^{-1}\mathbf{x}_0}\ \le\ y_0\ \le\ \hat{y}_0 + 2\hat{\sigma}\ \sqrt{1+\mathbf{x}_0{}^T(\mathbf{X}^T\mathbf{X})^{-1}\mathbf{x}_0} \quad (4.12)$$

In most real life applications the assumptions about the polynomial model do not hold. Specifically, the analytical form of $\hat{y}$ is not exact because the relation between the regression variables and the response y is unknown. As a result, when we try to approximate an unknown function with a polynomial the error between observations (measurements) and model predictions is not due to noise. However, in practice, we still use equations 4.10 and 4.11to estimate the accuracy in the model predictions.

4.3.8 Calculating K_b and its Confidence Interval

Based on the translator A for the stiffness of the B-pillar joint without bulkheads (K) developed by Long (1998) and a response surface of K_b / K, which can be developed using the method described in Section 4.3.7 and this section, we can calculate the stiffness of B-pillar joints with bulkheads.

The translator will use the following equation (see equation 4.1):

$$K_b = (K_b / K) \times K$$

Denote $y_1 = K_b / K$, and $y_2 = K$,

Then, $K_b = f(y_1, y_2) = y_1 \times y_2$ (4.13)

Expanding f as Taylor series at $(\bar{y}_1, \bar{y}_2)$,

$$f(y_1, y_2) = f(\bar{y}_1, \bar{y}_2) + \sum_{i=1}^{2} \frac{\partial f}{\partial y_i}(y_i - \bar{y}_i) \cong \bar{f} + \sum_{i=1}^{2} \frac{\partial f}{\partial y_i}(y_i - \bar{y}_i) \quad (4.14)$$

Then, $\mathrm{Var}(f) = \mathrm{E}\left[f - \mathrm{E}(f) \right]^2 = \mathrm{E}\left[\sum_{i=1}^{2} \frac{\partial f}{\partial y_i}(y_i - \bar{y}_i) \right]^2$

$$= \sum_{i=1}^{2} \left(\frac{\partial f}{\partial y_i}\right)^2 Var(y_i) + 2 \sum_{\substack{i=1 \\ j=1}}^{2} \frac{\partial f}{\partial y_i} \frac{\partial f}{\partial y_j} Cov(y_i, y_j)$$

$$\leq \sum_{i=1}^{2} \left(\frac{\partial f}{\partial y_i}\right)^2 \sigma_{yi} + 2 \sum_{\substack{i=1 \\ j=1}}^{2} \frac{\partial f}{\partial y_i} \frac{\partial f}{\partial y_j} \sigma_{yi} \sigma_{yj}$$

$$= \left[\sum_{i=1}^{2} \left(\frac{\partial f}{\partial y_i}\right) \sigma_{yi} \right]^2 \quad (4.15)$$

An upper bound for the standard deviation of K_b can be determined using the above equation:

$$\text{std.}(K_b) = \text{std.}(f)$$

$$= \sum_{i=1}^{2} \left(\frac{\partial f}{\partial y_i}\right)\sigma_{yi} = \bar{y}_2\,\sigma_{y1} + \bar{y}_1\sigma_{y2}$$

$$= K \times \text{std.}\,(K_b/K) + (K_b/K) \times \text{std.}\,(K) \qquad (4.16)$$

The 95% confidence interval for K_b is:

$$K_b \pm 2\ \text{std.}\,(K_b) \qquad (4.17)$$

4.3.9 Translator A for the Joints with Bulkheads

For a B-pillar to rocker joint without bulkheads, Long (1998) developed translator A using polynomials and neural networks. We used the polynomial translator A to predict the stiffness of B-pillar to rocker joint without bulkhead (K) since we used a polynomial to predict the stiffness ratio K_b/K.

Using the method described in Sections 4.3.7 and 4.3.8, we can develop a linear polynomial for K_b/K (the ratio of stiffness with transverse bulkheads to stiffness without bulkhead). Then, the stiffness with transverse bulkheads is predicted as the product of K and K_b/K (equation 4.1). The 95% confidence interval is predicted according to the equations derived in Section 4.3.8.

The translator A for predicting stiffness of the B-pillar to rocker joint with transverse bulkheads is implemented in a Fortran program and a spreadsheet format (MS Excel).

4.4 Results and Discussion

In the regression, a value of 0.05 was used as the significance probability to determine how important a term should be in order to be included in the regression model.

As described in Section 2.3.3, R^2 can be used to validate and test the regression model. The higher the R^2, the better the regression model. Table 4.8 presents the values of R^2 for the translator A (with bulkheads). For I/O stiffness, its value is 0.9422 for fitting and 0.9371 for testing. For the F/A stiffness, its value is 0.9510 for fitting and is reduced to 0.8580 for testing. Thus, for both I/O stiffness and F/A stiffness, the regression is better for fitting than for testing.

The standard deviations of the ratio of translator predictions (with bulkheads) over observations (FEA results) are presented in Table 4.9. For I/O stiffness, its value is 9.14% for fitting and 10.71% for testing, which is little higher compared to that for the B-pillar joint without bulkheads, 8.8% for fitting and 9.8% for testing (Long 1998). For the F/A stiffness, its value is 4.6% for fitting and 10.77% for testing while for the B-pillar joint without bulkheads, its value is 5.08% for fitting and 4.47% for testing (Long 1998). Thus, for both I/O stiffness and F/A stiffness, the standard deviations of the ratio of translator predictions (with bulkheads) over observations (FEA results) for testing are increased compared to that for fitting.

Based on the above observations, the translator A for the stiffness of the B-pillar joint with bulkheads predicts the stiffness with bigger errors for testing designs, especially for F/A stiffness, which can also be observed from the correlation plots in Figures 4.9 – 4.12. This can be improved by using more fitting designs.

Figures 4.13 - 4.16 show the predicted stiffness ($K_{I/O}$, $K_{F/A}$) and 95% confidence intervals for fitting and testing designs. The stiffnesses calculated from FEM are all covered by the 95% confidence interval, which seems conservative. Due to the high computational cost associated with FEA, we only analyzed 66 designs with 48 designs for fitting. This makes the confidence interval quite large. Further efforts to improve the predictions with smaller confidence interval can be made also by using more designs for fitting.

The I/O stiffness ($K_{I/O}$) and F/A stiffness ($K_{F/A}$) can be improved significantly by putting bulkheads in the appropriate position (i.e. the defined best position). Specifically, it is found that the I/O stiffness increases between 10% to 56% while the F/A stiffness increases between 4% to 22%. This will be very useful for design of automotive joints as bulkheads will increase the stiffness considerably but will increase very little mass of a joint (from 0.4% to 2.6% of the mass without the bulkheads).

Chapter 5

Application Of Methodology For Developing Translator B For The B-Pillar To Rocker Joint

The B-pillar to rocker joint is a simple "T" shaped joint lying between the front and rear doors (Figures 1.2, 1.3). Comparing to the other types of car joints, it is simple in structure. But it is also an important joint in the car overall structure. After consultation with engineers of a US automotive company, the B-pillar to rocker joint was selected as the first car joint to develop translator A and B in our research project.

Since translator A has been developed for the B-pillar to rocker joint of an actual car (Long 1998), the next step is to develop translator B for the B-pillar to rocker joint. In this chapter, we applies the general methodology, which is described in Chapter 3, to develop translator B for the B-pillar to rocker joint of an actual car. The work presented in this chapter was completed in close collaboration with Mr. L. Long (Long 1998). There are two main differences between the work completed by the author of this thesis and Long's work:

- First, the author of this thesis developed a *Mathematica* program, in which the polynomial translator and a subroutine for SLP algorithm from the course tutorials of AOE/ESM 4084, "*Engineering Design Optimization*" were used. Long wrote a Fortran program using DOT. The *Mathematica* program was

used to validate the Fortran program (using DOT). Both programs were used to solve the same optimization problem. The results obtained using *Mathematica* program well agreed with that obtained using the DOT program, and thus validated the DOT program.

- Second, to obtain more accurate results using the NN translator and compare the NN translator with the RSP translator, we fixed some design variables, which were not used in the NN translators but used in the RSP translators at the corresponding values of optimum designs obtained using RSP translator B. See Table 5.1 for these design variables. Long (1998) did not fixed these design variables when using the NN translator B.

The outline of this Chapter is as following:

- Section 5.1 describes the formulation of the optimization problem used in developing translator B for the B-pillar to rocker joint of an actual car. In this section, four types of design variables and ranges of these design variables are first described. Then the objective function and the constraints are described and explained in detail.
- Section 5.2 presents the results and discussion. Validations of the optimization results for the B-pillar to rocker joint are first presented, including check of convergence of the optimization program and check with FEA results. Then we compare the polynomial translator B with neural network translator B since we have developed both the polynomial translator B and neural network translator B for the B-pillar to rocker joint. The optimum results from translator B are also compared with FEA results for some actual design problems. Parametric study is performed to examine change of optimum mass when stiffness requirements change and when upper and lower limits of some dimensions change. Finally, the obtained results for

the B-pillar to rocker joint are discussed, and also are compared with what Min Zhu (1994) had obtained.

5.1 Formulation of the Optimization Problem for Developing a Translator B for a B-Pillar to Rocker Joint

For the B-pillar to rocker joint, the task of translator B is to find the dimensions and mass of the most efficient, feasible B-pillar to rocker joint meeting given targets on stiffness. It is actually an optimization problem.

To solve this optimization problem, we use translator A to simulate the relations between the design parameters of a joint design and the stiffness and mass of the joint to avoid the costly FEA. We encode translator A in the program for translator B. Since we have both polynomial translator A and neural network translator A, we also develop two translator B, one is polynomial translator B, the other is neural network translator B.

The optimization problem is described in detail in the following sections.

5.1.1 Design variables

The B-pillar to rocker joint can have different reinforcements and thus have different types of construction. After discussion with engineers in automotive industry, we decided to use one common type of construction in this study. This type of B-pillar to rocker joint has extended pillar reinforcement and centerplate with generic type of rocker cross section, i.e. center plate connected to the bottom of the front rocker and the rear plate of the rocker (Figures 1.3, 5.23 and 5.24). Bulkheads and pillar bridge are not

considered in the joint. The corresponding control parameters (defining the construction type) in the parametric model are set accordingly.

Totally 48 design variables are used in the translator B for the B-pillar to rocker joint since design parameters defining the bulkheads and pillar bridge are not considered (Table 5.1). As Chapter 3 has described, they are divided into four sets: 1) those fixed by the program because of design rules and conventions, 2) those fixed by designers, 3) those determined by other independent parameters, 4) those changed by the optimizer (independent design variables)

Some design variables are generally fixed from packaging, manufacturing, and styling requirements. Designers can fix them with specified requirements for the actual design problems when using translator B. Some design variables are determined as per design rules and conventions. They are fixed by the program and can not be changed by designers. To fairly compare the stiffness of different joint designs, the rocker branch and the B-pillar branch are cut at the same length for different joint designs.

The first set of design variables has one design variable, which is *Rocker_length*. It is fixed so that different B-pillar joint designs can be compared fairly (Figure 5.22).

There are seven design variables in the second set (fixed by designers). They are *pillar_angle, pillar_io_angle, pillar_location, aft_pillar_hole, length_of_flange, spot_weld_spacing* and *spot_weld_placement* (Figures 5.16, 5.18, 5.20, 5.22). Specifically, *pillar_angle* and *pillar_io_angle* are fixed from styling considerations because designers usually decide the orientation of the joint branches at the beginning of design process. *Pillar_location* and aft_pillar_hole are fixed from packaging consideration. *Length_of_flange, spot_weld_spacing* and *spot_weld_placement* are fixed because of manufacturing requirements.

In our study, *length_of_flange* is fixed at 19.00 mm. *Spot_weld_spacing* is fixed at 47.50 mm. *Spot_weld_placement* is fixed at 9.5 mm. *Pillar_angle* and *pillar_io_angle* are both fixed at 90 degree. *Pillar_location* is fixed at 150 mm. *Rocker_length* is fixed at 485 mm and *aft_pillar_hole* is fixed at 15 mm.

There are six design variables dependent on other independent design variables. They are *fwd_outer_ver_blending_rad*, *fwd_outer_hor_blending_rad*, *aft_outer_ver_blending_rad*, *aft_outer_hor_blending_rad*, *pillar_height*, and *pillar_reinforcement_depth* (Figures 5.18, 5.19). Specifically, the outer blending radius such as *fwd_outer_ver_blending_rad* is dependent on the corresponding inner blending radius such as *fwd_inner_ver_blending_rad* because they are assumed to take the same values. *Pillar_height* is determined by several other independent design variables and the length of B-pillar branch. In this study, the length of B-pillar branch is defined as the distance from the top of the pillar to the center of the rocker (Figure 5.26), and is fixed to allow for fair comparison of the stiffness and mass of different joint designs. *Pillar_reinforcement_depth* is dependent because the pillar reinforcement is assumed to touch the bottom of rocker.

In the optimization of the B-pillar to rocker joint, these fixed by the program and designers as well as dependent design variables (totally 14 design variables) are excluded from the optimization process. The rest 34 design variables can be changed by the optimizer. Thus, the optimization problem of B-pillar to rocker joint has 34 independent design variables.

The ranges of the design variables are shown in Table 5.2. They are consistent with the database that was used to develop translator A for the B-pillar to rocker joint, and prevent the dimensions from assuming values that are out of the ranges that were used to create the database.

5.1.2 Objective Function

The objective function of translator B for the B-pillar to rocker joint can be expressed as

$$F = \alpha\ M\ +\ (1-\alpha)\sqrt{(\frac{K_{I/O}-\hat{K}_{I/O}}{\overline{K}_{I/O}})^2+(\frac{K_{F/A}-\hat{K}_{F/A}}{\overline{K}_{F/A}})^2+(\frac{K_{Tor}-\hat{K}_{Tor}}{\overline{K}_{Tor}})^2} \qquad (5.1)$$

Here *M* is the mass of a given joint. $K_{I/O}, K_{F/A}$, and K_{Tor} are the I/O, F/A and torsion stiffness of the joint. $\hat{K}_{I/O}, \hat{K}_{F/A}$, and $\hat{K}_{Tor}$ are the user-specified requirements (targets) for I/O, F/A and torsion stiffness. $\overline{K}_{I/O}, \overline{K}_{F/A}$, and $\overline{K}_{Tor}$ are the stiffness values used to normalize the stiffness. α is a weighting factor used to include the effects of stiffness on objective function.

For most of the cases studied in this project, α was set to be 1, which means only the mass was considered in the objective function. But we can also set α to be a value between 0 and 1 (for example, set α to be 0.5). This makes the objective function to be the sum of mass and the specified measure (i.e. 0.5) of difference between the stiffness of a design from given stiffness targets. The optimal joint design then will be a joint with not only low mass but also its stiffness close to the stiffness targets.

For some cases in our parametric study, one of the stiffness ($K_{I/O}, K_{F/A}$ and K_{Tor}) is selected as the objective function. In such case, the objective function can be expressed as

$$F = -K_{type} / \overline{K}_{type}, \quad (type = I/O, F/A, \text{or Tor}) \tag{5.2}$$

Here K_{type} is the stiffness. $\overline{K}_{type}$ is used to normalize the stiffness

5.1.3 Constraints

As described in Chapter 3, the constraints used in the optimization program for the B-pillar to rocker joint are divided into packaging constraints, manufacturing constraints, styling constraints, mathematical constraints, performance target constraints, and side constraints on the ranges of design variables. In these constraints, the default maximum values and minimum values of some design variables and some measures used in the program were specified as per design rules and conventions and discussion with design engineers in automotive industry. Designers can also specify their values as necessary for some actual design problems.

- Packaging Constraints

Packaging Constraints for B-pillar and Pillar Reinforcement

1) Space must be provided for the door latch (Figure 5.17).

$$pillar\_outer\_length - pillar\_inner\_length \leq 0 \tag{5.3}$$

2) The pillar outer length must exceed a minimum value to leave enough space between the front door and the rear door (Figure 5.17).

$$minimum\ value\ of\ pillar\_outer\_length - pillar\_outer\_length \leq 0 \tag{5.4}$$

3) Space must be provided for the door latch (Figure 5.17)

$$\textit{minimum value of outer\_pillar\_width} - \textit{outer\_pillar\_width} \leq 0 \tag{5.5}$$

4) – 5) The pillar angle is constrained in a range so that it is easy to get in and out of the car. Styling considerations may also constrain the angle (Figure 5.16).

$$\textit{minimum value of pillar angle} - \textit{pillar\_angle} \leq 0 \tag{5.6}$$

$$\textit{pillar\_angle} - \textit{maximum value of pillar angle} \leq 0 \tag{5.7}$$

6) – 7) The pillar inboard/outboard angle is constrained in a range so that it is easy to get in and out of the car. Styling considerations may also constrain the angle (Figure 5.16).

$$\textit{minimum value of pillar\_io\_angle} - \textit{pillar\_io\_angle} \leq 0 \tag{5.8}$$

$$\textit{pillar\_io\_angle} - \textit{maximum value of pillar\_io\_angle} \leq 0 \tag{5.9}$$

8) The pillar reinforcement should not intersect with the side or the bottom piece of the rocker. The values of d3, H_int1 and H_int2 are derived in terms of the design variables using trigonometry (Figure 5.28)

Case 1: If *pillar_reinforcement_depth* < d3 then,

$$\textit{pillar\_reinf\_base\_width} - \textit{H\_int1} \leq 0; \tag{5.10a}$$

Case 2: If *pillar_reinforcement_depth* ≥ d3, then,

$$pillar\_reinf\_base\_width - H\_int2 \leq 0 \quad (5.10b)$$

9) – 10) There is a range for *pillar_reinf_depth* (Figure 5.19).

$$min.\ value\ of\ pillar\ reinforcement\ depth - pillar\_reinf\_depth \leq 0 \quad (5.11)$$

$$pillar\_reinf\_depth - max.\ value\ of\ pillar\ reinforcement\ depth \leq 0 \quad (5.12)$$

Packaging Constraints for Blending Radii

11) – 18) Blending radius can not be too large and too small from packaging (also styling) considerations (Figure 5.18). In the following constraints, *Bld_Mi* is the minimum value of blending radius given by the designer, and a default value of 30 mm was used in this study. *Bld_Mx* is the maximum value of blending radius given by the designer, with a default value of 200 mm.

$$Bld\_Mi - fwd\_inner\_ver\_blending\_rad \leq 0 \quad (5.13)$$

$$fwd\_inner\_ver\_blending\_rad - Bld\_Mx \leq 0 \quad (5.14)$$

$$Bld\_Mi - aft\_inner\_ver\_blending\_rad \leq 0 \quad (5.15)$$

$$aft\_inner\_ver\_blending\_rad - Bld\_Mx \leq 0 \quad (5.16)$$

$$Bld\_Mi - fwd\_inner\_hor\_blending\_rad \leq 0 \quad (5.17)$$

$$fwd\_inner\_hor\_blending\_rad - Bld\_Mx \leq 0 \quad (5.18)$$

$$Bld\_Mi - aft\_inner\_hor\_blending\_rad \leq 0 \quad (5.19)$$

$$aft\_inner\_hor\_blending\_rad - Bld\_Mx \leq 0 \quad (5.20)$$

Packaging Constraints for Rocker Cross Section (Figure 5.21)

19) – 20) The rocker height and width can not exceed a maximum value

$$rocker\_height - maximum\ value\ of\ rocker\_height \leq 0 \quad (5.21)$$

$$rocker\_width - maximum\ value\ of\ rocker\_width \leq 0 \quad (5.22)$$

21) – 22) The door edge height and width must be large enough to accommodate the sealant and the door edge. A value of 3.0 mm was used as the default value for both minimum values in this study.

$$minimum\ value\ of\ door\_edge\_height - door\_edge\_height \leq 0 \quad (5.23)$$

$$minimum\ value\ of\ door\_edge\_width - door\_edge\_width \leq 0 \quad (5.24)$$

23) – 24) There is a range for A1 to allow for water drainage

$$minimum\ value\ of\ A1 - A1 \leq 0 \quad (5.25)$$

$$A1 - 90 \leq 0 \quad (5.26)$$

25) – 26) There is a range for A5 from seat packaging considerations. The maximum value for A5 was specified at 90 degree in this study.

$$\textit{minimum value for A5} - A5 \leq 0 \tag{5.27}$$

$$A5 - \textit{maximum value for A5} \leq 0 \tag{5.28}$$

27) – 28) There is a range for A3 from packaging (also styling) considerations.

$$\textit{Minimum value of A3} - A3 \leq 0 \tag{5.29}$$

$$A3 - \textit{Maximum value of A3} \leq 0 \tag{5.30}$$

29) There must be a slope for water to run off. The default minimum value of *A6* for water to run off was 3.0 degree in this study (Figure 5.30).

$$\textit{minimum value of A6 for water to run off} - A6 \leq 0 \tag{5.31}$$

30) The slope of the top plate of inner rocker cell should be small (Figure 5.31).

$$\textit{atan (d7/h4) - maximum value of slope} \leq 0 \tag{5.32}$$

31) The width of inner rocker cell can not be too large from seat packaging considerations.

$$\textit{rocker\_width} - \textit{outboard\_cell\_width - max. value for inner cell} \leq 0 \tag{5.33}$$

- Manufacturing Constraints

Manufacturing constraints include stamping and welding constraints. Very detailed information about the geometry is needed to determine if a given design is feasible. However, this information is not available in the early design stage. We used crude equations to check if a design can be manufactured or not.

Manufacturing Constraints for Rocker Cross Section

1) – 8) The length of each edge of rocker cross section should be greater than a minimum value so that the rocker inner and outer shells can be stamped. The default minimum value was 10 mm in this study (Figure 5.29).

$$\textit{minimum value of the length of edge plates} - BR\_Li \leq 0 \quad (i=1, \ldots, 8) \tag{5.34}$$

9) – 16) Angles between two adjacent edges should be greater than the minimum value so as to avoid a sharp angle between the edge plates. The default minimum value was 20 degree in this study (Figure 5.30).

$$\textit{minimum value of angle} - BR\_Anglei \leq 0 \quad (i=1, \ldots, 8) \tag{5.35}$$

17) – 18) The angle of the upper and the lower edges of the outer rocker cell should be able to avoid die lock. The default minimum angle to avoid die lock was 3.0 degree in this study (Figures 5.33, 5.34).

$$\textit{minimum value of die angle} - (90 - A1) \leq 0 \tag{5.36}$$

$$\textit{minimum value of die angle} - (90\text{-}A2) \leq 0 \tag{5.37}$$

19) Draw angle of the outer rocker cell should be controlled to avoid high residual stresses. The maximum value of draw angle was 30 degree in this study (Figures 5.35, 5.36).

$$|\,(180+A1\text{-}A2)/2 - 90\,| - \textit{maximum value of Draw Angle} \leq 0 \tag{5.38}$$

20) Depth of draw for outer rocker cell should not be too large relative to width to ensure that plastic strains are not too high. The maximum ratio was specified at 1.5 in this study (Figure 5.35).

$$\textit{Depth of draw (outer rocker cell) /Width of draw (outer rocker cell) - maximum ratio} \leq 0 \tag{5.39}$$

21) There should be no sudden changes in depth of draw (Figure 5.35).

$$\textit{Changes in depth of draw - maximum value for the change between the depths of any two adjacent plates} \leq 0 \tag{5.40}$$

22) -23) The angle of the upper and lower piece of inner rocker cell should be able to avoid die lock. (Figures 5.33, 5.34)

$$\textit{minimum angle to avoid die lock} - (90\text{-}A8) \leq 0 \tag{5.41}$$

$$\textit{minimum angle to avoid die lock} - BR\_1Ang \leq 0 \tag{5.42}$$

24) Draw angle of the inner rocker cell should be controlled to avoid high residual stresses. (Figure 5.35, 5.36)

$$|(180\text{-}A8 + 90 - BR\_1Ang)/2 - 90| - \text{maximum value of Draw Angle} \leq 0 \quad (5.43)$$

25) Depth of draw for inner rocker cell should not be too large relative to width to ensure that plastic strains are not too high (Figure 5.35).

$$\text{Depth of draw (inner rocker cell) / width of draw (inner rocker cell)} - \text{maximum ratio} \leq 0 \quad (5.44)$$

26) – 35) Manufacturing constraints are required for *Spring Back* of the rocker plates. In the constraints, *spBkMi* is the minimum angle for Spring Back, which allows two adjacent plates to have a permanent deformation. 20 degree was used as its default value in this study (Figures 5.32).

$$spBkAng0 - (180 - spBkMi) \leq 0 \quad (5.45)$$

$$spBkAng1 - (180 - spBkMi) \leq 0 \quad (5.46)$$

$$spBkAng2 - (180 - spBkMi) \leq 0 \quad (5.47)$$

$$spBkAng3 - (180 - spBkMi) \leq 0 \quad (5.48)$$

$$spBkAng4 - (180 - spBkMi) \leq 0 \quad (5.49)$$

$$spBkAng5 - (180 - spBkMi) \leq 0 \quad (5.50)$$

$$spBkAng6 - (180 - spBkMi) \leq 0 \quad (5.51)$$

$$spBkAng7 - (180 - spBkMi) \leq 0 \quad (5.52)$$

$$spBkAng8 - (180 - spBkMi) \leq 0 \quad (5.53)$$

$$spBkAng9 - (180 - spBkMi) \leq 0 \quad (5.53)$$

Manufacturing Constraints for B-pillar

36) – 37) Depth of pillar plates should not be too large relative to width to avoid excessive plastic strains (Figure 5.17).

$$outer\_pillar\_width / pillar\_outer\_length \ - maximum\ ratio \leq 0 \quad (5.55)$$

$$inner\_pillar\_width / pillar\_inner\_length \ - \ maximum\ ratio \leq 0 \quad (5.56)$$

- Styling Constraints

1) The bottom flange of rocker should not be visible by a person standing at one side of the car (Figure 5.37).

$$BR\_alpha - BR\_beta \leq 0 \quad (5.57)$$

2) The slope of the outer rocker cell, A3, should be approximately equal to the slope of the door (Figure 5.38). In the constraint, *Ang_door* is the slope of the door, and

ABDrMx is the maximum allowable value for the difference between A3 and the slope of door.

$$| A3 - Ang\_door | - ABDrMx \leq 0 \quad (5.58)$$

- Mathematical Constraints

Mathematical Constraints on Rocker Cross Section

1) The inner rocker height plus the height of *BR_L6* should not exceed the rocker height (Figures 5.21, 5.29).

$$inner\_rocker\_height + vertical\ length\ of\ BR\_L6 - rocker\_height \leq 0 \quad (5.59)$$

2) The inner flange distance plus the outboard cell width should not exceed the rocker width (Figure 5.21).

$$inner\_flange\_distance + outboard\_cell\_width - rocker\_width \leq 0 \quad (5.60)$$

3) The door edge height plus the height minus clearance of low door should not exceed the rocker height (Figure 5.21)

$$low\_door\_ht\_minus\_clearance + door\_edge\_height - rocker\_height \leq 0 \quad (5.61)$$

4) The inner pillar base can not go out of the top plate of inner rocker cell. (Figures 5.25, 5.29)

$$inner\_pillar\_base\_width - horizontal\ distance\ of\ BR\_L8 \leq 0 \quad (5.62)$$

Mathematical Constraints on Blending Radii (Figure 5.18)

5) – 6) The inner vertical blending radii can not exceed the pillar height.

$$aft\_inner\_ver\_blending\_rad - pillar\_height \leq 0 \quad (5.63)$$

$$fwd\_inner\_ver\_blending\_rad - pillar\_height \leq 0 \quad (5.64)$$

7) The after inner horizontal blending radius should be smaller than the *pillar_location* so that the after blending area will not extend outside the after end of the rocker

$$aft\_inner\_hor\_blending\_rad - pillar\_location \leq 0 \quad (5.65)$$

8) The lengths of the forward horizontal blending radii added to the *pillar_base* and *pillar_location* can not exceed the overall rocker length so that the forward blending area will not extend outside the forward end of the rocker. 20 is a margin to ensure that the design can be created by the parametric model.

$$fwd\_inner\_hor\_blending\_rad + pillar\_base + pillar\_location + pillar\_inner\_length - pillar\_outer\_length + 20 - rocker\_length \leq 0 \quad (5.66)$$

- Performance Target Constraints

Typically, the stiffness of a joint must satisfy two types of requirements. It should not be less than a minimum required value and/or should be close to a target value. Since

the second requirement (i.e. the stiffness should be close to a target) is vague, we tried to account for it by adding to the objective function a term that measure the difference between the stiffness and the corresponding target.

The first requirement, that is the stiffness (K) of a design should be greater than a required value ($\hat{K}$) so that the joint design satisfies the performance (stiffness) targets, is expressed as follows:

$$\frac{(-K_{I/O} + \hat{K}_{I/O})}{\overline{K}_{I/O}} \leq 0 \tag{5.67}$$

$$\frac{(-K_{F/A} + \hat{K}_{F/A})}{\overline{K}_{F/A}} \leq 0 \tag{5.68}$$

$$\frac{(-K_{Tor} + \hat{K}_{Tor})}{\overline{K}_{Tor}} \leq 0 \tag{5.69}$$

- Constraints on the ranges of design variables are implemented in the optimization program as side constraints, which can not be changed by designers. This keeps the optimal designs inside the database and ensures the accuracy of the optimization results (translator B)

5.2 Results and Discussions

All the constraints for the optimization problem of the B-pillar to rocker joint limit the feasible design space to a great extent. This makes the nonlinear problem

behave like a linear problem. We used DOT (Design Optimization Tools Manual 1995) with both Sequential Linear Programming (SLP) and Modified Feasible Direction Method (MFD) to solve this optimization problem. During the testing period, a *Mathematica* program using polynomial translator and SLP algorithm was also developed to check the DOT program.

In section 5.2.1, we first checked the convergence of the optimization program using RSP translators with SLP and MFD method. Then we visually examined the optimum designs in Pro/Engineer, and compared the optimization results (for RSP translators) with the FEA results. In section 5.2.2, we present and compare the results obtained by using neural network translator and polynomial translator. In Section 5.2.3, we redesigned two actual car joints using translator B. In section 5.2.4, the parametric study was performed to exam change of optimum mass when stiffness requirements change and when upper and lower limits of some dimensions change. Finally, the results are discussed in Section 5.2.5.

5.2.1 Validation of the Results

Since our problem is actually a nonlinear problem, the optimizer can stop at different final designs (local optimum) when we use different initial designs. Therefore, we must check the results to see if the program converges to a global optimum design.

5.2.1.1 Checking Convergence of the Optimization Program using RSP

In this section, we first check the results obtained by using response surface polynomial (RSP). To check the convergence of the optimization program (translator B), we can do:

1) Solve the problem from different initial designs to see if the program find the same optimum design.
2) Solve the problem again from the obtained optimum design to see if the optimum design will be improved or not.

In this study, we used two different optimization algorithms, i.e. Sequential Linear Programming (SLP) and Modified Feasible Direction (MFD) method to solve the same problem to see if the optimization program converges to the same point.

Eight randomly generated designs were used as initial designs. The measured stiffnesses of an actual car joint were used as the stiffness targets. We only considered the mass in the objective function (α was set to be 1 in equation 5.1).

Due to numerical errors, we can not expect the optimum designs converge to the exactly same value. We regard the optimum designs converge to the same design if the values of the objective function (mass) are very close with a small relative difference and the first 2 to 3 digits of design variables are generally the same. We regard there is no improvement for the optimum design if the improvement is very small.

Table 5.6a shows the optimum results obtained by starting from the eight initial designs with SLP method for RSP translator. We found that the optimum designs obtained with SLP method all converged to the same design. The maximum relative difference between the optimum designs was 0.1%. The first 2 to 3 digits of design variables were generally the same. There was also no improvement (less than 0.1%) can

be obtained by solving the problem again starting from the obtained optimum design. So, the program with SLP method can find the global optimum design. The obtained optimization results from DOT program (DOT manual 1995) agreed with the results obtained by using the *Mathematica* program, which used the RSP translator and SLP method.

The program with MFD method also converged to the global optimum design when starting from the eight initial designs. However, the optimization with MFD method needed more iterations than that with SLP method. SLP was more efficient than MFD for the optimization of the B-pillar joint in this study. The reason can be that the problem for the B-pillar joint behaves like a linear problem because many constraints limit the range in which the design variables can vary.

We chose SLP as the default method in RSP translator B for the B-pillar to rocker joint. All the optimization results (from RSP translator) presented in later parts were obtained by using SLP method. Designers can switch to the MFD method by changing the method identification number in the translator B.

5.2.1.2 Comparison of Results of (RSP) Translator B with FEA Results

Translator B finds the efficient and feasible joint design with smaller mass but higher stiffness, which are equal to or higher than the given target values. To validate translator B, we compared the mass and stiffness of the optimum designs obtained using translator B with that from FEA.

We first randomly selected a number of required stiffness values as performance targets. The selected stiffness targets must be smaller than their maximum limits,

otherwise translator B (the optimization program) can not find a design meeting both the stiffness targets and all the constraints (especially the limits for the design variables). Tables 5.3 - 5.5 show the maximum limits for $K_{I/O}, K_{F/A}$ and K_{Tor} (using RSP translator) when the allowable mass changes. Corresponding to each set of the stiffness targets, we used translator B to obtain an optimum design.

These optimum designs were visually examined in Pro/Engineer and were found to be feasible designs. MSC/NASTRAN were used to obtain the FEA results for the Pro/E models (optimum designs). Table 5.7a shows the optimum results compared with the FEA results when RSP translators are used. Figures 5.1 – 5.3 show the correlation plots for I/O, F/A and torsional stiffness (for RSP translators).

From the obtained results, we found the optimum mass fit the FEA results well. The optimum stiffness ($K_{I/O}$, $K_{F/A}$, K_{Tor}) generally fit the FEA results well if the stiffness targets were not too high. Specifically, the optimum F/A stiffness and torsional stiffness fit the FEA results (Figures 5.2, 5.3) better than the optimum I/O stiffness (Figure 5.1). For some designs with high stiffness target in one direction and low stiffness target in another, the stiffness of optimum designs did not fit the FEA results well. The reason can be that the optimum designs might be close to the boundary of the region in the database that we used to created translator A or even out of this region. The predictions from translator A deteriorate when a design approaches the boundary of the database. In such cases, translator A and B will not predict the stiffness of the optimum design accurately.

From observing the scatter plots of $K_{I/O}$ versus $K_{F/A}$, and $K_{I/O}$ versus K_{Tor} of the designs in the database (Figures 5.13a, 5.13b), we find $K_{I/O}$, $K_{F/A}$ and K_{Tor} are actually correlated to each other. For example, a design with a large value of $K_{I/O}$ often

has large values of $K_{F/A}$ and K_{Tor} while a design with a small value of $K_{I/O}$ often has small values of $K_{F/A}$ and K_{Tor}. There are limits on the ranges in which each stiffness can vary. We could not specify a very high $K_{I/O}$ target but very low $K_{F/A}$ and K_{Tor} targets for a design, otherwise translator B might find an optimum design whose stiffness poorly correlate with FEA results.

To avoid these problems, we should divide the database into several zones according to the combination of the stiffness $K_{I/O}$, $K_{F/A}$ and K_{Tor} since they actually correlated to each other. The combination of stiffness ($K_{I/O}$, $K_{F/A}$, K_{Tor}) targets should be within these zones of the database to ensure that the optimum design from translator B have a better correlation with FEA results. Table 5.9 shows eight zones of the database. They were decided by investigating the scatter plots of the stiffnesses of designs in the database.

We again select the stiffness target combinations (for 12 designs) that are within the zones, and use translator B to find the optimum designs corresponding to these stiffness targets. Table 5.7c shows the optimum results for the new 12 designs (using RSP translators) compared with the FEA results. Figures 5.4 – 5.6 show the correlation plots for the results of the new 12 designs when RSP translators are used. Figure 5.4 shows that the correlation between the optimum I/O stiffness and the FEA results is much improved compared to Figure 5.1.

The *correlation coefficient* can be used to measure the correlation between two data sets, which is defined as the covariance of two data sets divided by the product of their deviations:

$$\rho_{Y_1,Y_2} = \frac{\mathrm{cov}(\mathbf{Y}_1, \mathbf{Y}_2)}{\sigma_{Y_1} \times \sigma_{Y_2}}, \tag{5.70}$$

Where $$\mathrm{cov}(\mathbf{Y}_1, \mathbf{Y}_2) = \frac{1}{n}\sum (y_{1,j} - \mu_{Y_1})(y_{2,j} - \mu_{Y_2}), \tag{5.71}$$

$$\sigma_{Y_1}^2 = \frac{1}{n}\sum (y_{1,j} - \mu_{Y_1})^2, \tag{5.72}$$

$$\sigma_{Y_2}^2 = \frac{1}{n}\sum (y_{2,j} - \mu_{Y_2})^2 \tag{5.73}$$

μ_{Y_1}, μ_{Y_2} are means of data sets $\mathbf{Y}_1$ and $\mathbf{Y}_2$.

In general, a correlation coefficient larger than 0.9 shows good agreement between the predictions of translator B and FEA results.

The correlation coefficients for all the designs (using RSP translator) are presented in Table 5.10a. From the table, we can find that the correlation are generally good and that the correlation between the two data sets improves considerably if the stiffness targets are constrained within the defined zones. Specifically, the correlation coefficient for the I/O stiffness increased from 0.9254 to 0.9733 when we constrained the stiffness targets. The correlation coefficient for the torsional stiffness improved slightly from 0.9794 to 0.9872 while that for the F/A stiffness decreased slightly from 0.9771 to 0.9676.

Accordingly, we implement these zones in the translator B (optimization program), which will give designers a warning message indicating that the optimization result may be inaccurate if the combination of stiffness targets is beyond the zones.

5.2.2 Comparison of Polynomial Translator B with Neural Network Translator B

We also tested the Neural Network (NN) translator B using both the SLP and MFD methods for optimization. The optimization program converged to the same solution with both SLP and MFD method from all the eight initial designs used for testing the convergence properties of the polynomial (Section 5.2.1.1). Table 5.6b shows the optimum results obtained by starting from the eight initial designs with SLP method for the NN translator. The maximum relative difference between the optimum designs was 0.06%. Tables 5.6a, 5.6b show that the optimum mass from NN translator was about 10% higher than that from RSP translator for the particular joint design used for testing the convergence properties.

We chose SLP as the default method in NN translator B for the B-pillar to rocker joint because SLP was more efficient than MFD. All the optimization results (from NN translator) presented in later parts were obtained by using SLP method. Designers can select MFD method by changing the method identification number in translator B.

Table 5.7b shows the optimum results compared with the FEA results when NN translators are used. Figures 5.7 – 5.9 show the correlation plots for I/O, F/A and torsional stiffness when NN translators are used. The optimum stiffnesses of some designs did not fit well with FEA results, especially when the stiffness targets were high. The reason is that the stiffness targets for these designs were selected randomly and some of them might be outside the region corresponding to the designs of the database. Comparing Figures 5.1, 5.2 and 5.3 with Figures 5.7, 5.8, and 5.9, it is also observed that the correlation for NN translator was not as good as that for RSP translator in general when the stiffness combinations of these designs were selected randomly (not all within the zones). The correlation coefficients for RSP translator were between 0.92 and 0.98

(Table 5.10a) while the correlation coefficients for NN translator were between 0.84 and 0.93 (Table 5.10b).

We again select the combinations of the stiffness targets for 12 designs in a way that the corresponding designs are within the database used for training (Section 5.2.1.2), and use the NN translator B to find the optimum designs corresponding to these stiffness targets. Table 5.7d shows the optimum results for the new 12 designs (using NN translators) compared with the FEA results. Figures 5.10 – 5.12 show the correlation plots for I/O, F/A and torsional stiffness. Table 5.10b shows the correlation coefficients for the stiffnesses of the optimum designs obtained using NN translator. It is observed from the table that the correlation is improved for each stiffness (I/O, F/A and torsional) when the stiffness targets are selected within the zones defined in Section 5.2.1.2. Specifically, the correlation coefficient for I/O stiffness is improved from 0.9201 to 0.9642. For F/A stiffness, it is improved from 0.8838 to 0.96, and for the torsional stiffness, it is improved most significantly from 0.8401 to 0.9975. Figures 5.7 – 5.12 also show the improvements in correlation. Comparing Figures 5.4, 5.5 and 5.6 with Figures 5.10, 5.11 and 5.12, it is observed that both RSP translator and NN translator correlate FEA results well for F/A and torsional stiffnesses when the stiffness combinations of these designs are selected within the zones. But for I/O stiffness, they do not correlate the FEA results well when the stiffness is high (large than 6.0 E+7). The correlation coefficients for the RSP translator are between 0.96 and 0.99 (Table 5.10a) while the correlation coefficients for the NN translator are between 0.96 and 1.00 (Table 5.10b).

Thus, when the stiffness targets are not high and their combinations are selected within the zones (defined in Section 5.2.1.2), an optimum design can be obtained by using either RSP translator B or NN translator B (Tables 5.8a, 5.8b). It is hard to say which translator B is better. The optimum design obtained by different translator B (RSP

or NN) can be different in terms of the values of some design variables while most of them are quite close.

Further investigation of the results in Tables 5.7a - 5.7d indicates that, in general, the masses of the optimum designs obtained using the NN translator B are about 6% ~16% higher than those using the RSP translator. The RSP translator underestimates the mass compared to the mass obtained from FEA. The NN translator tends to overestimate the mass when the I/O and F/A stiffness requirements are low and to underestimate the mass when the I/O and F/A stiffness requirements are high. Both the RSP and NN translators tend to overestimate the stiffness when the required I/O and F/A stiffnesses are low and to underestimate the stiffness when they are high.

Since the NN translators use fewer design variables than the RSP translators in this study, some design variables do not affect the stiffness and mass when using the NN translator (Table 5.1). To obtain more accurate results using the NN translator and compare the NN translator with the RSP translator, we fixed these design variables at the corresponding values of optimum designs obtained using RSP translator B when using the NN translator B to obtain the above results. If we do not fix these design variables, the NN translator B will use some variables that have no effect on the stiffness and mass, and might find different optimum designs and obtain different results (Long 1998).

5.2.3 Redesign of the Joints of Actual Cars Using Translator B

We also used translator B to redesign two actual car joints. The stiffnesses of the actual car joints are set as the performance targets. The optimum designs are obtained using translator B. Tables 5.8a - 5.8d show the results of the optimum designs and FEA results, from which we can get the following observations for the B-pillar joint:

For the B-pillar of optimum designs (Figures 5.17, 5.18),

- The *pillar_outer_length* tends to become equal to their upper limits. This helps to increase the dimensions of the B-pillar in forward/afterward direction and thus improve the forward/afterward stiffness.
- The *outer_pillar_width* increases when the stiffness requirements increase. This helps to increase the dimension of the B-pillar in inboard/outboard direction and help to improve the inboard/outboard stiffness.
- The *pillar_base* increase when the stiffness requirements of the joint increase. This is reasonable because the stiffness of the joint is expected to increase significantly when the section modulus of the beams leading to the joint increase.

For the pillar reinforcement of the optimum designs (Figure 5.19),

- The *pillar_reinforcement_depth* is a dependent design variable and takes a value between its lower and upper limits.
- The *pillar_reinf_base_width* and the *pillar_reinf_expansion* tend to become equal to their lower limits to reduce the mass of the joint because they have little effect on the joint stiffness.

For the rocker cross section of the optimum designs (Figure 5.21),

- The *rocker_height*, the *low_door_ht_minus_clearnce* tend to become equal to their lower limits, and the *outboard_cell_width* takes a value close to its lower limit. The *inner_flange_distance*, the *inner_rocker_height* and the *rocker_width* take some values between their lower and upper limits.
- The *door_edge_height* tends to take a large value as while the *door_edge_width* tends to take a value as small as possible. Translator B tends to minimize the *door_edge_width* since the stiffnesses increase rapidly when the *door_edge_width* decrease. Zhu (1994) also observed this trend.
- Angles A1, A3 and A8 tend to take their lower limits while angles A2 and A7 tend to get close to their upper limits. The front part of the rocker tends to be vertical when A7 becomes large and A3 becomes small (Figure 5.27). A large A2 tends to make the bottom of the rocker to be horizontal.

For the pillar hole of the optimum designs (Figure 5.20),

- The *bottom_pillar_hole* and the *fwd_pillar_hole* tend to become equal to their upper limits while the *aft_pillar_hole* is fixed in this study. The optimum design tends to make the pillar hole as small as possible.

For the thicknesses of the plates of the optimum designs (Figure 5.25),

- The *thickness of the outer rocker cell plate (frontrock)* takes its lower limit for car 2 and a value between its lower and upper limits for car 1. The parametric study in Section 5.2.3 indicates that both the stiffness and the mass can be increased if the *thickness of rocker outer cell plate* is increased. Therefore, there is a trade-off for an optimum design to take a suitable value between its lower and upper limits. The *thickness of the outer rocker cell plate* reaches the lower limit to reduce the mass if small stiffness targets are required. It

takes a value between its lower and upper limits for high stiffness requirements.

- The *thickness of the pillar reinforcement*, the *thickness of centerplate* and the *thickness of backrock* tend to become equal to their lower limits. The reason should be that they do not affect the joint stiffness and the mass can be reduced when they take smaller values.
- The *thickness of pillarback* increases when the stiffness requirements increase. As indicated in the parametric study in Section 5.2.3, increasing the *thickness of pillarback* can increase the stiffness considerably.

5.2.4 Parametric Study

To study the effect of stiffness requirements on the mass of the optimum designs, we changed one stiffness and fixed other two stiffnesses at the measured stiffnesses of an actual car joint. Figures 5.14a – 5.14c show the effect of the stiffness targets on the mass of the optimum designs. It is observed that the mass of the final design increases with the stiffness targets increasing. However, the trends are nonlinear. Specifically, the mass increases only slightly for low values of the stiffness requirements. The mass increases rapidly after the stiffness exceeds a certain value. It is also observed that $K_{F/A}$ have a larger effect on the mass than the stiffness $K_{I/O}$ and K_{Tor}. Thus, for the range of stiffnesses considered in this project, the stiffness $K_{F/A}$ requirement mainly determines the mass of the optimum design.

From the optimum designs, it is observed that some design variables tend to reach their lower or upper limits and some others assume values between their lower and upper

limits. Thus, the mass of the optimum design will change when the corresponding lower and upper limits of these design variables change. Figures 5.15a – 5.15i, Tables 5.11 – 5.19 show the effect of the upper and lower bounds of *the thickness of rocker outer cell, the thickness of pillarback, pillar_base, outer_pillar_width, pillar_inner_length, door_edge_width, rocker_width* and *outboard_cell_width* on the mass of optimum design. The tables also show the effect of changes in the limits of these variables on the optimum values of some important design variables such as *the thickness of rocker outer cell*. We selected these design variables because they were very important to the joint stiffness and mass. See Figures 5.17, 5.18 and 5.21 for the definition of these design variables. The measured stiffnesses of an actual car joint were used as the targets in the study.

Figures 5.15a – 5.15i show that the mass of the optimum design will increase when we increase the lower limit or decrease the upper limit of these design variables. This is because the design space in which the optimizer can search for an optimum design is reduced.

Both the stiffness and mass increase when the *thickness of the outer rocker cell (frontrock)* increases. Table 5.11 shows that increasing the lower limit of the *thickness of rocker outer cell* increases the mass of the optimum design. Tables 5.12 – 5.16 shows that the optimum designs tends to increase the *thickness of rocker outer cell* to increase the joint stiffness when the lower or upper limits of *the thickness of pillarback, pillar_base, outer_pillar_width* and *pillar_inner_length* change. Therefore, determining the optimum value of the *thickness of rocker outer cell* involves a trade off between high stiffness and low mass requirements.

The *thickness of pillar back* of the optimum designs tends to increase when the stiffness requirements increase since increasing its value improves the stiffness. When its

upper limit is reduced, the optimum design tends to increase *the thickness of rocker outer cell* to improve its stiffness.

The *pillar_base* is also an important design variable of the B-pillar to rocker joint. Tables 5.13 and 5.14 show the mass of the joint increases when its lower and upper limits change. As we observed in Section 5.2.1.2, it tends to take a large value to increase the stiffnesses of the joint. When the upper limit of *pillar_base* decreases, the thickness of outer rocker cell increases to compensate for the loss of stiffness, which increases the mass (Table 5.14).

It is also observed that increasing the lower limits of *door_edge_width*, *rocker_width* and *outboard_cell_width* (Figure 5.21) and decreasing the upper limit of the *outer_pillar_width, pillar_inner_width* (Figure 5.17) increase the joint mass respectively (Tables 5.15, 5.17-5.19).

5.2.5 Discussion of Results

Comparing the stiffness of optimum designs that were predicted by translator B with FEA results, we conclude that, when using translator B, it is important to specify the stiffness targets in a way that their combination falls within the database. Also the stiffness requirements should not be high. This will ensure that translator B predicts the stiffnesses of these designs accurately. When the combination of the stiffness targets was set within the defined eight zones and the stiffness targets are not high, both RSP and NN translators could find the optimum design, which correlated well with the FEA results. Zhu (1994) found that the predictions of NN were slightly more accurate than those of RSP. However, in this study, we can not get this conclusion. We found that it is hard to

say one translator (NN or RSP) predicts the stiffness of the optimum designs more accurately than the other does with comparison to the FEA results. The reason might be that Zhu (1994) used a completed second-degree polynomial instead of using stepwise regression to create the RSP. This included some statistically unimportant terms and made the predictions of the translator to have large errors.

Several observations of the optimum designs should be useful for design of car joints. They can serve as rules of thumb for improving the joint stiffness and help engineers design more efficient joints. For example, in our study, it was observed that the *pillar_base* and after horizontal blending radii tended to assume large values while the forward horizontal blending radii tended to assume small values to leave space for a large *pillar_base* (Figure 5.18). This indicated that the optimum designs tended to make a large joint connection between the rocker and the B-pillar. This agrees with rules of thumb published in an internal report of an automotive manufacturer. This report stated that increasing the joint blending radii and section modulus leading into the joint is a good way to improve the joint stiffness.

For the optimum designs, the *bottom_pillar_hole* and the *fwd_pillar_hole* (Figure 5.20) tended to become equal to their maximum values. This maked the pillar hole of the optimum designs as small as possible. This is also consistent with guidelines reported by an automotive manufacturer.

Zhu (1994) found that the rocker section tends to take its maximum allowable height at the optimum. This is opposite to our observations. In our study, we observed that the *rocker_height* tended to become equal to its minimum value. This might be because our study used different parametric models, databases and constraints for the B-pillar to rocker joint than Zhu (1994).

Zhu (1994) suggested increasing the minimum allowable stiffness by 10% in order to cover the offset between the stiffness overestimated by the RSP and NN translator B and the FEA results, and therefore, ensure that the optimum design has acceptable stiffness. In our study, the translator B did not always overestimate the stiffness. Thus, we do not suggest increasing the stiffness targets slightly for the optimum designs.

Chapter 6
Concluding Remarks

6.1 Summary

This thesis presented general methodologies for developing two design tools, called translator A and translator B, for car joints. Translator A quickly predicts the stiffness and mass of a given joint. Translator B finds the dimensions and mass of the most efficient joint design according to the given requirements on stiffness. The methodology for developing translator B was demonstrated on the B-pillar to rocker joint of an actual car. The effect of transverse bulkheads on the B-pillar to rocker joint was investigated. A translator A for joints without bulkheads, developed by Long (1998), was extended so that it can predict the stiffness of joints with transverse bulkheads. This translator uses response surface polynomials.

The generic model for the B-pillar to rocker joint used in this study was developed by Long (1998) in Pro/Engineer. Based on this model, the effect of the transverse bulkheads on the stiffness of the B-pillar joint was studied. A linear polynomial was used to predict the ratio of the stiffness of the joint with bulkheads to that of the same joint without bulkheads (K_b / K). Stepwise regression was used to determine the most important design variables. A statistical method for calculating the confidence interval for the predicted stiffness of the B-pillar to rocker joint with

transverse bulkheads was also developed. The extended translator A for the B-pillar to rocker joints with bulkheads quickly predicts the effect of the transverse bulkheads on the stiffness.

A response surface polynomial (RSP) translator B and a neural network (NN) translator B were developed. MATHEMATICA and Fortran programs were written for translator B. Designers can choose either the RSP translator B or the NN translator B to find the efficient joint design. The developed translator B accounts for a large number of manufacturing, packaging, styling, performance targets and mathematical constraints. These constraints ensure that the obtained optimum design is a reliable and feasible design meeting the performance requirements. During the development of translator B, the Modified Feasible Direction (MFD) and Sequential Linear Programming (SLP) methods were tested. Both algorithms converged to the global optimum design. However, SLP is the default algorithm used in translator B since SLP was the most efficient optimization technique. Designers can switch to the MFD algorithm in translator B by changing the method identification number in the translator B.

To ensure that translator B translates the performance (stiffness) requirements into a feasible design, the stiffness and mass of the optimum design were checked against the FEA results. It was found that there were relatively large errors between the FEA results and the results from translator B for some designs with high stiffness requirements. Further study of the joint stiffness of the designs in the database showed that these stiffnesses were in certain ranges and were quite strongly correlated. To avoid using improper combinations of stiffness targets, we further divided the database into several zones. The optimum designs from both RSP translator B and NN translator B correlate the FEA results well when the stiffness target combinations are selected within these zones and the stiffness targets are not high.

Conclusions of this study are summarized as following:

- Transverse bulkheads in the rocker are effective in increasing the stiffness of joints. For the B-pillar to rocker joint, putting transverse bulkheads in the inner rocker cell can increase the I/O stiffness and F/A stiffness considerably without any appreciable effect on mass.
- The developed translator A for the B-pillar to rocker joint with bulkheads can quickly predict the stiffness of the joint with transverse bulkheads and provide a 95% confidence interval for the stiffness.
- The translator B is not good for high stiffness targets. Designers can use both the RSP translator B and the NN translator B to find the efficient joint designs when the stiffness targets are not high and their combinations are selected within a prescribed range. The predicted stiffness and mass of the optimum designs have considerable accuracy compared to FEA results.
- No translator (RSP or NN) was found consistently better than the other was.
- The NN translator produces heavier designs than the RSP translator does.
- Both the RSP and the NN translator tend to overestimate the stiffness when the I/O and F/A stiffness requirements are low and tend to underestimate the stiffness when they are high.
- The optimum designs for the B-pillar to rocker joint tend to have a low rocker since the *rocker_height* tend to become small as possible at the optimum.
- The optimum designs for the B-pillar joint tend to have a large blending area
- At the optimum, the pillar hole tends to become as small as possible.
- The thickness of the outer rocker cell and the pillar back are important design parameters. Increasing the thickness of rocker outer cell increases both the stiffness and the mass considerably. At the optimum, the outer rocker thickness assumes values between the lower and upper limits. Increasing the thickness of pillar back can also increase the joint stiffness considerably.

6.2 Future Work

During the development of translator A for the B-pillar to rocker joint with transverse bulkheads, we analyzed 66 designs and used 48 designs for fitting the polynomial regression model of K_b / K. We did not analyze more designs because of the high computational cost associated with FEA. In some cases, the error in the stiffness was considerable and the obtained 95% confidence intervals were quite large. Therefore, more designs should be used to improve the accuracy of the translator.

As we have found in Chapter 5, there were relatively large errors between the predicted stiffness from translator B and the FEA results for some designs especially with high stiffness requirements. To improve the predictions of translator B, a second regression can be used based on more optimum designs obtained from translator B and their FEA results.

Besides the transverse bulkheads, it is important to study other reinforcements. Based on the translator A developed by Long (1998), other translators A for the B-pillar to rocker joint that account for other reinforcements can be following a similar approach for transverse bulkheads.

Using the developed translator A and translator B, a database including many suitable joint designs for various combinations of performance targets can be developed. This database will be much helpful to the design engineers in the automotive industry.

With the progress in the CAD/CAM packages, it will be of great help to integrate the design tools into the CAD/CAM package. This will enable design engineers to

design an efficient joint, evaluate its performance and produce manufacturing drawings in a single environment.

The methodologies for developing translator A and translator B for design guidance can also be applied to other B-pillar to rocker joints with different types of construction. Furthermore, they can be extended to other components of the overall car structure. We believe that all the translators will help to reduce the time and cost required for the design of the components of a car body. They and serve as the efficient design tools for a rational hierarchical design approach of overall car body.

Bibliography

Anderson, J. A., 1995, "An Introduction to Neural Networks", MIT Press.

Ali, H., 1994, "Optimization for Finite Element Applications", Mechanical Engineering, Vol. 116, No. 12, pp. 68 – 76.

Balabanov, Vladimir O., 1997, “Development of Approximations for HSCT Wing Bending Material Weight Using Response Surface Methodology”, Ph.D. Dissertation, Department of Aerospace and Ocean Engineering, Virginia Polytechnic Institute and State University.

Berke, L., and Hajela, P., 1992, “Application of artificial neural nets in structural mechanics”, Structural Optimization, Vol.4, pp. 90 – 98.

Belegundu, A. D., 1993, "Optimizing the Shapes of Mechanical Components", Mechanical Engineering, Vol. 115, No. 1, pp. 46 – 48.

Botkin, M. E., and Lust, R. V., 1995, “A Neural Network Application to Shape Optimization”, 961102, General Motors Research and Development Center.

Chang, D.C., 1974, “Effects of Flexible Connections on Body Structural Response”, SAE Transactions, Vol. 83, pp. 233 – 244.

Carpenter, W. C., Barthelemy, J. M., 1992, “A Comparison of Polynomial Approximations and Artificial Neural Nets as Response Surface”, Proceedings of the 33rd AIAA/ASME/ASCE/AHS/ASC SDM Meeting, Dallas, Texas, pp. 2474 – 2482.

"Design optimization Tools Manual", 1995, Vanderplaats Research & Development, Inc.

Draper, N. R. and Smith, H., 1981, "Applied Regression Analysis", Second Edition, John Wiley & Sons, Inc.

Edwards, Allen L., 1984, "An Introduction to Linear Regression and Correlation", Second Edition, W.H. Freeman and Company, New York.

Giunta, Anthony A., 1997, “Aircraft Multidisciplinary Design Optimization Using Design of Experiments Theory and Response Surface Modeling Methods”, Ph.D. Dissertation, Department of Aerospace and Ocean Engineering, Virginia Polytechnic Institute and State University.

Guyot, N., and Nikolaidis, E., 1997, "Fuzzy Sets and Utility Theory-Based Multi-Objective Optimization of Automotive Joints", International Journal of Advanced Manufacturing Systems, Vol. 1, Issue 1.

Hagan, Martin T., Demuth, Howard B. and Beale, Mark, 1996, "Neural Network Design", PWS Publishing Co.

Hajela, P., and Berke, L., 1990, “Neurobiological Computational Models in Structural Analysis and Design”, AIAA/ASME/ASCE/AHS/ASC 31st Structures, Structural Dynamics, and Materials Conference, A Collection of Technical Papers, pp. 345 - 353.

"JMP Statistics and Graphics Guide", 1995, Version 3.1 of JMP, SAS Institute Inc.

Lee, K. and Nikolaidis, E., 1991, "Identification of Flexible Joints in Vehicle Structures", AIAA Journal, Vol. 30, No. 2, pp. 482 – 489.

Long, L., 1998, " Design-Oriented Translators for Automotive Joints ", Ph.D. Dissertation, Department of Aerospace and Ocean Engineering, Virginia Polytechnic Institute and State University.

McMCUEN, Richard H., 1985, "Statistical Methods for Engineers", Prentice-Hall, Inc., Englewood Cliffs, N.J.

Montgomery, Douglas C., and Peck, Elizabeth A., 1992, "Introduction to Linear Regression Analysis", Second Edition, John Wiley & Sons, Inc.

Murphy, S. T., 1995, "A Parametric Model for Rapid Analysis of Automotive Joints", M.S. Master's Thesis, Department of Aerospace and Ocean Engineering, Virginia Tech.

Myers, Raymond H., 1971, "Response Surface Methodology", Boston, Allyn and Bacon.

Nikolaidis, E. and Lee, K., 1992, "A 3-D Joint Model for Automotive Structures", 8th International Conference on Vehicle Structural Mechanics and CAE, Traverse City, Michigan.

Nikolaidis, E. and Zhu, M., 1991, "Analysis the I/O Bending of T-Shaped Joint by Using Vlasov's Theory", Report to Ford, Virginia Polytechnic Institute and State University.

Rogers, J. L., 1994, "Simulating Structural Analysis with Neural Network", Journal of Computing in Civil Engineering, Vol. 8, No. 2, pp. 252 – 265.

Sunami, Y., Yugawa, T. and Yoshida, Y., 1987, "Analysis of the Joint Rigidity In-Plane Bending of Plane-Joint Structures", Japanese Society of Automotive Engineers, Vol. 9, No. 2, pp. 44 – 51.

Sunami, Y., Yugawa, T. and Yoshida, Y., 1990, "Analysis of the Joint Rigidity of the Automotive Body Structure - Out-of-Plane Bending of Plane-Joint Structures", Japanese Society of Automotive Engineers, Vol. 11, No. 3, pp. 59 – 66.

Swift, R. A., and Batill, S. M., 1991, “Application of Neural Network to Preliminary Structural Design”, AIAA/ASME/ASCE/AHS/ASC 32nd Structures, Structural Dynamics, and Materials Conference, A Collection of Technical paper, pp. 335 – 343.

Vanderplaats, Garret N., 1984, "Numerical optimization techniques for engineering design with applications", New York, McGraw-Hill.

Zhu, M., 1994, "Translators for Design Guidance of Joints in Automotive Structures", Ph.D. Dissertation, Department of Aerospace and Ocean Engineering, Virginia Polytechnic Institute and State University.

Table 4.1 B-pillar to Rocker Joint Design Parameters

No.	Design parameters	Remarks
1	*length_of_flange*	
2	*spot_weld_spacing*	
3	*spot_weld_placement*	
4	*pillar_base*	
5	*pillar_angle*	
6	*pillar_io_angle*	
7	*pillar_height*	
8	*pillar_lacation*	
9	*outer_pillar_width*	
10	*inner_pillar_width*	
11	*pillar_outer_length*	
12	*pillar_inner_length*	
13	*fwd_inner_ver_blending_rad*	
14	*fwd_inner_hor_blending_rad*	
15	*fwd_outer_ver_blending_rad*	
16	*fwd_outer_hor_blending_rad*	
17	*aft_inner_ver_blending_rad*	
18	*aft_inner_hor_blending_rad*	
19	*aft_outer_ver_blending_rad*	
20	*aft_outer_hor_blending_rad*	
21	*inner_pillar_base_width*	
22	*rocker_length*	
23	*pillar_reinforcement_depth*	
24	*pillar_reinf_base_width*	
25	*pillar_reinf_expansion*	
26	*A1*	
27	*A2*	
28	*A3*	
29	*A5*	
30	*A7*	
31	*A8*	
32	*rocker_height*	
33	*inner_flange_distance*	
34	*inner_rocker_height*	
35	*rocker_width*	
36	*outboar_cell_width*	
37	*door_edge_height*	
38	*door_edge_width*	
39	*low_door_ht_minus_clearance*	
40	*fwd_bulk_head_position*	Only used for joint with transverse bulkheads
41	*aft_bulk_head_position*	Only used for joint with transverse bulkheads
42	*top_pillar_hole*	
43	*bottom_pillar_hole*	
44	*fwd_pillar_hole*	

Table 4.1 (Continued)

No.	Design parameters	Remarks
45	*aft_pillar_hole*	
46	*thickness of frontrock*	
47	*thicknes of pillar_reinf*	
48	*thickness of pillarback*	
49	*thickness of backrock*	
50	*thickness of centerplate*	
51	*thickness of pillar_bridge*	not used when pillar bridge is not present
52	*thickness of bulkheads*	only used for joint with transverse bulkheads

Table 4.2 Stiffness due to Putting Bulkheads in Inboard Rocker Cell vs. in Outboard Rocker Cell (Thickness of Bulkhead = 1.2 mm)

Design No.	L1 (mm)		Stiffness without bulkheads	Stiffness with bulkheads in inboard rocker cell		Stiffness with bulkheads in outboard rocker cell	
			K	K_b	percent increase (%)	K_b	percent increase (%)
9	15	F/A	4.2499 E+08	4.2796 E+08	0.70	4.2810 E+08	0.73
		Tor	5.9260 E+07	5.9475 E+07	0.36	5.6931 E+07	-3.9 *
		I/O	3.9205 E+07	3.9891 E+07	1.75	4.0170 E+07	2.46
	25	F/A	4.2499 E+08	4.2937 E+08	1.03	4.3217 E+08	1.69
		Tor	5.9260 E+07	5.9453 E+07	0.33	5.7282 E+07	-3.3 *
		I/O	3.9205 E+07	3.9927 E+07	1.84	4.1563 E+07	6.01
14	15	F/A	3.9848 E+08	3.9906 E+08	0.15	4.0092 E+08	0.61
		Tor	1.1340 E+07	1.1341 E+08	0.00	1.1370 E+08	0.26
		I/O	4.7571 E+07	4.7937 E+07	0.77	4.8617 E+07	2.20
	35	F/A	3.9848 E+08	4.0766 E+08	2.30	4.1039 E+08	2.99
		Tor	1.1340 E+07	1.1412 E+08	0.63	1.1450 E+08	0.96
		I/O	4.7571 E+07	5.2009 E+07	9.33	5.2587 E+07	10.55
25	15	F/A	2.9416 E+08	2.9634 E+08	0.74	2.9700 E+08	0.97
		Tor	5.3362 E+07	5.3417 E+07	0.10	5.3699 E+07	0.63
		I/O	2.3340 E+07	2.3675 E+07	1.43	2.3959 E+07	2.65
	35	F/A	2.9416 E+08	3.0829 E+08	4.80	3.0068 E+08	2.22
		Tor	5.3362 E+07	5.3521 E+07	0.30	5.3561 E+07	0.37
		I/O	2.3340 E+07	2.5826 E+07	10.65	2.5413 E+07	8.88

* We consider the negative values are due to errors in FEA and round off errors. The torsional stiffness should be slightly improved when adding bulkheads. Since the improvement is very small, the increase percent might be close to zero but positive.

In the table, L1 is the distance between the bulkheads and the ends of rocker (see Figure 4.8). Here L1 takes the same value for both ends of the rocker. K is the stiffness without bulkheads. K_b is the stiffness with bulkheads in outboard or inboard rocker cells. Design No. 9, 14, 25 are the design numbers used in our database.

Table 4.3 Comparison between the Stiffness Improvements due to Putting Bulkheads at the Defined Best Positions and the Largest Stiffness Improvement ($K_{I/O}$)

Design No.	Stiffness improvement due to putting bulkheads at the defined best position		The largest stiffness improvement		100% × K_b(best)/ K_b(largest)
	K_b(best)	increase percent (%)	K_b(largest)	increase percent (%)	
9	4.5250 E+07	15.42	4.5560 E+07	16.21	95.13
14	6.1861 E+07	30.04	6.2156 E+07	30.66	97.98
25	3.2322 E+07	38.48	3.3006 E+07	41.41	92.92
27	3.2228 E+07	25.05	3.2628 E+07	26.60	94.17
33	2.8397 E+07	32.29	2.8619 E+07	33.30	96.97
34	2.9734 E+07	34.65	3.0045 E+07	36.07	96.06
42	3.6876 E+07	21.19	3.7205 E+07	22.27	95.15

Table 4.4 Effect of Bulkhead Thickness on the Stiffness (Design No. = 9, Distance between the Bulkhead and Rocker End L1= 15, 25mm)

	Bulkhead thickness (mm)	Forward/Afterward		Torsion		Inboard/Outboard	
		K_b	increase percent (%)	K_b	increase percent (%)	K_b	increase percent (%)
L1 = 15	0.8	4.277 E+08	0.64	5.947 E+07	0.35	3.984 E+07	1.62
	1.0	4.278 E+08	0.66	5.947 E+07	0.35	3.987 E+07	1.69
	1.2	4.280 E+08	0.71	5.948 E+07	0.37	3.989 E+07	1.74
	1.4	4.280 E+08	0.71	5.948 E+07	0.37	3.991 E+07	1.80
	1.6	4.282 E+08	0.76	5.948 E+07	0.37	3.993 E+07	1.85
	1.8	4.283 E+08	0.78	5.948 E+07	0.37	3.995 E+07	1.90
L1 = 25	0.8	4.288 E+08	0.90	5.944 E+07	0.30	3.981 E+07	1.54
	1.0	4.291 E+08	0.97	5.945 E+07	0.32	3.987 E+07	1.69
	1.2	4.294 E+08	1.04	5.945 E+07	0.32	3.993 E+07	1.85
	1.4	4.296 E+08	1.08	5.946 E+07	0.34	3.997 E+07	1.95
	1.6	4.298 E+08	1.13	5.946 E+07	0.34	4.001 E+07	2.05
	1.8	4.300 E+08	1.18	5.947 E+07	0.35	4.005 E+07	2.15

Table 4.5 Increase Percent of Stiffness of Joints with Bulkheads at the Defined Best Positions for Different Designs

Design No.	Increase percent of $K_{F/A}$ (%)	Increase percent of K_{Tor} (%)	Increase percent of $K_{I/O}$ (%)
25	12.09	1.32	38.48
30	11.47	1.08	22.98
34	15.34	1.52	34.65
42	12.50	0.56	21.19
48	12.98	0.97	44.69
55	18.21	0.70	34.19
65	10.02	1.19	20.20
71	11.30	0.69	16.54
72	9.80	1.33	27.01
85	17.42	1.41	30.18
91	22.21	1.07	34.17
106	9.42	0.20	26.50
107	8.69	1.34	20.79
108	14.82	1.89	40.24
114	7.58	0.83	37.92
116	15.94	0.53	20.04
117	7.09	0.75	34.01
130	15.47	0.51	41.99
135	13.16	1.69	36.15
136	8.55	0.74	30.45
147	12.62	1.01	31.02
151	16.50	1.35	33.09
154	16.56	0.69	30.92
162	13.19	1.62	31.70

Table 4.6 Important Design Variables for I/O Stiffness

Rank	Design variables
1	*outboar_cell_width*
2	*rocker_width*
3	*A5*
4	*thickness of backrock*
5	*A2*
6	*thickness of pillar_reinf*

Table 4.7 Important Design Variables for F/A Stiffness

Rank	Design variables
1	*A5*
2	*pillar_inner_length*
3	*outboar_cell_width*
4	*rocker_width*
5	*pillar_base*
6	*thickness of backrock*
7	*aft_inner_hor_blending_rad*
8	*thickness of frontrock*
9	*door_edge_width*
10	*fwd_inner_hor_blending_rad*
11	*low_door_ht_minus_clearance*
12	*outer_pillar_width*

Table 4.8 R^2 of the Translator A for the B-pillar to Rocker Joint with Bulkheads

		Fitting (48 designs)	Testing (18 designs)
R^2	I/O Stiffness (with bulkheads)	0.9422	0.9371
	F/A Stiffness (with bulkheads)	0.9510	0.8580

Table 4.9 Standard Deviation of the Ratio of Stiffness Predictions over FEA Results for the B-pillar to Rocker Joint with Bulkheads

		Fitting (48 designs)	Testing (18 designs)
Standard deviation of the ration (prediction over FEA results)	I/O Stiffness (with bulkheads)	0.0914	0.1071
	F/A Stiffness (with bulkheads)	0.0459	0.1077

Table 5.1 Design Variables of the B-pillar to Rocker Joint

Sequential No.	Name of Design Variable	Type of Design Variable
1	*length_of_flange*	# Fixed by the designers
2	*spot_weld_spacing*	# Fixed by the designers
3	*spot_weld_placement*	# Fixed by the designers
4	*pillar_base*	Independent
5	*pillar_angle*	# Fixed by designers
6	*pillar_io_angle*	# Fixed by designers
7	*pillar_height*	# Dependent
8	*pillar_location*	# Fixed by designers
9	*outer_pillar_width*	Independent
10	*inner_pillar_width*	## Independent
11	*pillar_outer_length*	## Independent
12	*pillar_inner_length*	## Independent
13	*fwd_inner_ver_blending_rad*	## Independent
14	*fwd_inner_hor_blending_rad*	## Independent
15	*fwd_outer_ver_blending_rad*	# Dependent
16	*fwd_outer_hor_blending_rad*	# Dependent
17	*aft_inner_ver_blending_rad*	## Independent
18	*aft_inner_hor_blending_rad*	## Independent
19	*aft_outer_ver_blending_rad*	# Dependent
20	*aft_outer_hor_blending_rad*	# Dependent
21	*inner_pillar_base_width*	## Independent
22	*rocker_length*	# Fixed by program
23	*pillar_reinforcement_depth*	# Dependent
24	*pillar_reinf_base_width*	## Independent
25	*pillar_reinf_expansion*	## Independent
26	*A1*	## Independent
27	*A2*	Independent
28	*A3*	## Independent
29	*A5*	## Independent
30	*A7*	## Independent
31	*A8*	## Independent
32	*rocker_height*	Independent
33	*inner_flange_distance*	Independent
34	*inner_rocker_height*	## Independent
35	*rocker_width*	Independent
36	*outboar_cell_width*	## Independent
37	*door_edge_height*	## Independent
38	*door_edge_width*	## Independent
39	*low_door_ht_minus_clearance*	## Independent
40	*top_pillar_hole*	## Independent
41	*bottom_pillar_hole*	## Independent
42	*fwd_pillar_hole*	## Independent
43	*aft_pillar_hole*	# Fixed by designers

44	*thickness of frontrock*	Independent
45	*thickness of pillar_reinf*	Independent
46	*thickness of pillarback*	Independent
47	*thickness of backrock*	Independent
48	*thickness of centerplate*	Independent

Design variables that are not independent design variables, and are excluded from the optimization problem.

Design variables that are not used in the NN translators but used in the RSP translators.

Table 5.2 Ranges of Design Variables of the B-pillar to Rocker Joint

Sequential No.	Name of Design Variable	Lower Bound	Upper Bound
1	*length_of_flange*	19.00	19.00
2	*spot_weld_spacing*	47.50	47.50
3	*spot_weld_placement*	9.50	9.50
4	*pillar_base*	157.00	215.00
5	*pillar_angle*	90.00	90.00
6	*pillar_io_angle*	90.00	90.00
7	*pillar_height*	210.00	250.00
8	*pillar_location*	150.00	150.00
9	*outer_pillar_width*	50.00	83.00
10	*inner_pillar_width*	6.00	25.00
11	*pillar_outer_length*	77.00	110.00
12	*pillar_inner_length*	122.00	160.00
13	*fwd_inner_ver_blending_rad*	120.00	155.00
14	*fwd_inner_hor_blending_rad*	80.00	125.00
15	*fwd_outer_ver_blending_rad*	120.00	155.00
16	*fwd_outer_hor_blending_rad*	80.00	125.00
17	*aft_inner_ver_blending_rad*	95.00	133.00
18	*aft_inner_hor_blending_rad*	100.00	135.00
19	*aft_outer_ver_blending_rad*	95.00	133.00
20	*aft_outer_hor_blending_rad*	100.00	135.00
21	*inner_pillar_base_width*	2.00	15.00
22	*rocker_length*	485.00	485.00
23	*pillar_reinforcement_depth*	10.00	100.00
24	*pillar_reinf_base_width*	20.00	60.00
25	*pillar_reinf_expansion*	2.00	15.00
26	*A1*	83.00	90.00
27	*A2*	65.00	78.00
28	*A3*	10.00	36.00

29	*A5*	75.00	87.00
30	*A7*	70.00	86.00
31	*A8*	80.00	90.00
32	*rocker_height*	110.00	120.00
33	*inner_flange_distance*	18.00	45.00
34	*inner_rocker_height*	90.00	110.00
35	*rocker_width*	115.00	147.00
36	*outboar_cell_width*	65.00	95.00
37	*door_edge_height*	6.00	38.00
38	*door_edge_width*	7.00	19.00
39	*low_door_ht_minus_clearance*	60.00	75.00
40	*top_pillar_hole*	22.00	80.00
41	*bottom_pillar_hole*	28.00	50.00
42	*fwd_pillar_hole*	17.00	30.00
43	*aft_pillar_hole*	15.00	15.00
44	*thickness of frontrock*	0.71	1.27
45	*thickness of pillar_reinf*	0.71	1.52
46	*thickness of pillarback*	0.89	1.27
47	*thickness of backrock*	1.27	1.98
48	*thickness of centerplate*	0.71	1.27

Table 5.3 Max. $K_{I/O}$ vs. Mass

Mass	Max. $K_{I/O}$ (without $K_{F/A}$, K_{Tor} requirements)
4.0	7.44072
4.5	8.49707
5.0	9.36228
5.5	10.2602
6.0	10.8954
6.5	11.1007
7.0	11.2224

Table 5.4 Max. $K_{F/A}$ vs. Mass

Mass	Max. $K_{F/A}$ (without $K_{I/O}$, K_{Tor} requirements)
4.0	4.6480
4.5	5.25192
5.0	5.85584
5.5	6.22053
6.0	6.35447
6.5	6.40857
7.0	6.41748
7.5	6.41748

Table 5.5 Max. K_{Tor} vs. Mass

Mass	Max. K_{Tor} (without $K_{I/O}$, $K_{F/A}$ requirements)
4.0	15.1234
4.5	17.8514
5.0	19.8691
5.5	21.8867
6.0	22.3810
6.5	22.3810
7.0	22.3810

Table 5.6a Comparison of Optimum Results (Polynomial Translator) Using SLP When Starting from Different Initial Points
($K_{I/O} > 4.3899E7, K_{F/A} > 5.2297E8, K_{Tor} > 7.9788E7$)

Seq. No	No. of Function Evaluation	Object Function
1	527	4.54870
2	527	4.54962
3	527	4.54821
4	492	4.54730
5	492	4.54704
6	492	4.54812
7	527	4.55183
8	528	4.55183

Table 5.6b Comparison of Optimum Results (Neural Network Translator) Using SLP When Starting from Different Initial Points
($K_{I/O} > 4.3899E7, K_{F/A} > 5.2297E8, K_{Tor} > 7.9788E7$)

Seq. No	No. of Function Evalation	Objective Function
1	740	4.97923
2	740	4.97973
3	705	4.98170
4	635	4.98150
5	600	4.97854
6	706	4.97915
7	705	4.98036
8	673	4.97942

Table 5.7a Checking Stiffness and Mass of Optimum Design
Using FEA (Polynomial Translator)
(18 Designs with Stiffness Target Combinations Randomly Selected)

No	Stiffness Targets			Optimum Designs				FEA Results			
	I/O ($\times 10^7$)	F/A ($\times 10^8$)	Tor ($\times 10^7$)	I/O ($\times 10^7$)	F/A ($\times 10^8$)	Tor ($\times 10^7$)	Mass	I/O ($\times 10^7$)	F/A ($\times 10^8$)	Tor ($\times 10^7$)	Mass
1	1.00	2.00	7.98	1.002	2.179	7.980	3.4998	1.023	2.010	6.348	3.7077
2	5.00	2.00	7.98	5.000	2.583	7.980	3.7344	4.258	2.632	9.094	3.8616
3	1.00	4.00	7.98	1.524	4.000	7.980	3.7296	1.263	3.462	7.147	3.8842
4	1.00	6.00	7.98	2.523	6.000	14.10	5.1213	3.274	6.262	13.66	5.2026
5	5.00	6.00	7.98	5.000	6.000	14.90	5.2164	6.365	6.902	17.74	5.3101
6	4.39	5.23	7.98	4.390	5.230	12.23	4.5558	4.384	5.422	14.29	4.6649
7	7.00	6.00	7.98	7.001	6.000	17.40	5.4655	8.921	6.470	20.93	5.5809
8	8.00	6.00	7.98	7.999	6.000	18.43	5.6318	10.37	6.540	22.30	5.8477
9	9.00	5.50	7.98	9.001	5.500	19.19	5.3538	13.46	6.466	22.14	5.5629
10	7.00	5.00	7.98	7.000	5.000	15.55	4.7136	8.173	5.084	18.38	4.8941
11	7.00	5.50	7.98	7.001	5.500	16.54	5.0583	8.535	5.764	19.74	5.1688
12	8.00	5.00	7.98	8.000	5.000	16.88	4.8547	11.70	5.725	19.19	5.0328
13	9.00	5.00	7.98	9.000	5.000	18.43	5.1157	11.78	5.648	21.92	5.2815
14	6.00	4.50	7.98	6.000	4.500	13.38	4.2500	6.225	4.290	15.37	4.3051
15	3.00	3.00	7.98	3.000	3.000	7.980	3.6211	2.308	2.681	8.409	3.7878
16	1.00	5.50	7.98	2.403	5.500	12.73	4.7085	2.853	5.541	12.24	4.8070
17	2.00	6.00	7.98	2.523	6.000	14.10	5.1213	3.306	6.311	13.76	5.2027
18	9.00	2.00	7.98	9.000	3.568	7.980	4.7821	6.706	3.147	8.253	5.0682

Table 5.7b Checking Stiffness and Mass of Optimum Design Using FEA (Neural Network Translator) (12 Designs with Stiffness Target Combinations Randomly Selected)

No	Stiffness Targets			Optimum Designs				FEA Results			
	I/O ($\times 10^7$)	F/A ($\times 10^8$)	Tor ($\times 10^7$)	I/O ($\times 10^7$)	F/A ($\times 10^8$)	Tor ($\times 10^7$)	Mass	I/O ($\times 10^7$)	F/A ($\times 10^8$)	Tor ($\times 10^7$)	Mass
1	1.00	2.00	7.98	1.000	2.460	7.980	3.9971	1.080	2.268	7.075	3.7650
2	5.00	6.00	7.98	5.778	6.000	14.20	5.6736	7.739	7.507	18.07	5.7414
3	4.39	5.23	7.98	4.546	5.230	13.26	4.9847	5.029	6.148	15.73	5.0135
4	7.00	6.00	7.98	7.104	6.000	15.37	5.7511	9.243	6.567	21.01	5.8856
5	1.00	4.00	7.98	1.191	4.000	10.13	4.1143	1.266	3.815	8.119	3.9962
6	7.00	5.00	7.98	7.000	5.194	14.59	5.2883	8.849	5.383	18.61	5.4774
7	3.00	3.00	7.98	3.000	3.503	7.980	4.3061	3.119	3.806	9.210	4.2005
8	2.00	6.00	7.98	4.309	6.000	13.78	5.653	3.806	6.674	14.53	5.6647
9	5.00	2.00	7.98	5.000	3.114	8.484	4.0441	4.396	3.030	1.118	3.9961
10	8.00	5.00	7.98	8.000	5.384	15.59	5.5944	15.31	6.844	20.06	5.7181
11	6.00	4.50	7.98	6.000	4.500	11.58	4.6253	7.765	5.054	13.70	4.7584
12	1.00	5.50	7.98	3.804	5.500	13.62	5.1920	3.054	3.845	9.197	4.2382

Table 5.7c Checking Stiffness and Mass of Optimum Design Using FEA (Polynomial Translator) (12 Designs with Stiffness Target Combinations Selected within the Zones Defined in Table 5.9)

No	Stiffness Targets			Optimum Designs				FEA Results			
	I/O ($\times 10^7$)	F/A ($\times 10^8$)	Tor ($\times 10^7$)	I/O ($\times 10^7$)	F/A ($\times 10^8$)	Tor ($\times 10^7$)	Mass	I/O ($\times 10^7$)	F/A ($\times 10^8$)	Tor ($\times 10^7$)	Mass
1	1.25	2.50	5.00	1.418	2.500	5.000	3.4099	1.099	2.349	4.196	3.6599
2	1.75	3.00	6.50	1.750	3.000	6.500	3.5445	1.542	2.852	6.076	3.7395
3	2.50	3.50	8.00	2.500	3.500	8.000	3.6865	2.041	3.075	9.091	3.8463
4	3.30	3.50	8.50	3.300	3.500	8.500	3.7138	2.572	3.292	9.646	3.8601
5	3.60	4.50	10.0	3.600	4.500	10.000	3.9397	3.140	4.336	11.245	4.0734
6	4.30	4.00	9.00	4.300	4.000	9.000	3.8364	4.445	4.234	10.483	3.9484
7	4.60	5.00	10.0	4.600	5.000	12.168	4.3960	5.118	5.408	14.206	4.5069
8	5.30	3.50	9.00	5.300	3.500	9.000	3.8585	5.130	3.466	9.292	3.9485
9	5.60	4.00	10.0	5.600	4.000	10.000	3.9898	5.255	3.778	11.264	4.0638
10	6.30	4.00	10.0	6.300	4.000	10.000	4.0835	7.258	4.315	10.337	4.2581
11	6.60	4.50	11.0	6.600	4.500	14.260	4.3461	8.570	4.936	15.774	4.4874
12	7.50	4.50	11.0	7.500	4.500	15.379	4.4949	9.915	4.962	16.824	4.6146

Table 5.7d Checking Stiffness and Mass of Optimum Design Using FEA (Neural Network Translator) (12 Designs with Stiffness Target Combinations Selected within the Zones Defined in Table 5.9)

No	Stiffness Targets			Optimum Designs				FEA Results			
	I/O ($\times 10^7$)	F/A ($\times 10^8$)	Tor ($\times 10^7$)	I/O ($\times 10^7$)	F/A ($\times 10^8$)	Tor ($\times 10^7$)	Mass	I/O ($\times 10^7$)	F/A ($\times 10^8$)	Tor ($\times 10^7$)	Mass
1	1.25	2.50	5.00	1.250	3.059	5.769	3.9723	1.145	2.949	5.032	3.7484
2	1.75	3.00	6.50	1.750	3.096	6.500	3.9820	1.430	2.949	6.219	3.7916
3	2.50	3.50	8.00	2.500	3.558	8.000	4.1605	2.331	3.866	8.305	4.058
4	3.30	3.50	8.50	3.300	3.500	9.364	4.0996	2.916	3.739	10.307	3.9265
5	3.60	4.50	10.0	3.717	4.500	11.757	4.4396	3.750	5.072	12.948	4.4181
6	4.30	4.00	9.00	4.300	4.000	9.535	4.1935	5.593	5.232	10.708	4.1973
7	4.60	5.00	10.0	4.731	5.000	13.148	4.8231	5.862	6.061	15.749	4.8545
8	5.30	3.50	9.00	5.309	3.500	9.333	4.1034	4.873	3.618	10.393	3.9985
9	5.60	4.00	10.0	5.600	4.148	9.999	4.3655	6.674	4.592	11.241	4.4696
10	6.30	4.00	10.0	6.300	4.252	10.887	4.5144	7.652	4.608	12.111	4.7210
11	6.60	4.50	11.0	6.600	4.738	12.987	4.8481	9.399	5.379	15.669	5.0877
12	7.50	4.50	11.0	7.500	4.943	14.762	5.2455	11.533	5.457	18.124	5.3899

Table 5.8a Comparison of Optimum Design and FEA Results for Car 1

No	Name of Design Variables	Status	Car 1		
			initial	Opt (poly)	Opt (NN)
1	*Length_of_flange*	# Fixed by user	20.00	19.00	19.00
2	*Spot_weld_spacing*	# Fixed by user	60.00	47.50	47.50
3	*Spot_weld_placement*	# Fixed by user	10.00	9.50	9.50
4	*Pillar_base*	Independent	177.00	185.15	185.00
5	*Pillar_angle*	# Fixed by user	90.00	90.00	90.00
6	*Pillar_io_angle*	# Fixed by user	90.00	90.00	90.00
7	*Pillar_height*	## Dependent	208.00	218.45	218.37
8	*Pillar_location*	# Fixed by user	163.00	150.00	150.00

9	*Outer_pillar_width*	Independent	55.00	82.99	83.00
10	*Inner_pillar_width*	Independent	23.00	6.00	23.00
11	*Pillar_outer_length*	Independent	110.00	109.99	110.00
12	*Pillar_inner_length*	Independent	154.00	159.84	159.99
13	*Fwd_inner_ver_blending_rad*	Independent	115.00	120.00	134.99
14	*Fwd_inner_hor_blending_rad*	Independent	85.00	80.00	80.00
15	*Fwd_outer_ver_blending_rad*	## Dependent	115.00	120.00	134.99
16	*Fwd_inner_hor_blending_rad*	## Dependent	85.00	80.00	80.00
17	*Aft_inner_ver_blending_rad*	Independent	100.00	132.99	133.00
18	*Aft_inner_hor_blending_rad*	Independent	100.00	135.00	100.00
19	*Aft_outer_ver_blending_rad*	## Dependent	100.00	132.99	133.00
20	*Aft_outer_hor_blending_rad*	## Dependent	100.00	135.00	100.00
21	*Inner_pillar_base_width*	Independent	2.00	15.00	2.32
22	*Rocker_length*	## Fixed by program	480.00	485.00	485.00
23	*Pillar_reinforcement_depth*	## Dependent	45.00	38.16	46.82
24	*Pillar_reinf_base_width*	Independent	16.00	20.00	20.00
25	*Pillar_reinf_expansion*	Independent	2.00	2.00	2.00
26	*A1*	Independent	83.00	83.00	83.00
27	*A2*	Independent	79.00	77.94	77.99
28	*A3*	Independent	30.00	10.00	10.00
29	*A5*	Independent	89.00	75.00	75.00
30	*A7*	Independent	89.00	85.95	85.95
31	*A8*	# Fixed by user	90.00	80.03	80.01
32	*Rocker_height*	Independent	115.00	110.01	110.01
33	*Inner_flange_distance*	Independent	41.16	37.57	36.94
34	*Inner_rocker_height*	Independent	110.00	106.16	106.19
35	*Rocker_width*	Independent	110.00	120.17	119.75
36	*Outboar_cell_width*	Independent	68.00	67.83	68.03
37	*Door_edge_height*	Independent	34.00	35.66	27.07
38	*Door_edge_width*	Independent	5.00	7.00	7.00
39	*Low_door_ht_minus_clearance*	Independent	68.00	60.05	60.00
40	*Top_pillar_hole*	Independent	35.00	80.00	80.00
41	*Bottom_pillar_hole*	Independent	34.00	49.99	50.00
42	*Fwd_pillar_hole*	Independent	20.00	30.00	30.00
43	*Aft_pillar_hole*	## Fixed by user	18.00	15.00	15.00
44	*Thickness of frontrock*	Independent	1.27	1.14	1.27
45	*Thickness of pillar_reinf*	Independent	1.27	0.71	0.71
46	*Thickness of pillarback*	Independent	1.27	1.27	1.27
47	*Thickness of backrock*	Independent	1.27	1.27	1.39
48	*Thickness of centerplate*	Independent	1.27	0.71	0.71

Table 5.8b Comparison of Optimum Design and FEA Results for Car 2

No	Name of Design Variables	Status	Car 2		
			initial	Opt (poly)	Opt (NN)
1	*Length_of_flange*	# Fixed by user	17.00	19.00	19.00
2	*Spot_weld_spacing*	# Fixed by user	45.00	47.50	47.50
3	*Spot_weld_placement*	# Fixed by user	10.00	9.50	9.50

4	*Pillar_base*	Independent	185.00	157.15	160.24
5	*Pillar_angle*	# Fixed by user	90.00	90.00	90.00
6	*Pillar_io_angle*	# Fixed by user	90.00	90.00	90.00
7	*Pillar_height*	## Dependent	220.00	218.72	217.62
8	*Pillar_location*	# Fixed by user	143.00	150.00	150.00
9	*Outer_pillar_width*	Independent	70.00	79.34	50.00
10	*Inner_pillar_width*	Independent	10.00	7.54	24.99
11	*Pillar_outer_length*	Independent	90.00	109.93	109.96
12	*Pillar_inner_length*	Independent	122.00	122.07	159.89
13	*Fwd_inner_ver_blending_rad*	Independent	130.00	120.01	155.00
14	*Fwd_inner_hor_blending_rad*	Independent	125.00	125.00	80.03
15	*Fwd_outer_ver_blending_rad*	## Dependent	130.00	120.01	155.00
16	*Fwd_inner_hor_blending_rad*	## Dependent	125.00	125.00	80.03
17	*Aft_inner_ver_blending_rad*	Independent	105.00	113.06	133.00
18	*Aft_inner_hor_blending_rad*	Independent	105.00	135.00	100.00
19	*Aft_outer_ver_blending_rad*	## Dependent	117.00	113.06	133.00
20	*Aft_outer_hor_blending_rad*	## Dependent	115.00	135.00	100.00
21	*Inner_pillar_base_width*	Independent	15.00	14.99	14.99
22	*Rocker_length*	## Fixed by program	490.00	485.00	485.00
23	*Pillar_reinforcement_depth*	## Dependent	70.00	43.17	47.88
24	*Pillar_reinf_base_width*	Independent	25.00	20.00	25.00
25	*Pillar_reinf_expansion*	Independent	10.00	2.00	10.00
26	*A1*	Independent	80.00	83.00	83.00
27	*A2*	Independent	75.00	77.94	78.00
28	*A3*	Independent	15.00	10.00	10.00
29	*A5*	Independent	75.00	75.00	80.12
30	*A7*	Independent	70.00	81.21	85.98
31	*A8*	# Fixed by user	80.00	80.04	80.00
32	*Rocker_height*	Independent	117.00	110.05	110.01
33	*Inner_flange_distance*	Independent	25.00	40.28	29.93
34	*Inner_rocker_height*	Independent	95.00	102.59	105.81
35	*Rocker_width*	Independent	140.00	120.10	119.64
36	*Outboar_cell_width*	Independent	65.00	65.05	74.93
37	*Door_edge_height*	Independent	6.00	30.73	26.65
38	*Door_edge_width*	Independent	19.00	7.00	7.00
39	*Low_door_ht_minus_clearance*	Independent	95.00	60.05	60.01
40	*Top_pillar_hole*	Independent	23.00	22.00	79.94
41	*Bottom_pillar_hole*	Independent	34.00	49.96	47.60
42	*Fwd_pillar_hole*	Independent	15.00	30.00	29.97
43	*Aft_pillar_hole*	## Fixed by user	20.00	15.00	15.00
44	*Thickness of frontrock*	Independent	0.89	0.71	0.71
45	*Thickness of pillar_reinf*	Independent	0.89	0.71	0.71
46	*Thickness of pillarback*	Independent	0.89	0.89	0.89
47	*Thickness of backrock*	Independent	1.78	1.27	1.27
48	*Thickness of centerplate*	Independent	0.89	0.71	0.71

Table 5.8c Comparison of FEA Results and Results from Translator B for B-pillar to Rocker Joint of Car 1 and Car 2

Cars/ Stiff. Requirement	Stiffness / Mass	Polynomial Translators		Neural Network Translators	
		FEA	Translator (err)	FEA	Translator (err)
Car 1 I/O>4.76E7 F/A >5.684E8 Tor >7.649E7	I/O	5.4527E7	4.7600E7 (-12.7%)	4.5713E7	4.7602E7 (4.1%)
	F/A	6.2650E8	5.6840E8 (-9.3%)	6.6915E8	5.6840E8 (-15.1%)
	Torsion	1.6285E8	1.3799E8 (-15.3%)	1.7093E8	1.3924E8 (-18.5%)
	Mass	5.0450	4.9475 (-1.9%)	5.4505	5.3570 (-1.7%)
Car 2 I/O>2.567E7 F/A>2.527E8 Tor > 6.521E7)	I/O	1.9929E7	2.5674E7 (28.8%)	4.0275E7	3.6564E7 (-9.2%)
	F/A	2.4668E8	2.5270E8 (2.4%)	3.6429E8	3.2990E8 (-9.4%)
	Torsion	5.7217E7	6.5211E7 (14.0%)	8.6064E7	6.5210E7 (-24.2%)
	Mass	3.7179	3.5204 (-5.3%)	3.9322	3.9231 (-0.2%)

Table 5.8d: Comparison of Mass of the Initial and Optimum Designs for Car 1 and Car 2

Cars	Initial Design (Kg)	Optimum Design (Kg) and Percentage Improvement	
		RSP	NN
Car 1	5.9312	5.0450 (14.9%)	5.4505 (8.1%)
Car 2	5.1268	3.7179 (27.5%)	3.9322 (23.3%)

Table 5.9 Zones of Database (According to the Combination of Stiffness)

Zone No.	Range of $K_{I/O}$ ($\times 10^7$)	Range of $K_{F/A}$ ($\times 10^8$)	Range of K_{Tor} ($\times 10^7$)
1	1.0~1.5	1.8~4.0	2.5~8.0
2	1.5~2.0	2.0~4.5	3.0~10.0
3	2.0~3.0	2.0~5.5	3.5~12.5
4	3.0~4.0	2.0~5.5	4.0~13.5
5	4.0~5.0	2.5~5.5	4.0~14.5
6	5.0~6.0	2.5~5.0	5.0~13.0
7	6.0~7.0	3.5~5.0	7.5~13.0
8	7.0~8.0	3.5~5.0	9.0~13.0

Table 5.10a Correlation Coefficients of Stiffness Using Polynomial Translator

Designs		Designs (old 18) with stiffness targets combination not strictly inside the defined zones (corresponding to figure 5.1-5.3)	Designs (new 12) with stiffness targets combination strictly inside the defined zones (corresponding to figure 5.4 – 5.6)
Polynomial translator	$K_{I/O}$	0.9254	0.9733
	$K_{F/A}$	0.9771	0.9676
	K_{Tor}	0.9794	0.9872

Table 5.10b Correlation Coefficients of Stiffness Using Neural Network Translator

Designs		Designs (old 12) with stiffness targets combination not strictly inside the defined zones (corresponding to figure 5.7-5.9)	Designs (new 12) with stiffness targets combination strictly inside the defined zones (corresponding to figure 5.10 – 5.12)
Neural Network translator	$K_{I/O}$	0.9201	0.9642
	$K_{F/A}$	0.8838	0.9600
	K_{Tor}	0.8401	0.9975

Table 5.11. Min. Mass vs. Lower Limit of Thickness of Outer Rocker Cell (frontrock)
(Range of Thickness of Outer Rocker Cell: 0.71 ~ 1.27)

Lower Limit of Thickness of Outer Rocker Cell	0.80	0.90	1.00	1.05	1.10	1.15	1.20
Min. Mass (Polynomial Translator)	4.5487	4.5506	4.5866	4.6332	4.6848	4.7414	4.7995
Min. Mass (Neural Network Translator)	4.9797	4.9797	4.9797	4.9797	4.9815	4.9810	5.0174

Table 5.12. Min. Mass vs. Upper Limit of Thickness of Pillar Back

(Range of Thickness of Pillar Back: 0.89 ~ 1.27)

Upper Limit of Thickness of Pillar Back	0.95	1.00	1.05	1.10	1.15	1.20
Min. Mass (Polynomial Translator)	4.6847	4.6623	4.6454	4.6191	4.6039	4.5800
Min. Mass (Neural Network Translator)	5.0272	5.0085	4.9996	4.9889	4.9836	4.9801

Note: with decrease of upper limit of thickness of pillar back, the thickness of outer rocker cell (frontrock) will increase.

Table 5.13. Min. Mass vs. Lower Limit of *pillar_base*

(Range of *pillar_base*: 157 ~ 215)

Lower Limit of *pillar_base*	157-185	190	195	200	205	210
Min. Mass (Polynomial Translator)	4.5487	4.5999	4.6546	4.7016	4.7533	4.7989
Min. Mass (Neural Network Translator)	4.9497	5.0417	5.1023	5.1605	5.2200	5.2926

Note: with increase of low limit of pillar base, pillar inner length will decrease, and thickness of frontrock will increase.

Table 5.14. Min. Mass vs. Upper Limit of *pillar_base*

(Range of *pillar_base*: 157 ~ 215)

Upper Limit of *pillar_base*	160	165	170	175	180	185-215
Min. Mass (Polynomial Translator)	4.7148	4.6774	4.6508	4.6115	4.5821	4.5487
Min. mass (Neural Network Translator)	5.1616	5.1217	5.0849	5.0519	5.0124	4.9797

Note: with decrease of upper limit of pillar base, thickness of frontrock will increase.

Table 5.15. Min. Mass vs. Upper Limit of *outer_pillar_width*

(Range of *outer_pillar_width*: 50 ~ 83)

Upper Limit of *outer_pillar_width*	55	60	65	70	75	80
Min. Mass (Polynomial Translator)	4.6479	4.6376	4.6149	4.5978	4.5815	4.5589
Min. Mass (Neural Network Translator)	5.2059	5.1544	5.1131	5.0742	5.0347	5.0004

Note: with decease of upper limit of outer pillar width, thickness of frontrock will increase.

Table 5.16. Min. Mass vs. Upper Limit of *pillar_inner_length*

(Range of *pillar_inner_length*: 122 ~ 160)

Upper Limit of *pillar_inner_length*	130	135	140	145	150	155
Min. Mass (Polynomial Translator)	4.8524	4.8026	4.7505	4.7015	4.6499	4.5963
Min. Mass (Neural Network Translator)	5.3811	5.2887	5.2198	5.1634	5.1035	5.0420

Note: with decrease of upper limit of pillar inner length, pillar base and thickness of frontrock will increase.

Table 5.17. Min. Mass vs. Lower Limit of *door_edge_width*

(Range of *door_edge_width*: 7 ~ 19)

Lower Limit of *door_edge_width*	8	10	12	14	16	18
Min. Mass (Polynomial Translator)	4.5583	4.5832	4.6078	4.6346	4.6652	4.7032
Min. Mass (Neural Network Translator)	4.9796	4.9837	4.9954	5.0072	5.0231	5.2343

Table 5.18. Min. Mass vs. Lower Limit of *rocker_width*

(Range of *rocker_width*: 115 ~ 147)

Lower Limit of *rocker_width*	125	130	135	140	145
Min. Mass (Polynomial Translator)	4.6050	4.6721	4.7534	4.8403	4.9287
Min. Mass (Neural Network Translator)	5.0077	5.0545	5.1019	5.1514	5.2022

Table 5.19. Min. Mass vs. Lower Limit of *outboard_cell_width*

(Range of *outboard_cell_width*: 65 ~ 95)

Lower Limit of *outboard_cell_width*	70	75	80	85	90
Min. Mass (Polynomial Translator)	4.5739	4.6241	4.6806	4.7628	4.8627
Min. Mass (Neural Network Translator)	5.0013	5.0252	5.0530	5.0847	5.1259

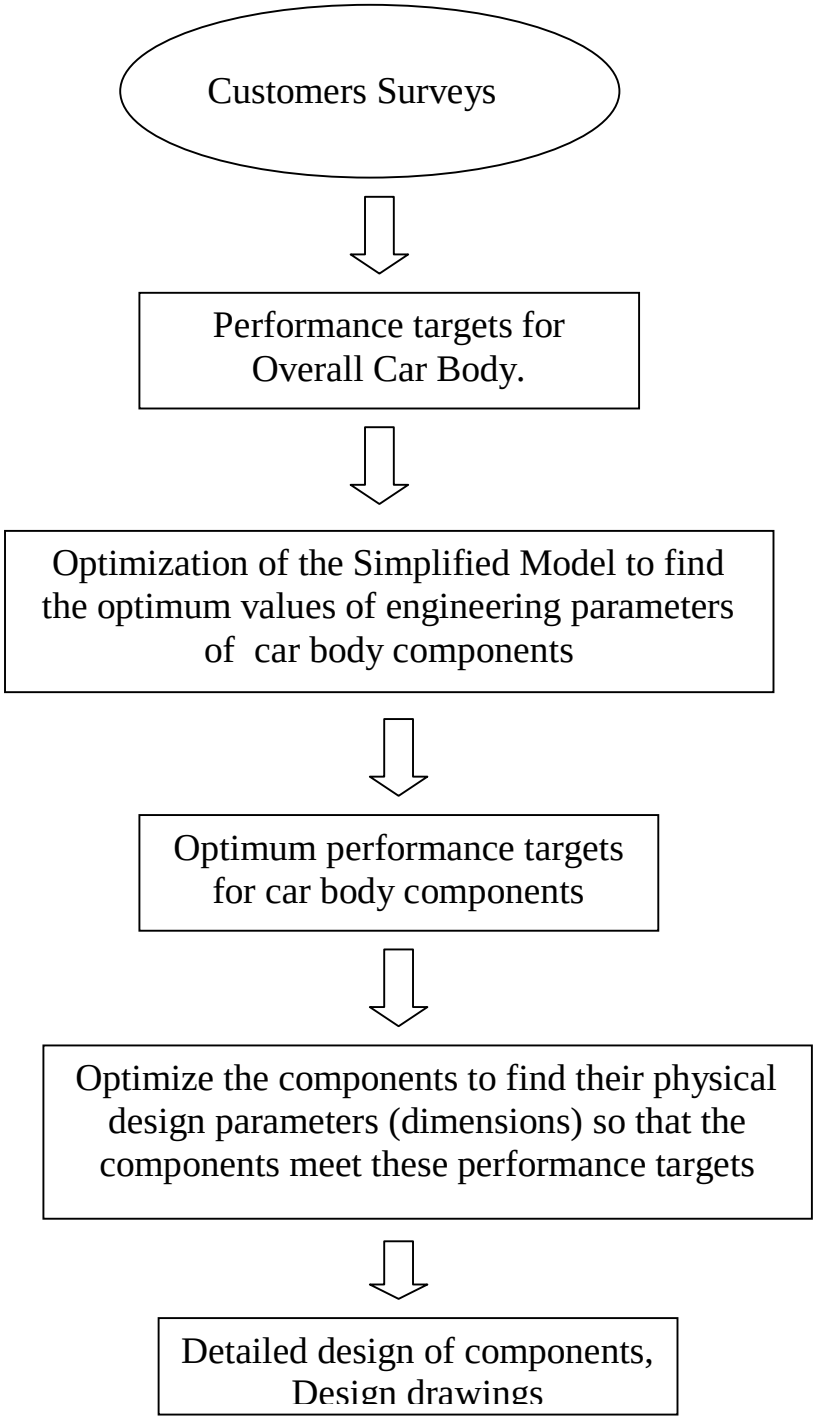

Figure 1.1 Design of Overall Car Body

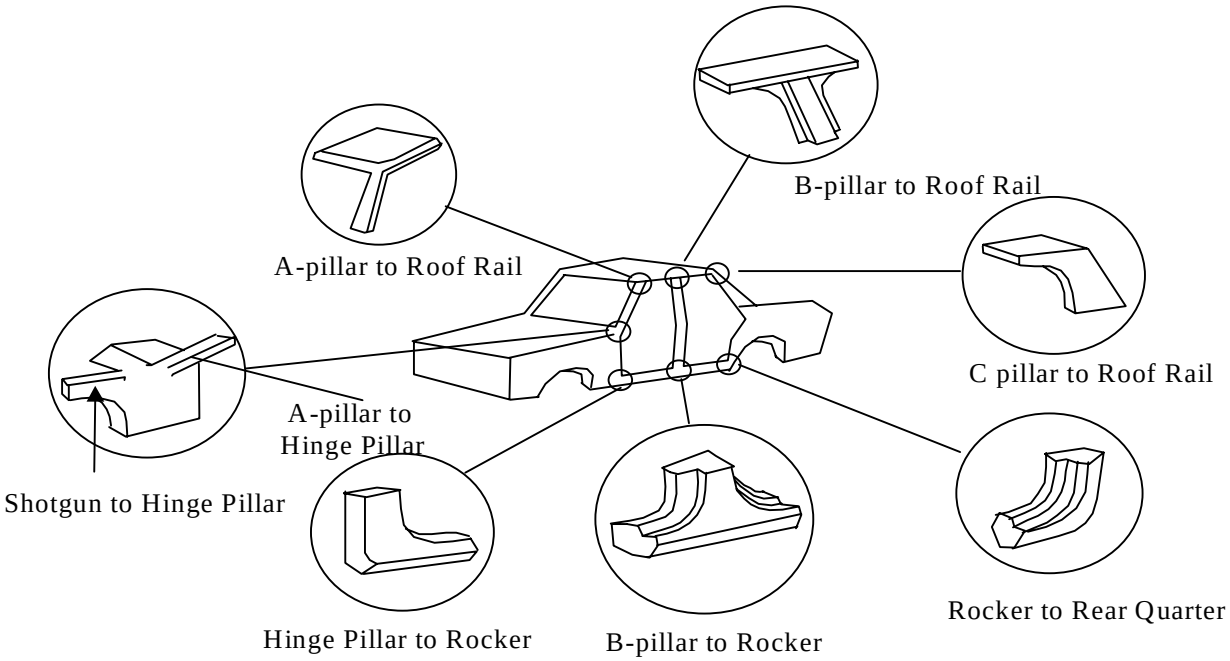

Figure 1.2 Car Body Structural Joints

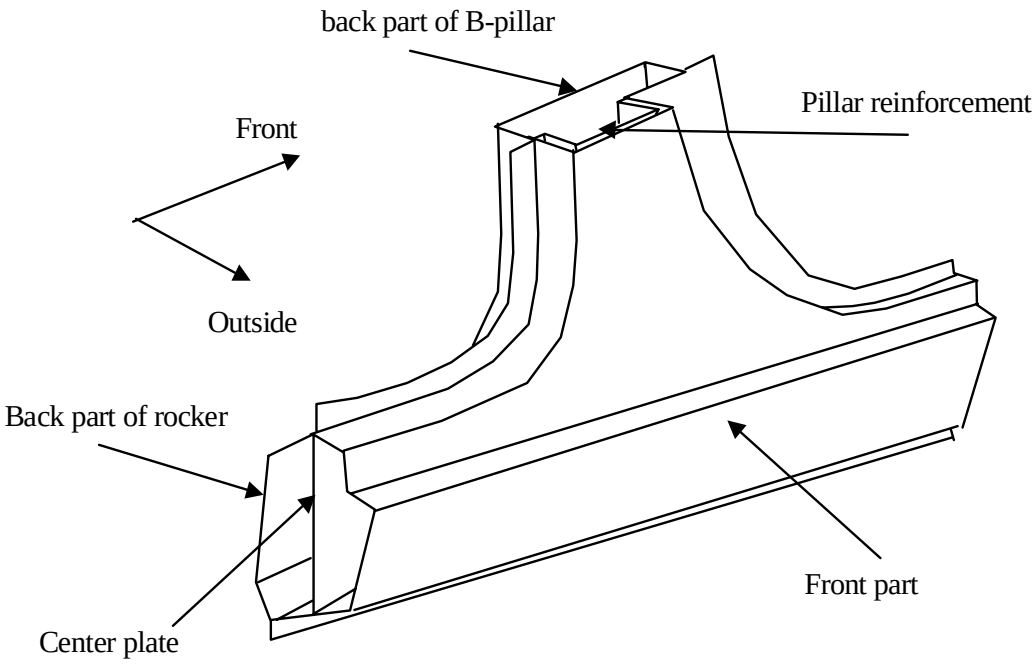

Figure 1.3 B-pillar to Rocker Joint

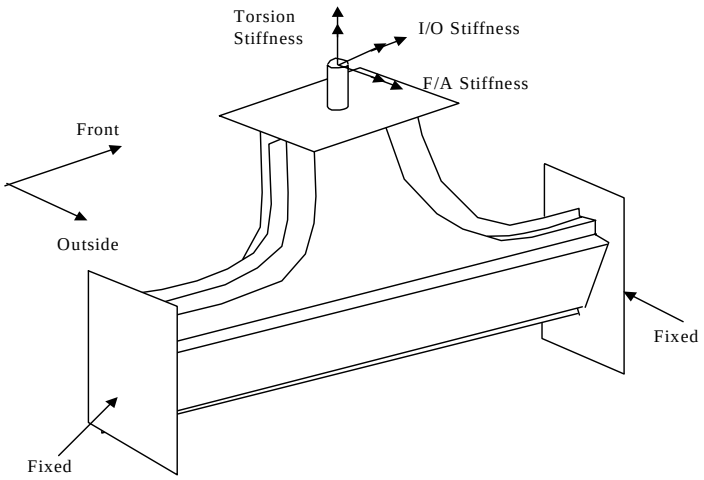

Figure 1.4 Definitions of the Stiffnesses for the B-pillar to Rocker Joint

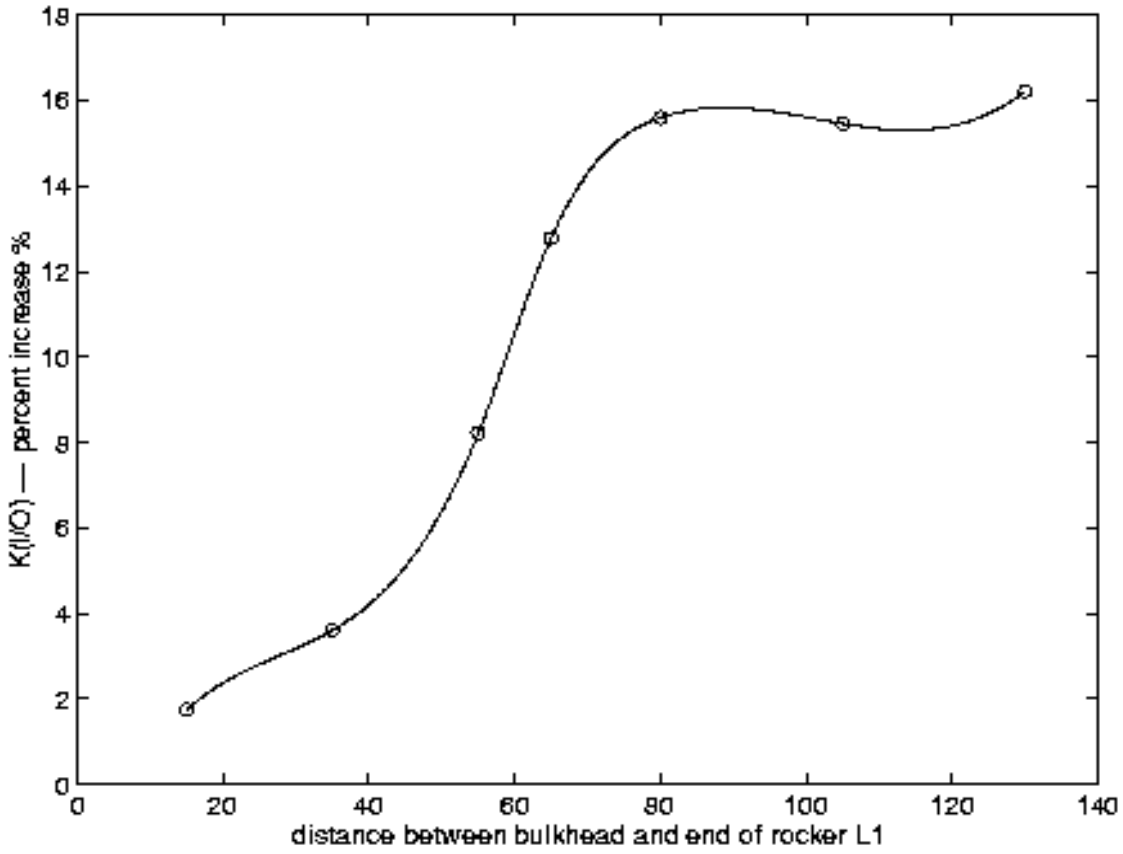

Figure 4.1 Design No.9 Bulkhead Location L1 to the Effect of $K_{I/O}$

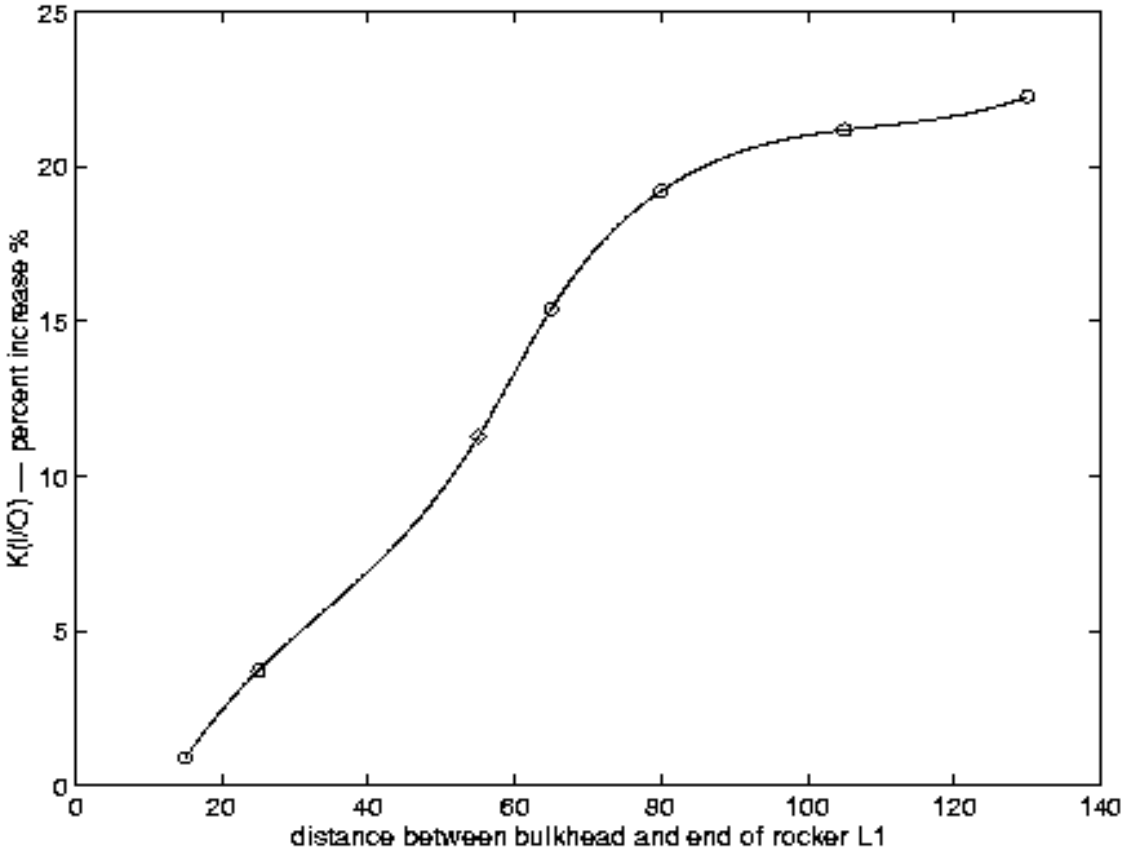

Figure 4.2 Design No. 42 Bulkhead Location L1 to the Effect of $K_{I/O}$

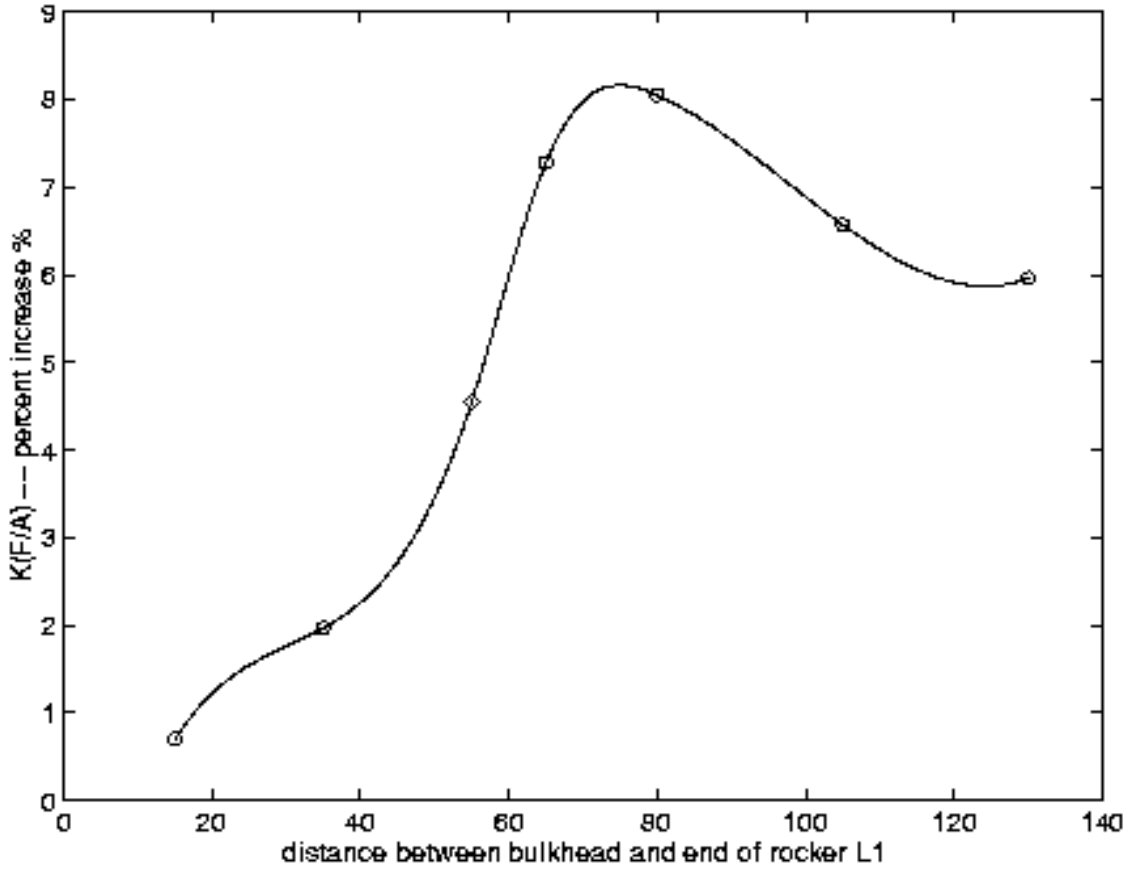

Figure 4.3 Design No.9 Bulkhead Location L1 to the Effect of $K_{F/A}$

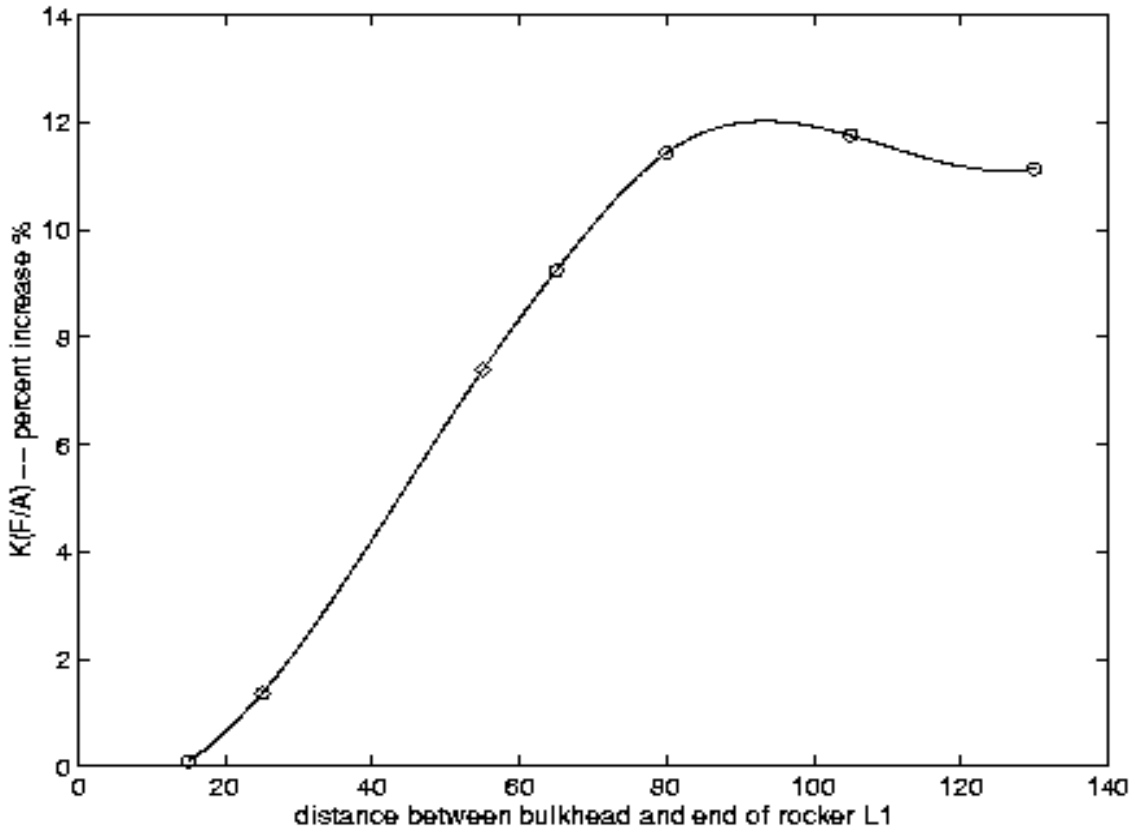

Figure 4.4 Design No.42 Bulkhead Location L1 to the Effect of $K_{F/A}$

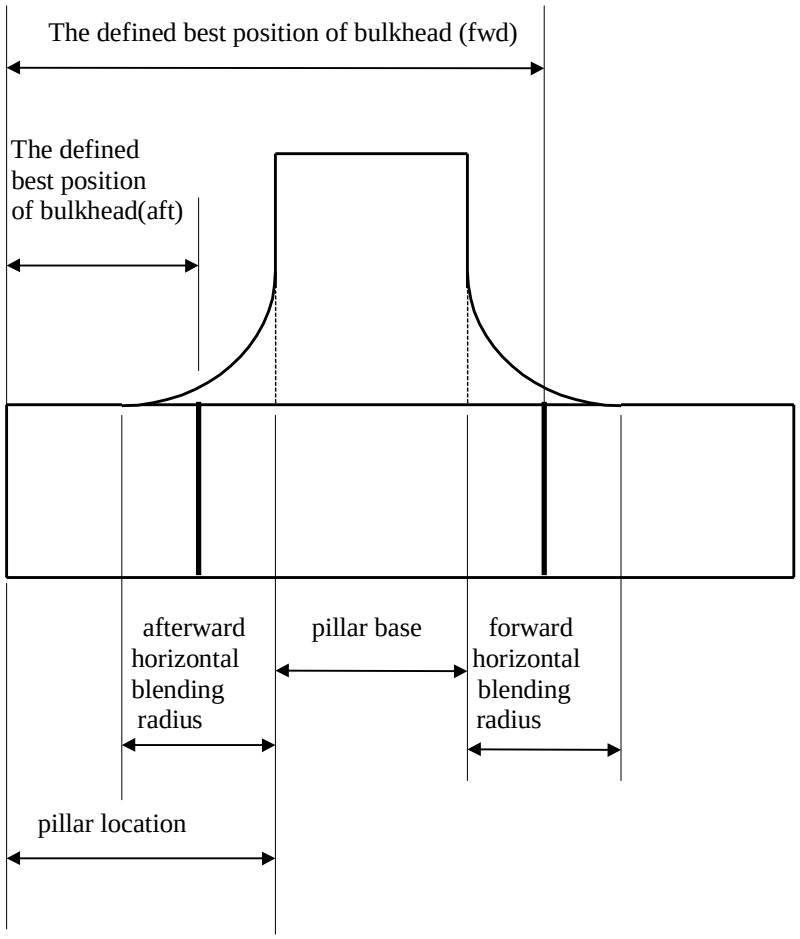

Figure 4.5 The Defined Best Position of Bulkheads

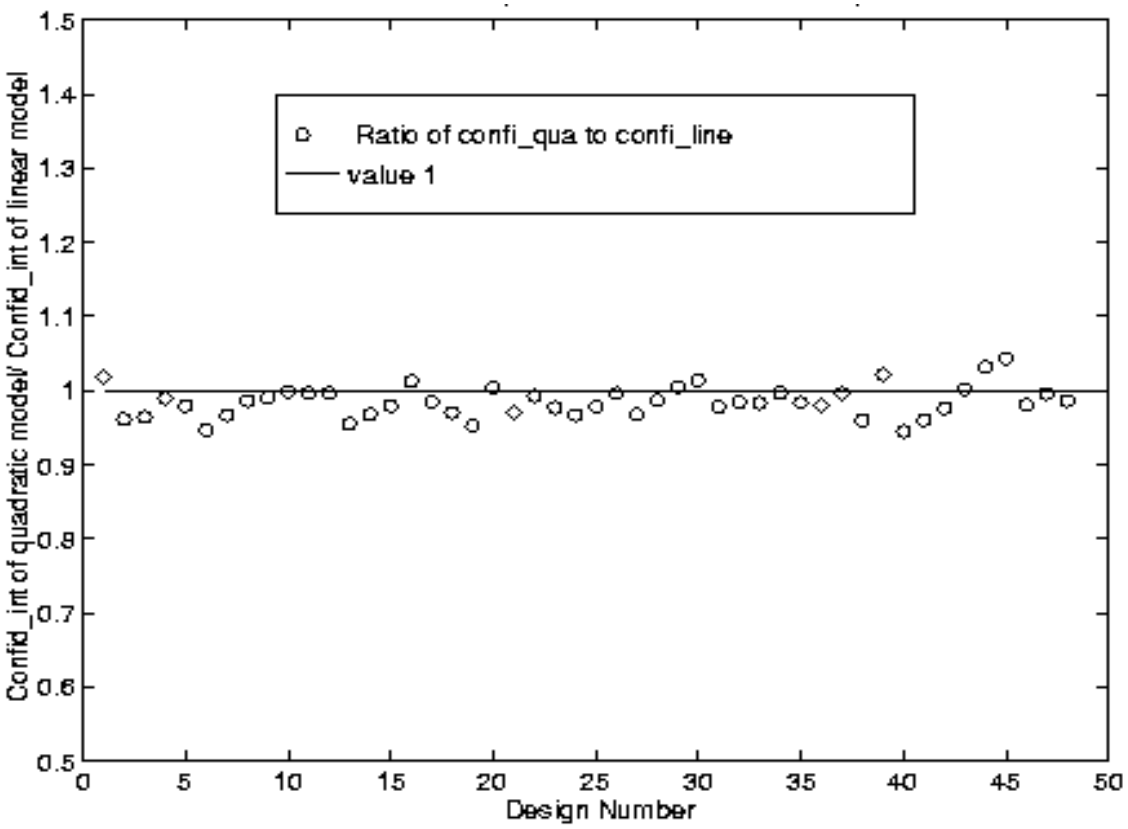

Figure 4.6 $K_{I/O}$ Confidence Interval Comparison between Linear and Quadratic Models, 48 Fitting Designs

(Note: Ratio of confi_qua to confi_line stands for the ratio of the confidence interval of the quadratic model to the confidence interval of the linear model.)

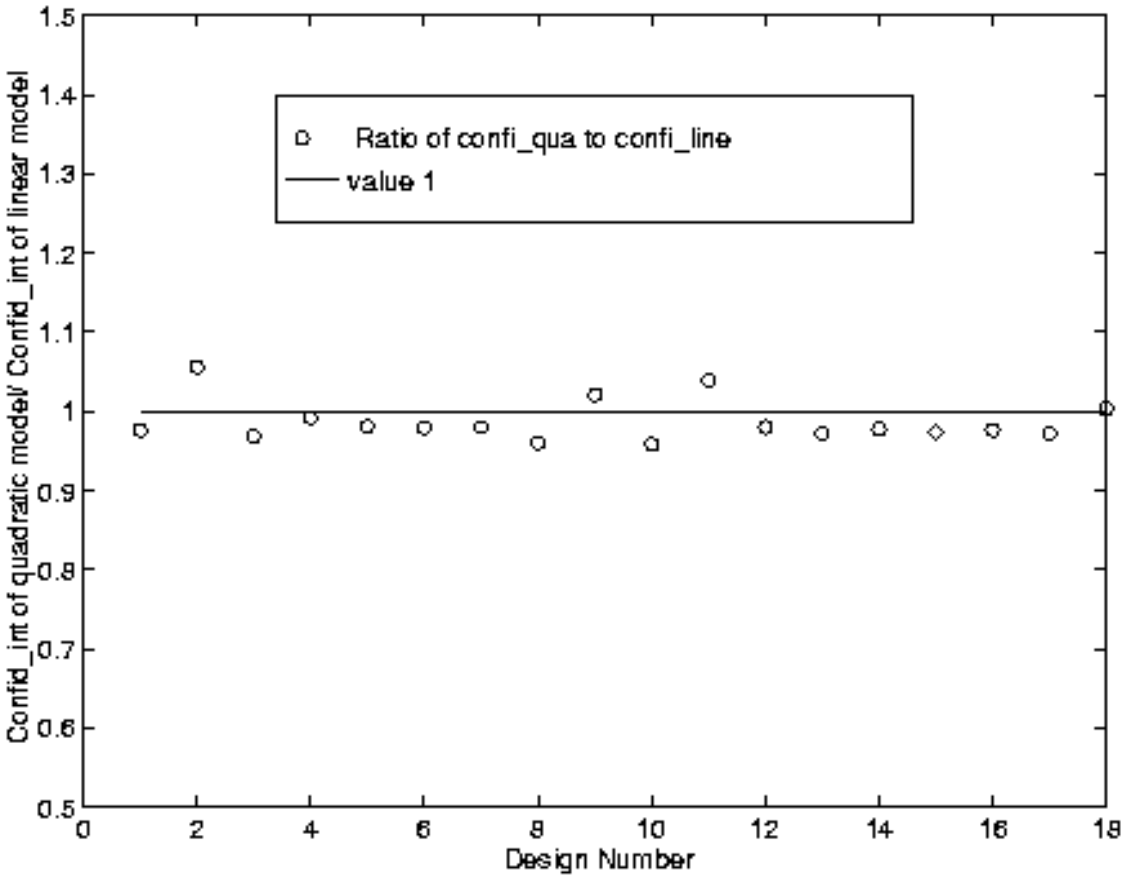

Figure 4.7 $K_{I/O}$ Confidence Interval Comparison between Linear and Quadratic Models, 18 Testing Designs

(Note: Ratio of confi_qua to confi_line stands for the ratio of the confidence interval of the quadratic model to the confidence interval of the linear model.)

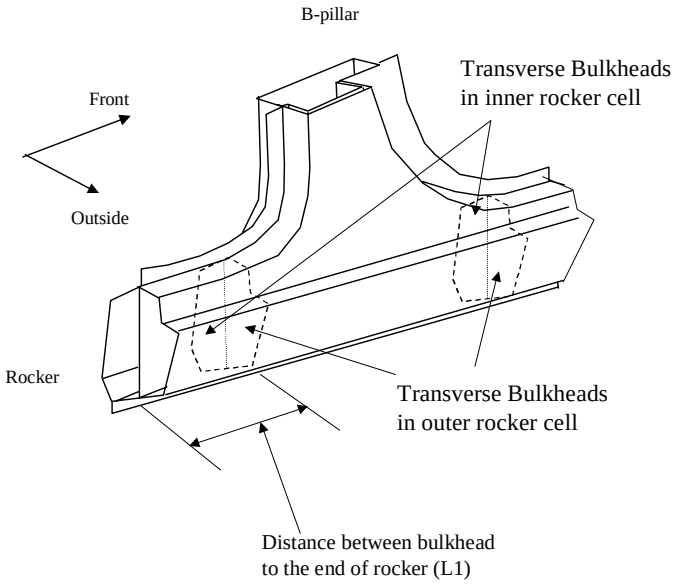

Figure 4.8 Transverse Bulkheads Reinforcements in Rocker Cells for the B-pillar to Rocker Joint

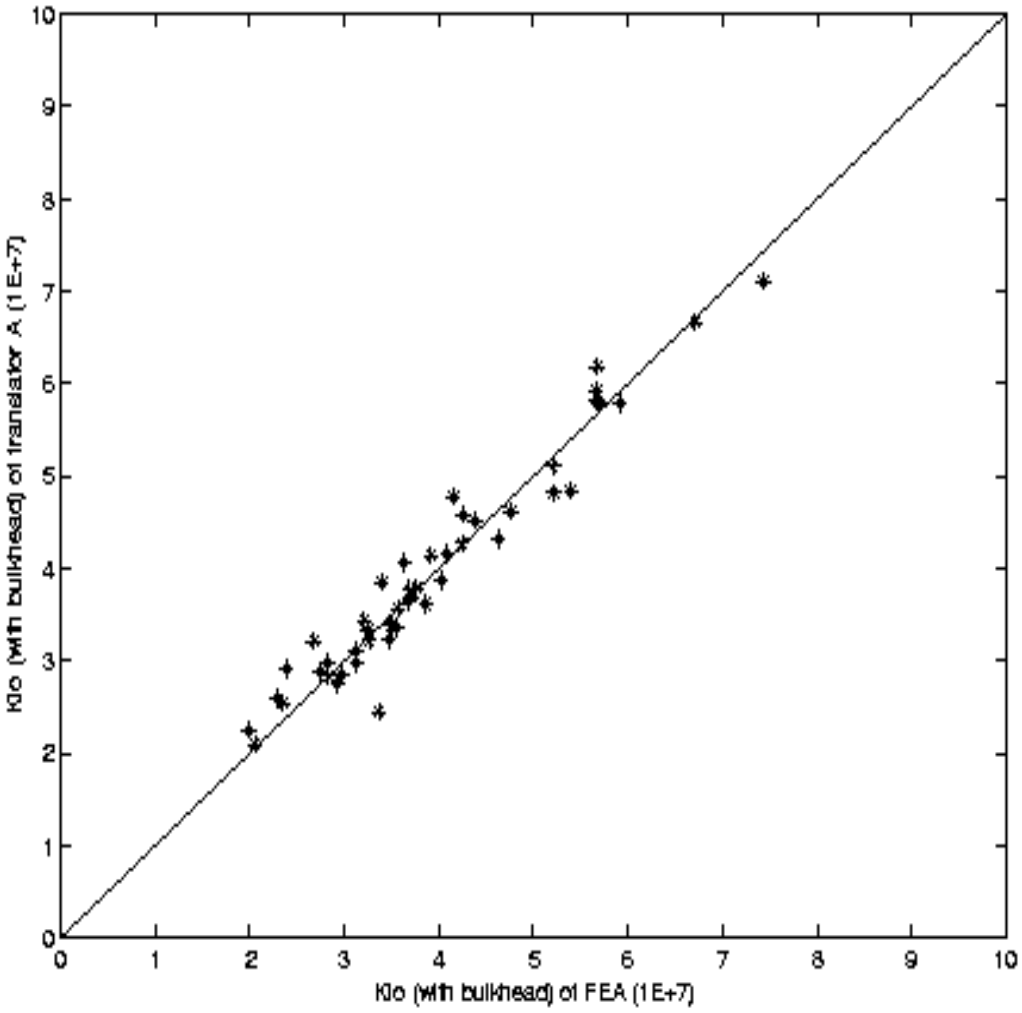

Figure 4.9 Validation of Translator A for the B-pillar to Rocker Joint with Transverse Bulkheads Using FEA Results, I/O Stiffness (48 Fitting Designs)

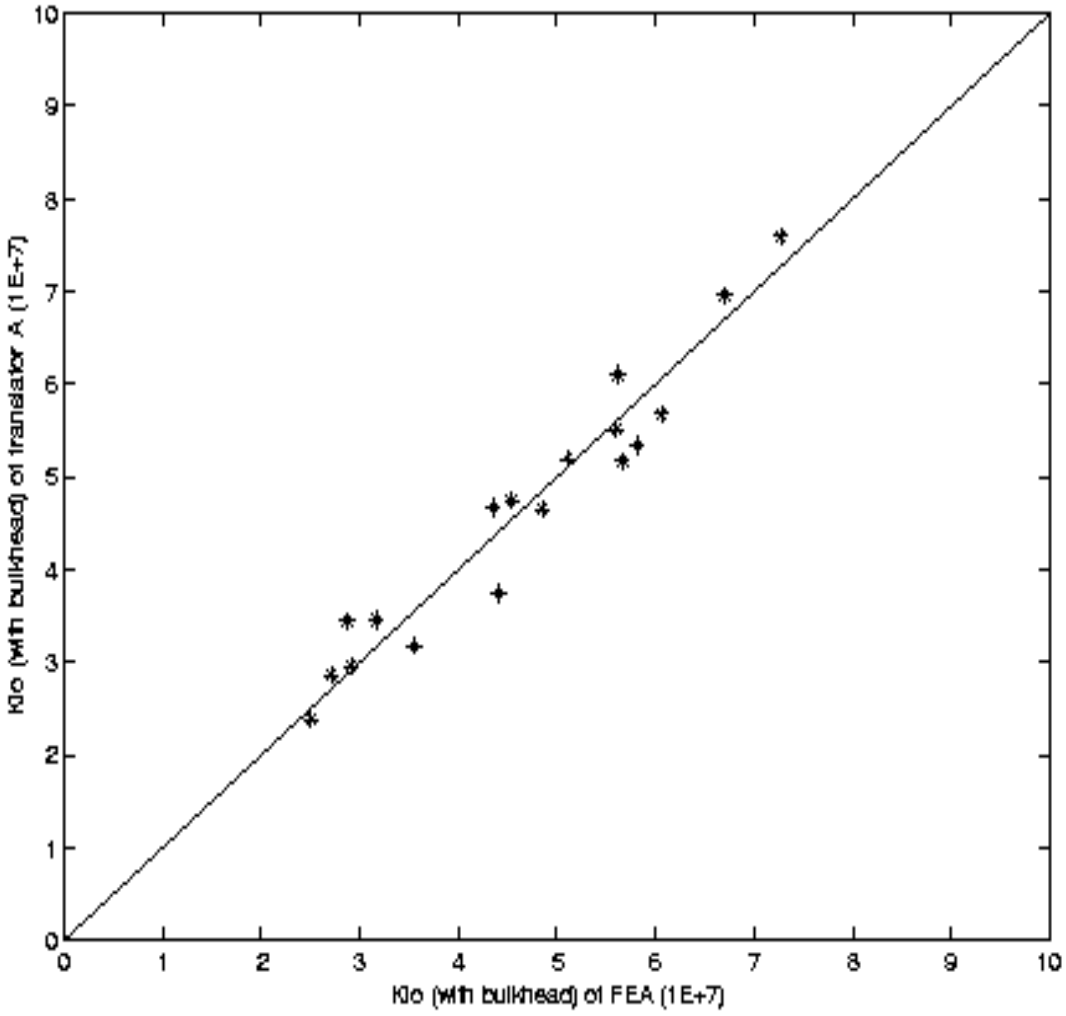

Figure 4.10 Validation of Translator A for the B-pillar to Rocker Joint with Transverse Bulkheads Using FEA Results, I/O Stiffness (18 Testing Designs)

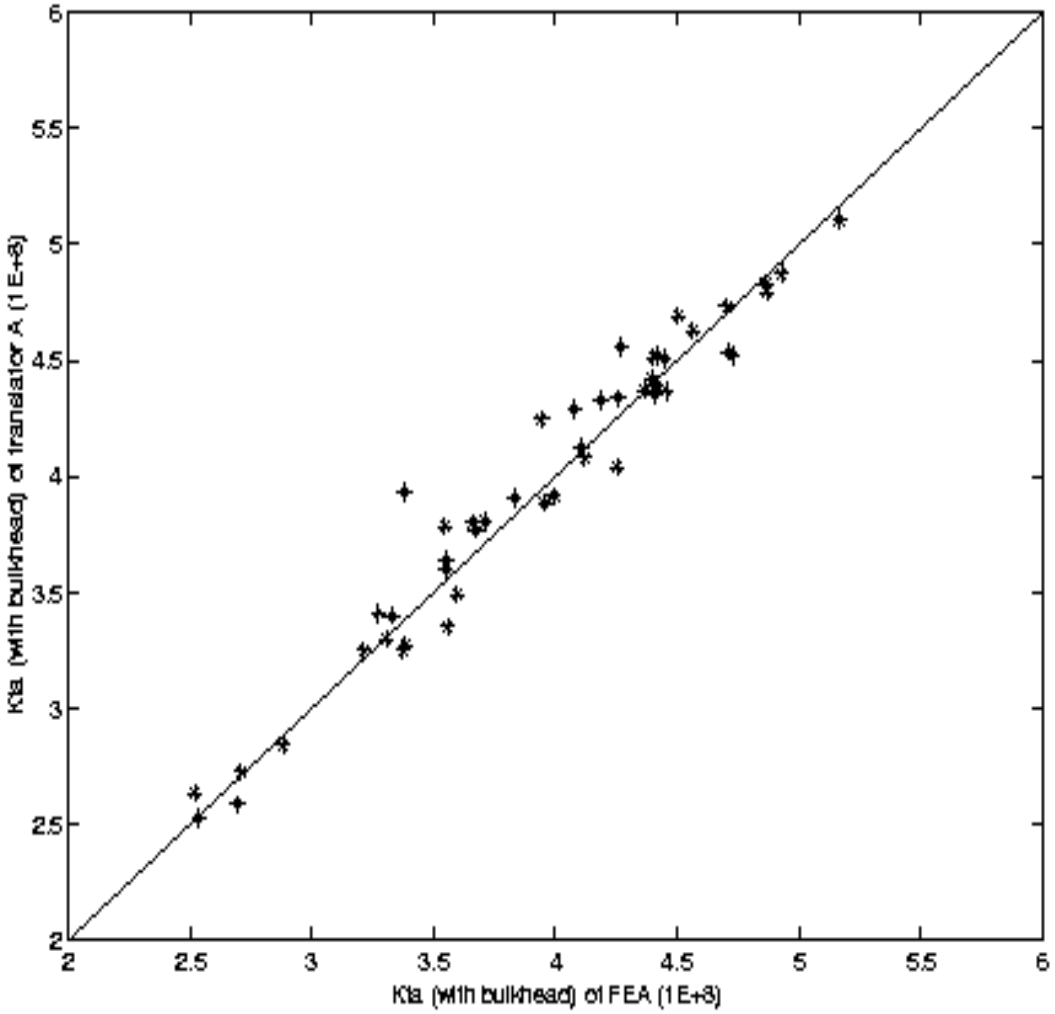

Figure 4.11 Validation of Translator A for the B-pillar to Rocker Joint with Transverse Bulkheads Using FEA Results, F/A Stiffness (48 Fitting Designs)

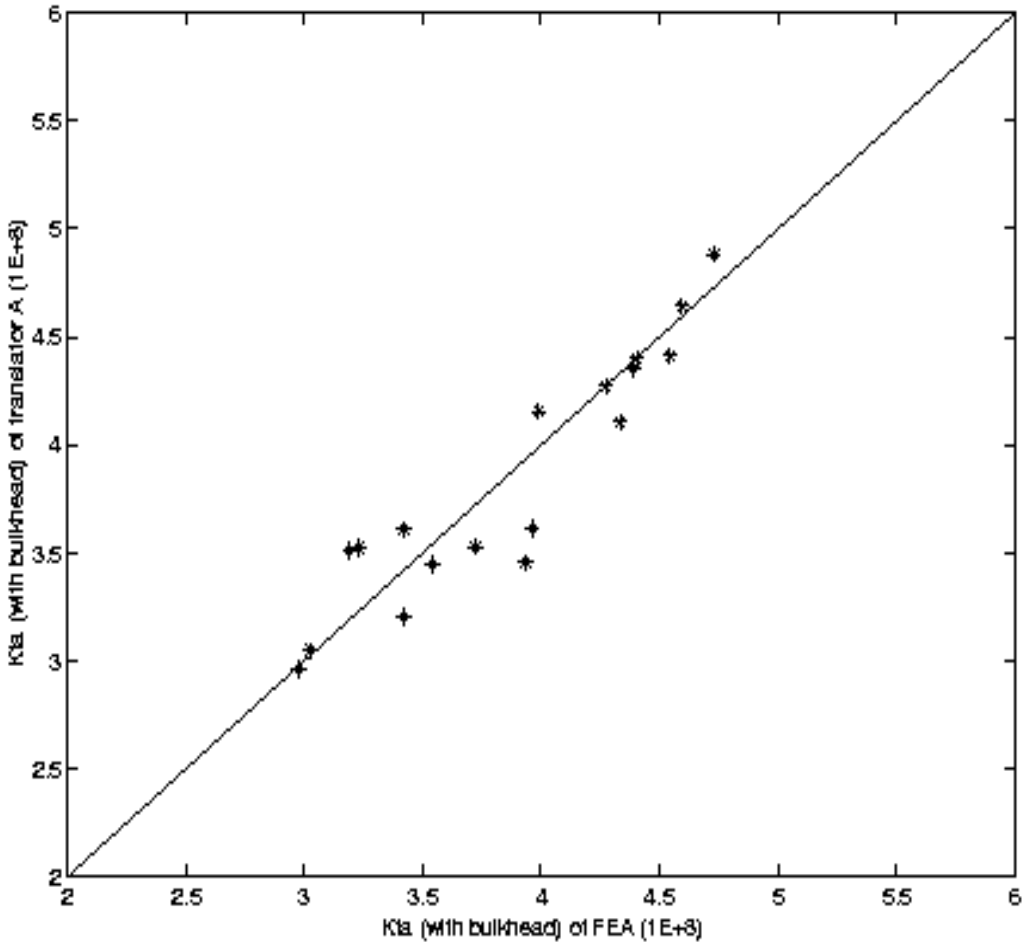

Figure 4.12 Validation of Translator A for the B-pillar to Rocker Joint with Transverse Bulkheads Using FEA Results, F/A Stiffness (18 Testing Designs)

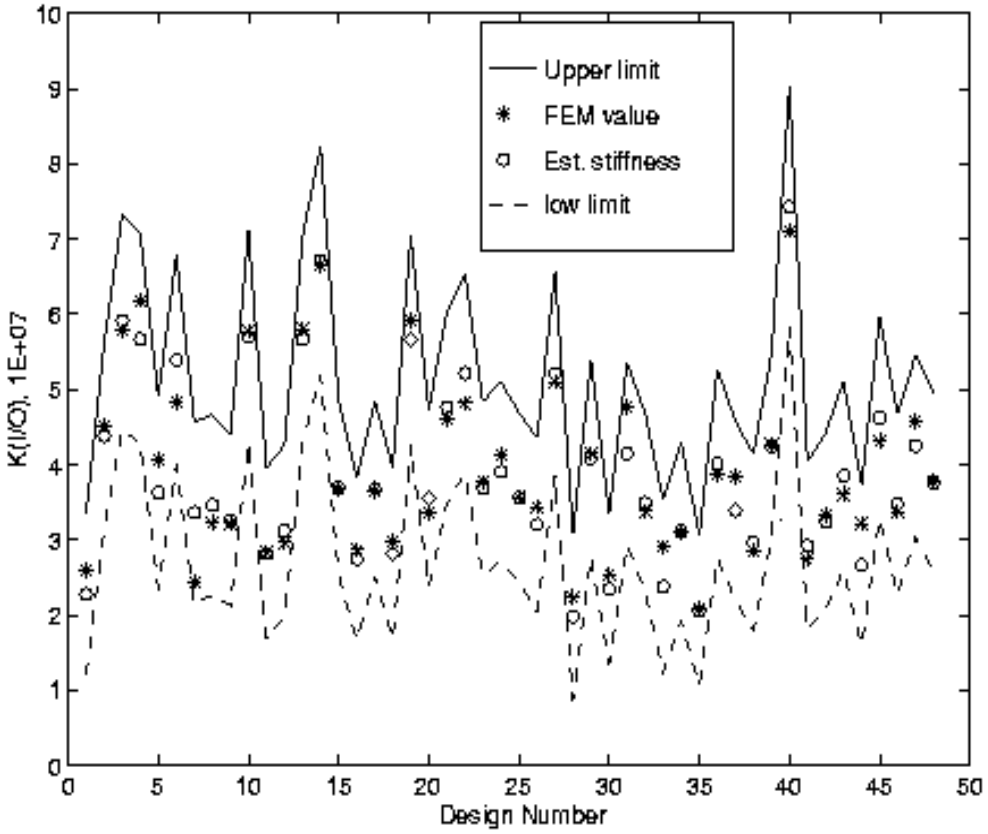

Figure 4.13 The Estimated Stiffness, FEM Value and Estimated 95% Confidence Interval, $K_{I/O}$ (with bulkheads), 48 Fitting Designs

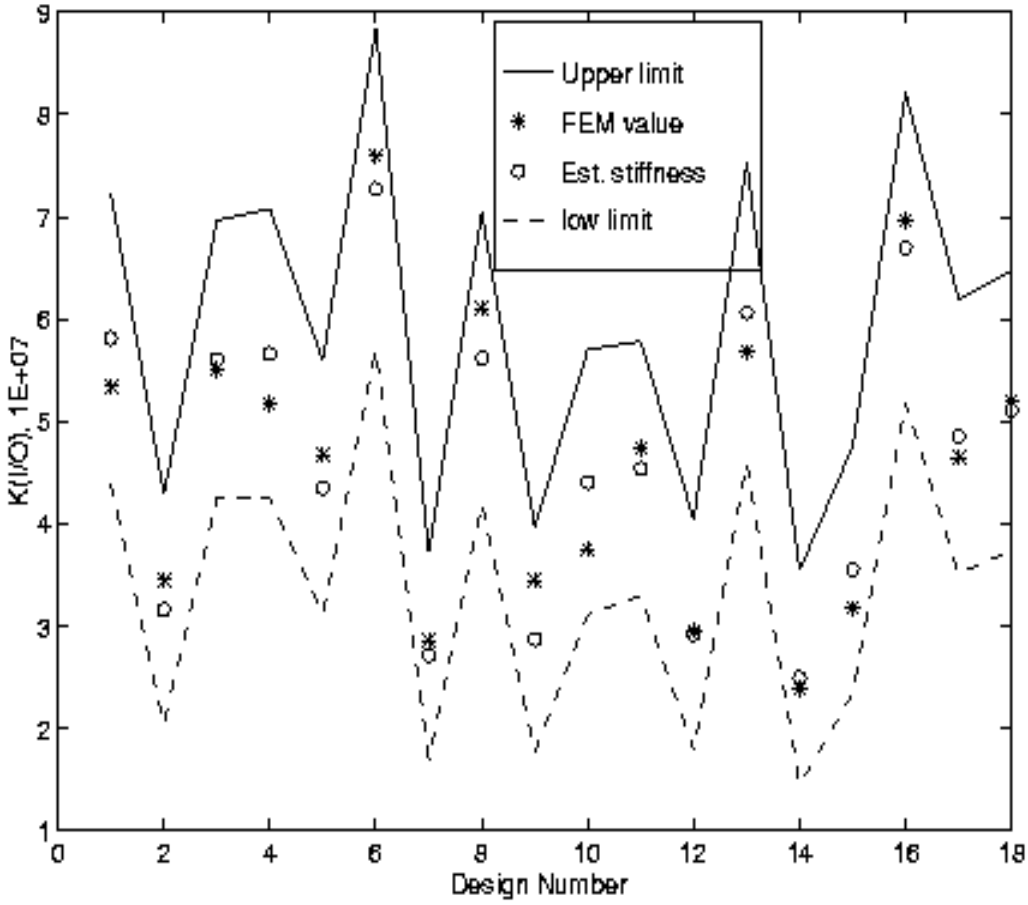

Figure 4.14 The Estimated Stiffness, FEM Value and Estimated 95% Confidence Interval, $K_{I/O}$ (with bulkheads), 18 Testing Designs

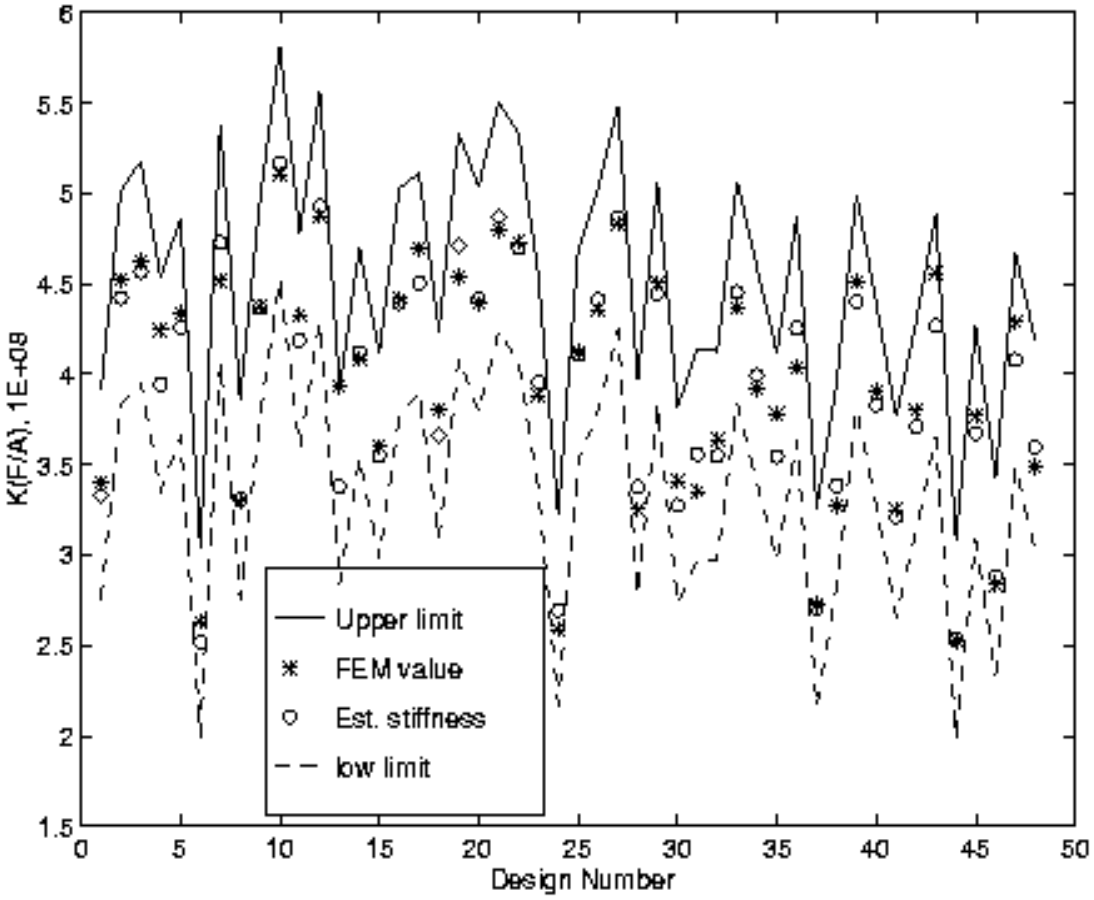

Figure 4.15 The Estimated Stiffness, FEM Value and Estimated 95% Confidence Interval, $K_{F/A}$ (with bulkheads), 48 Fitting Designs

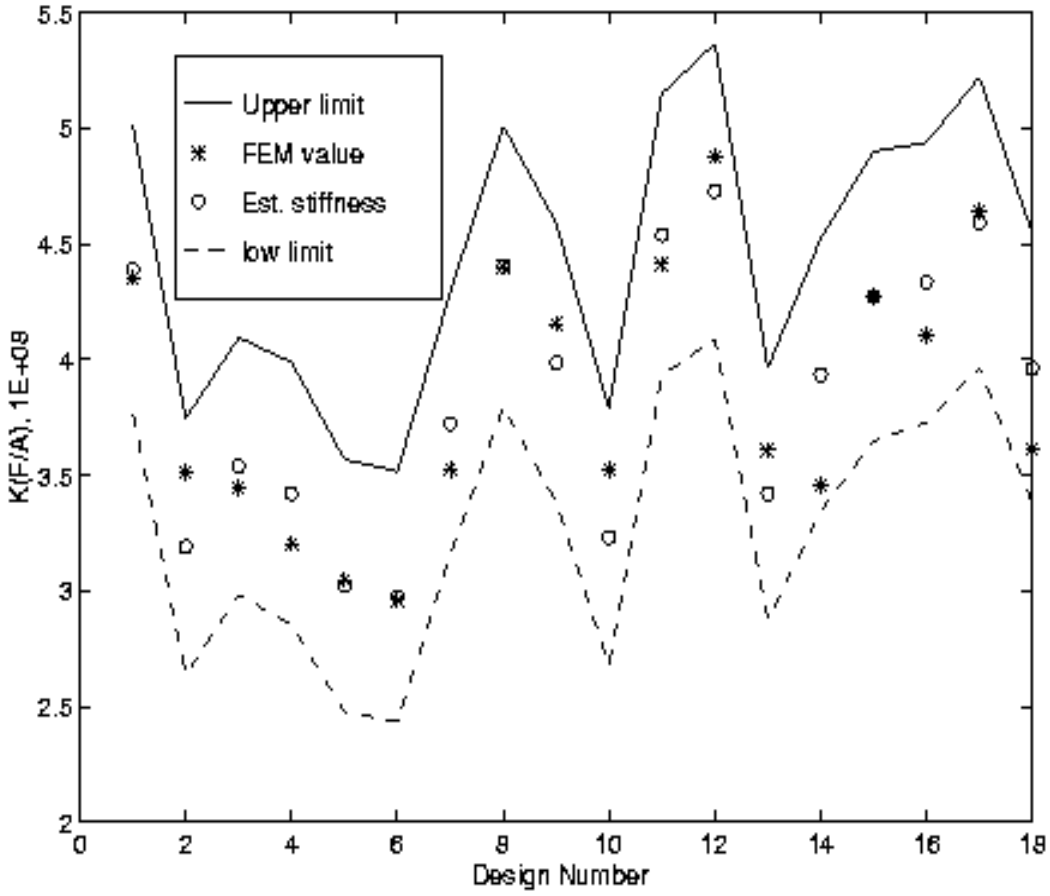

Figure 4.16 The Estimated Stiffness, FEM Value and Estimated 95% Confidence Interval, $K_{F/A}$ (with bulkheads), 18 Testing Designs

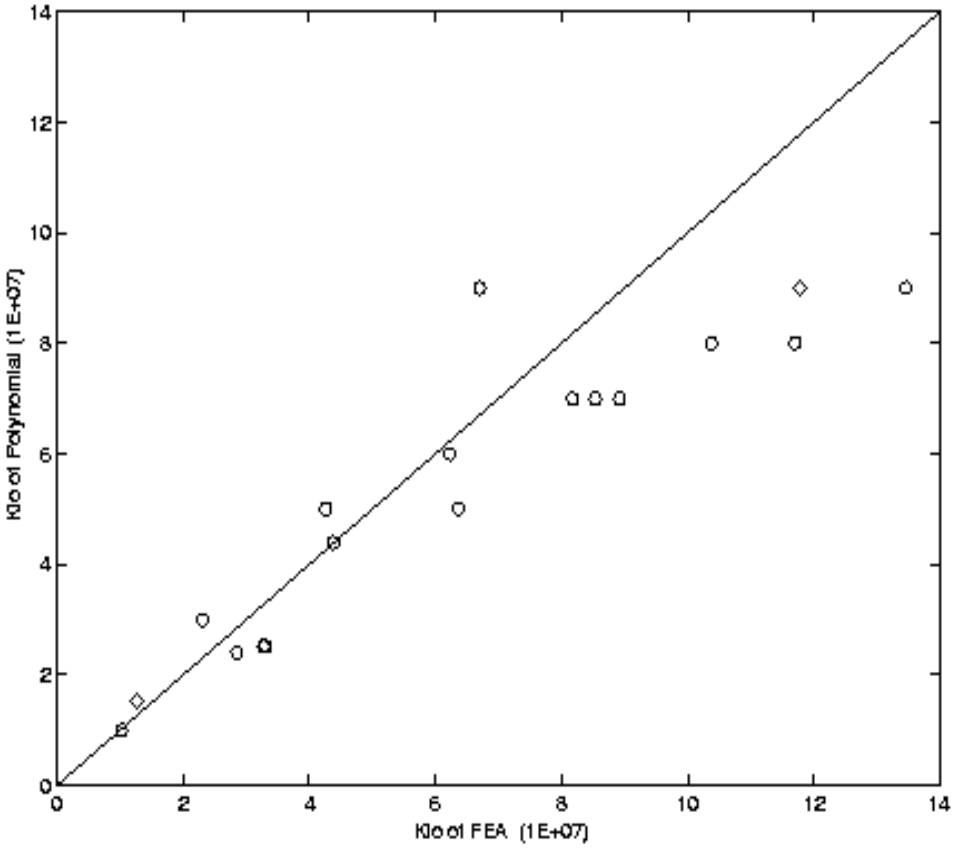

(Correlation coefficient = 0.9254)

Figure 5.1 Correlation Plot of $K_{I/O}$ (Using Polynomial Translator) vs. FEA
(Old 18 Designs with Stiffness Target Combination
not Strictly inside the Defined Zones)

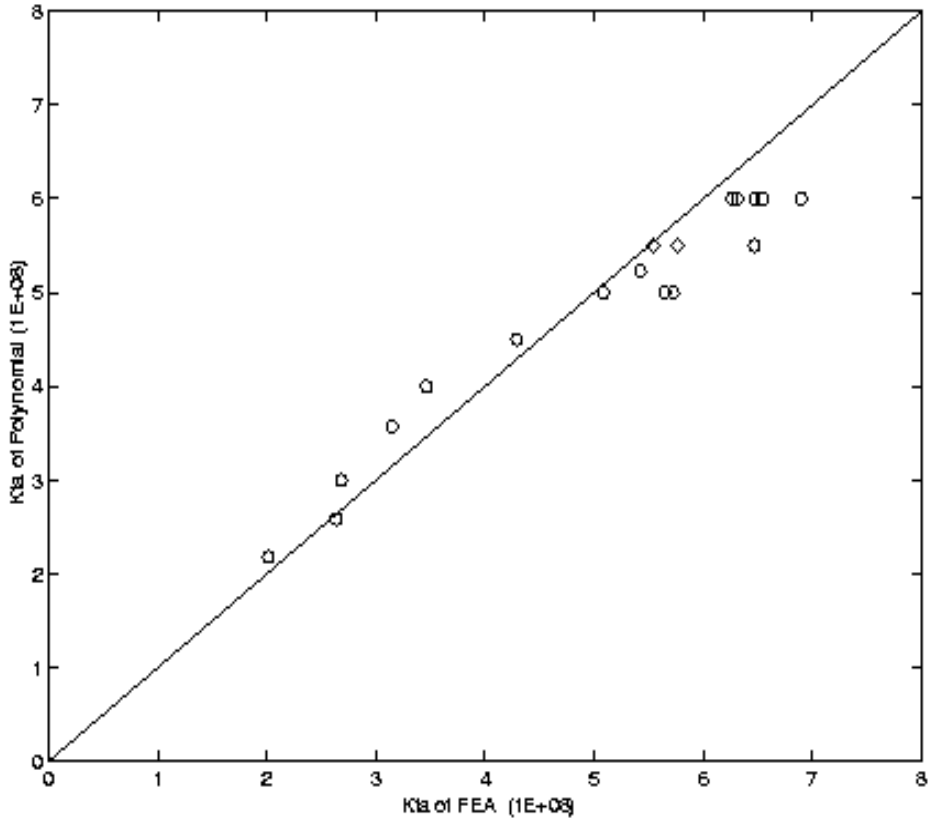

(Correlation coefficient = 0.9771)

Figure 5.2 Correlation Plot of $K_{F/A}$ (Using Polynomial Translator) vs. FEA
(Old 18 Designs with Stiffness Target Combination
not Strictly inside the Defined Zones)

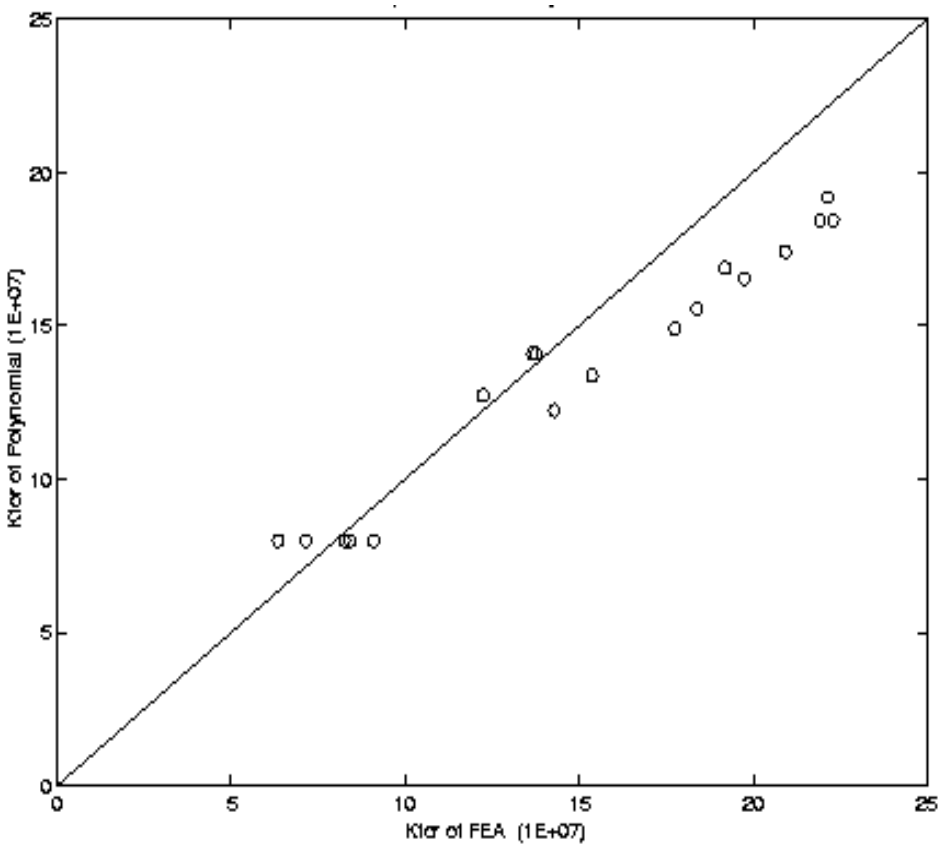

(Correlation coefficient = 0.9794)

Figure 5.3 Correlation Plot of K_{Tor} (Using Polynomial Translator) vs. FEA
(Old 18 Designs with Stiffness Target Combination
not Strictly inside the Defined Zones)

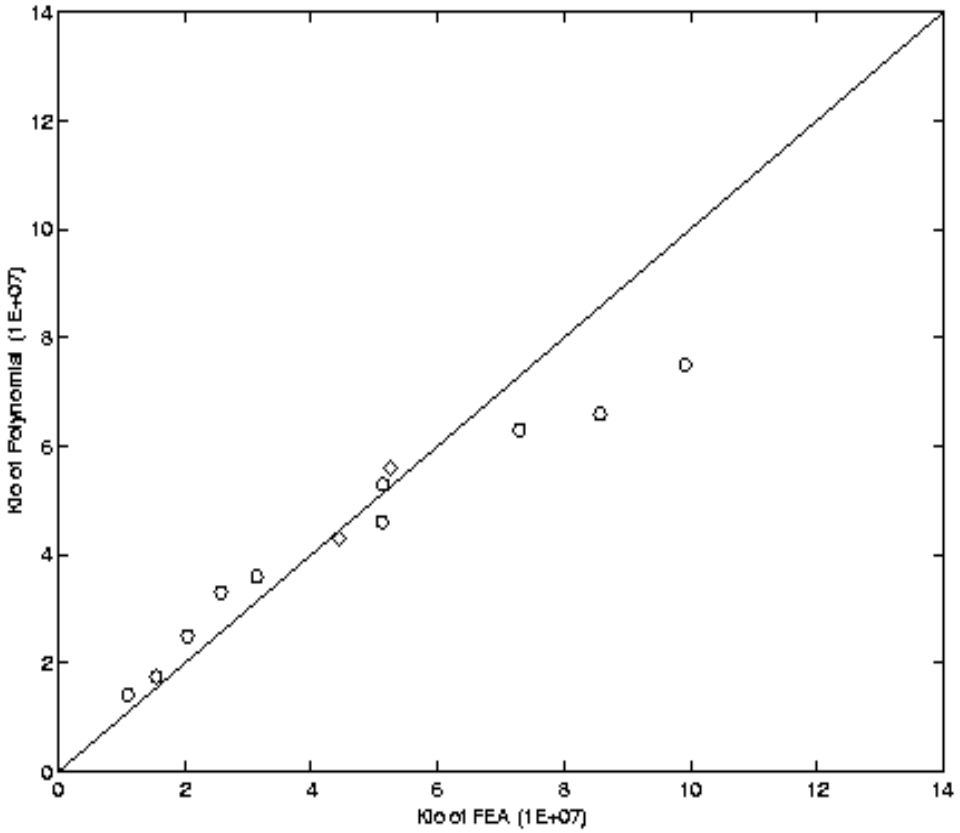

(Correlation coefficient = 0.9733)

Figure 5.4 Correlation Plot of $K_{I/O}$ (Using Polynomial Translator) vs. FEA
(New 12 Designs with Stiffness Target Combination
Strictly inside the Defined Zones)

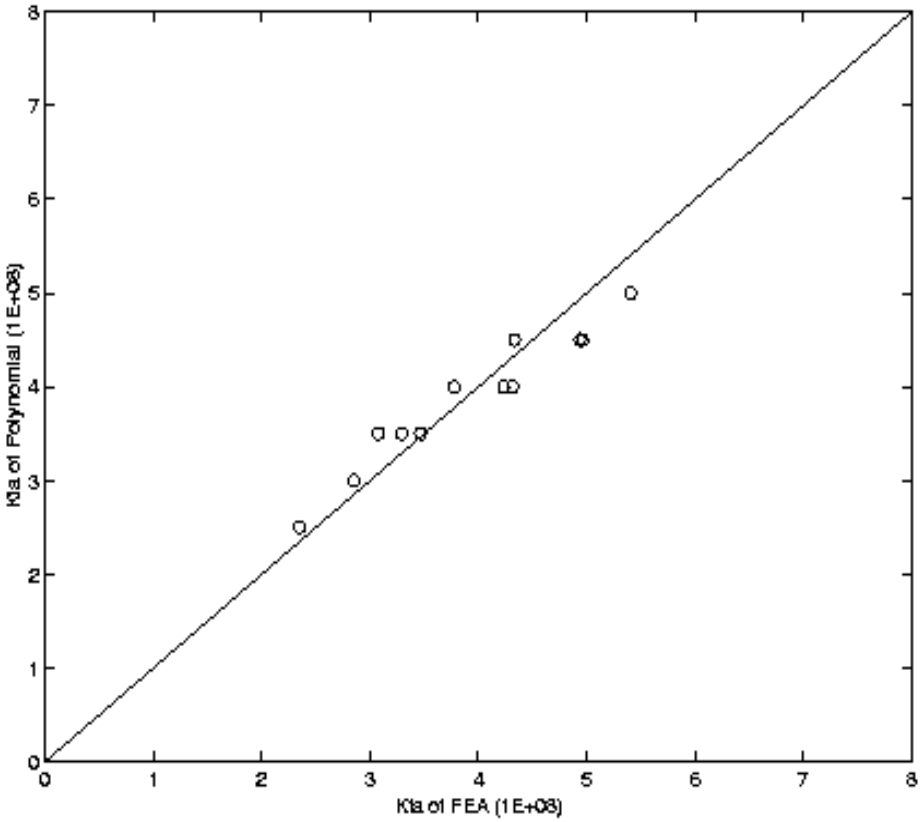

(Correlation coefficient = 0.9676)

Figure 5.5 Correlation Plot of $K_{F/A}$ (Using Polynomial Translator) vs. FEA
(New 12 Designs with Stiffness Target Combination
Strictly inside the Defined Zones)

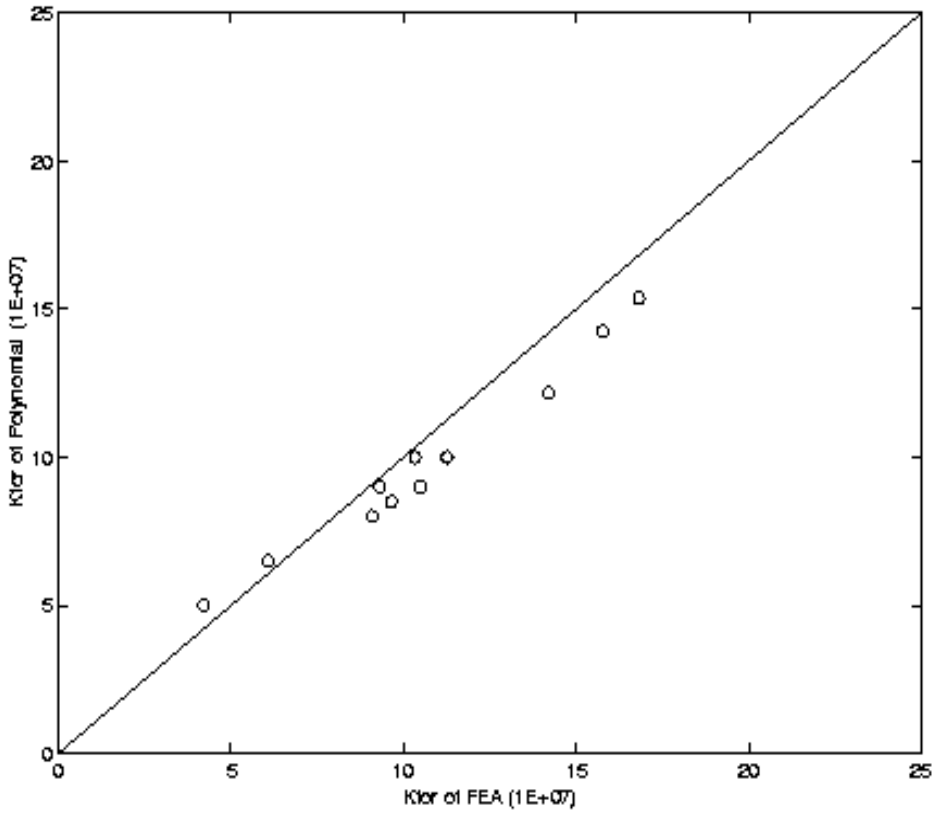

(Correlation coefficient = 0.9872)

Figure 5.6 Correlation Plot of K_{Tor} (Using Polynomial Translator) vs. FEA
(New 12 Designs with Stiffness Target Combination
Strictly inside the Defined Zones)

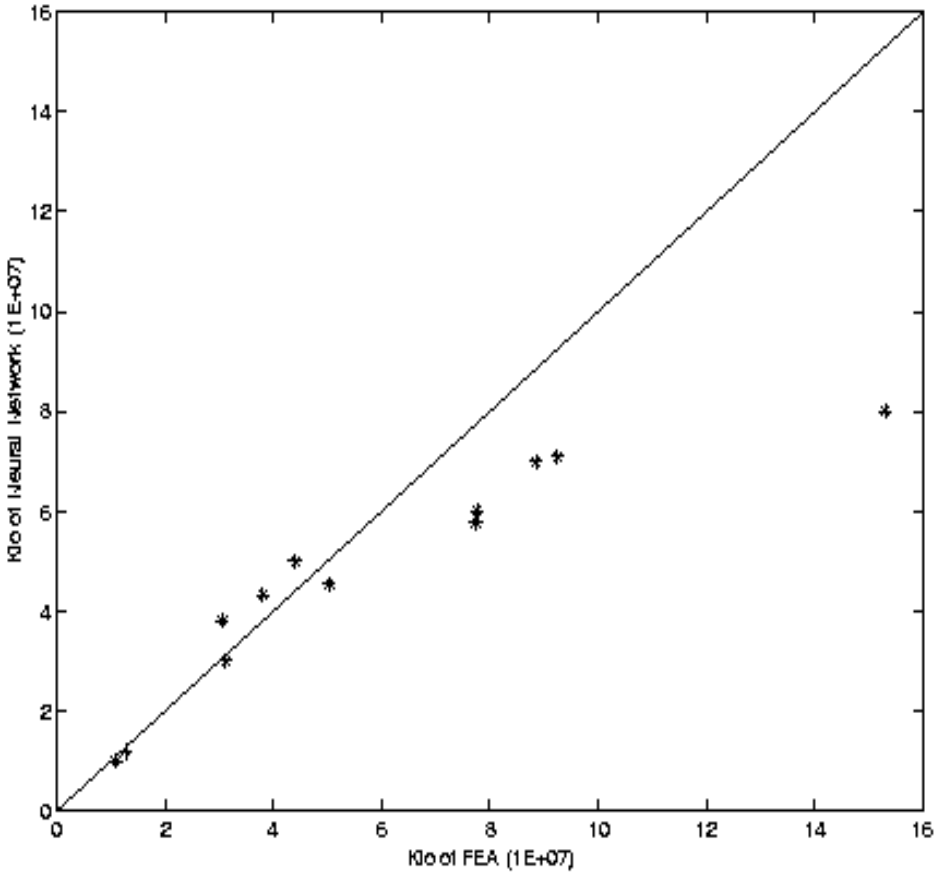

(Correlation coefficient = 0.9201)

Figure 5.7 Correlation Plot of $K_{I/O}$ (Using Neural Network Translator) vs. FEA (Old 12 Designs with Stiffness Target Combination not Strictly inside the Defined Zones)

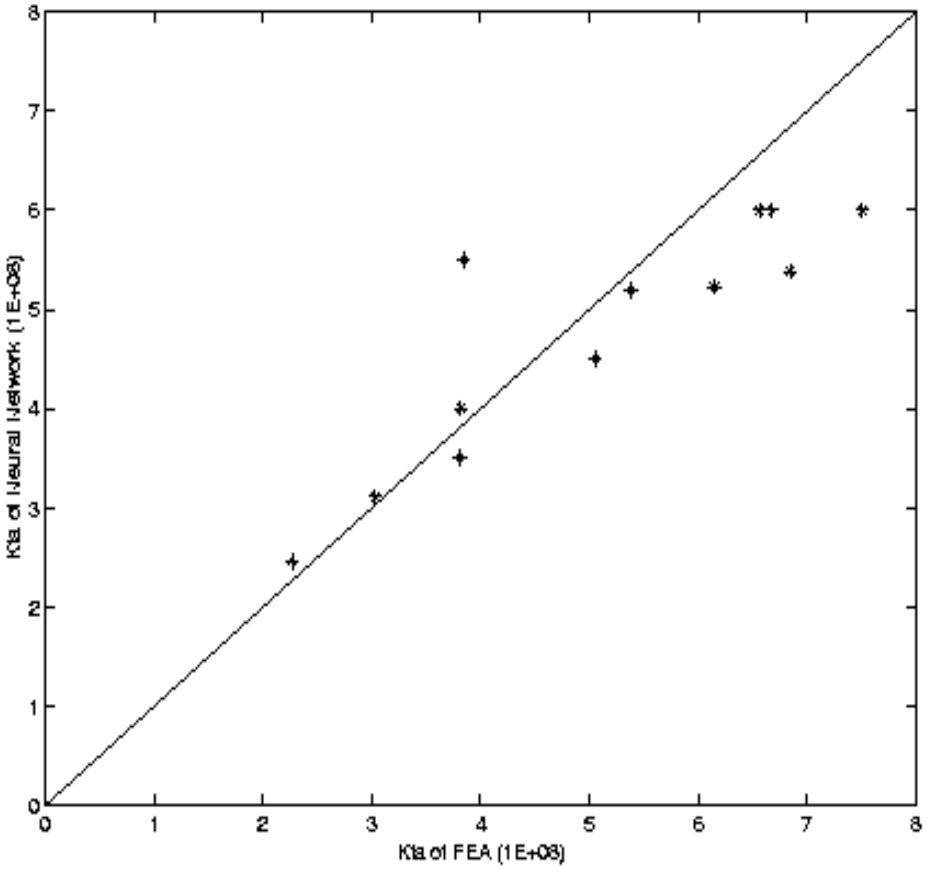

(Correlation coefficient = 0.8838)

Figure 5.8 Correlation Plot of $K_{F/A}$ (Using Neural Network Translator) vs. FEA (Old 12 Designs with Stiffness Target Combination not Strictly inside the Defined Zones)

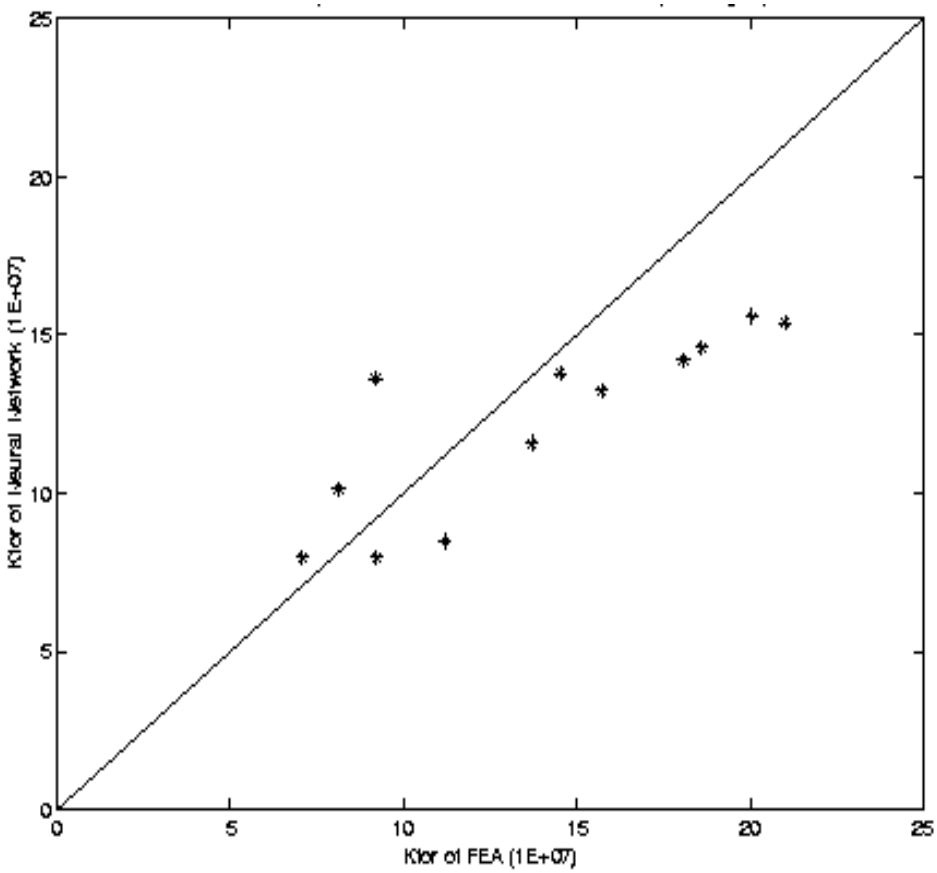

(Correlation coefficient = 0.8401)

Figure 5.9 Correlation Plot of K_{Tor} (Using Neural Network Translator) vs. FEA (Old 12 Designs with Stiffness Target Combination not Strictly inside the Defined Zones)

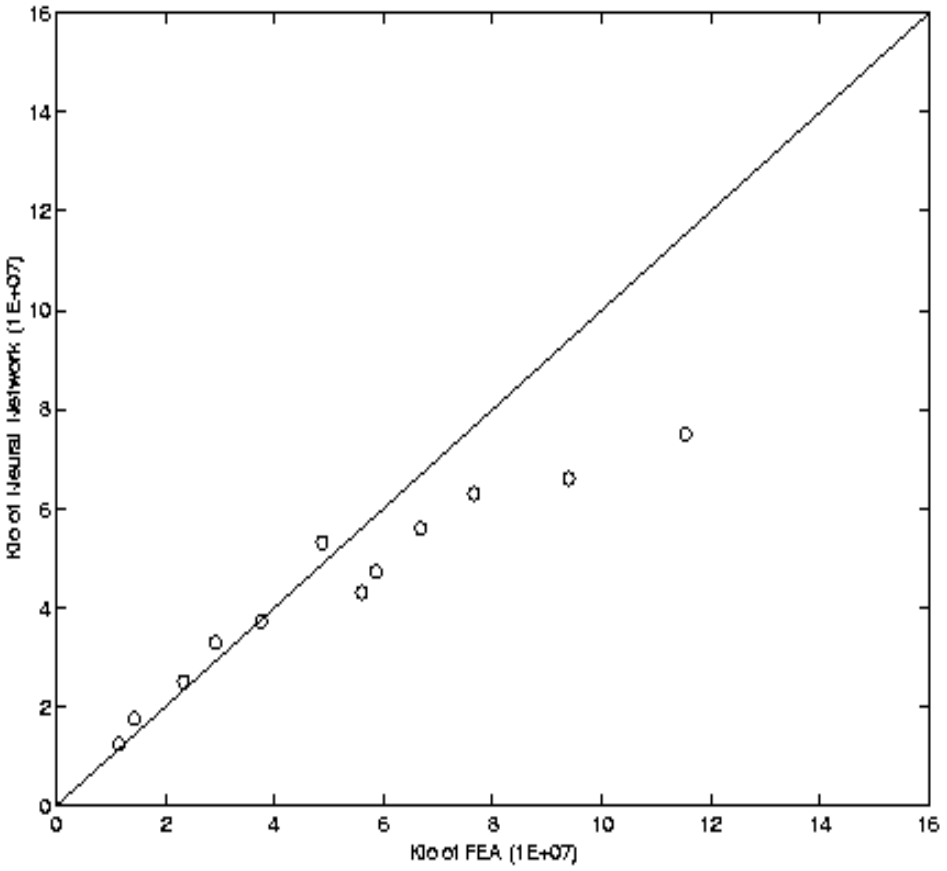

(Correlation coefficient = 0.9642)

Figure 5.10 Correlation Plot of $K_{I/O}$ (Using Neural Network Translator) vs. FEA (New 12 Designs with Stiffness Target Combination Strictly inside the Defined Zones)

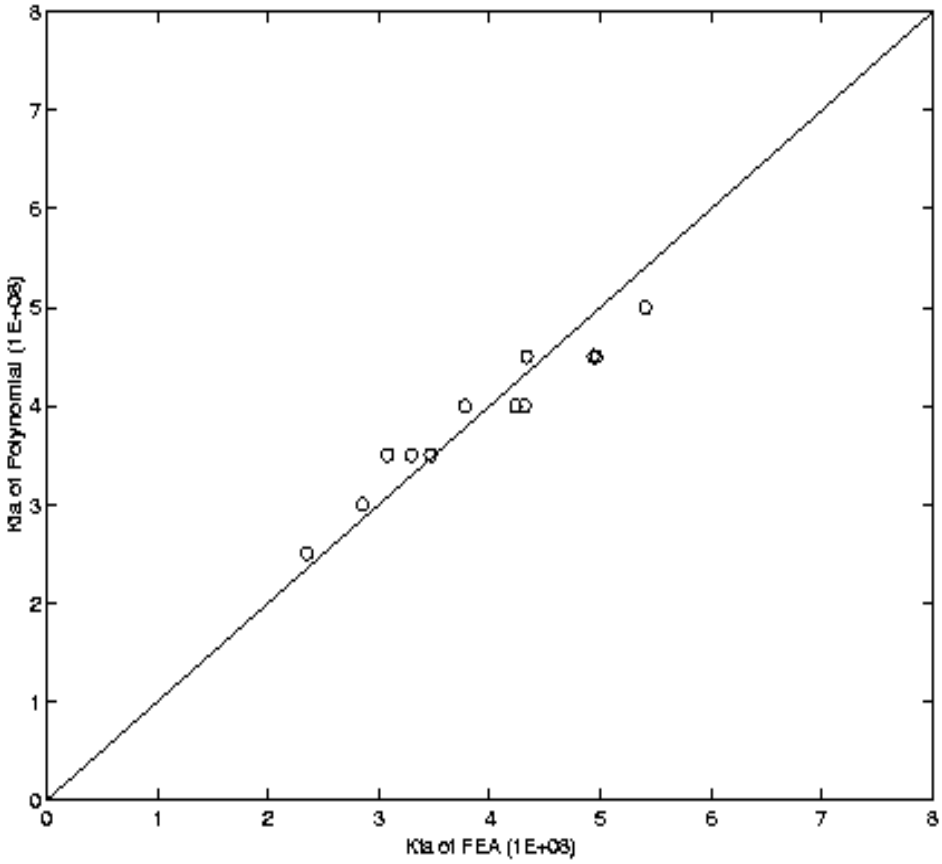

(Correlation coefficient = 0.9600)

Figure 5.11 Correlation Plot of $K_{F/A}$ (Using Neural Network Translator) vs. FEA (New 12 Designs with Stiffness Target Combination Strictly inside the Defined Zones)

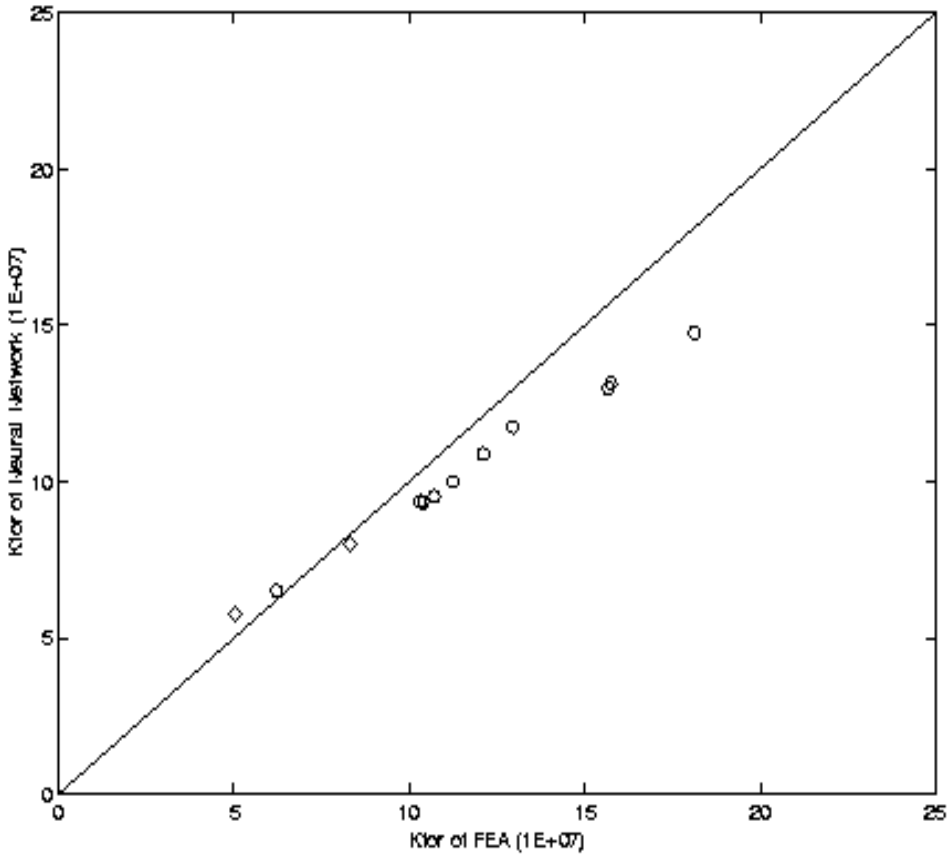

(Correlation coefficient = 0.9975)

Figure 5.12 Correlation Plot of K_{Tor} (Using Neural Network Translator) vs. FEA (New 12 Designs with Stiffness Target Combination Strictly inside the Defined Zones)

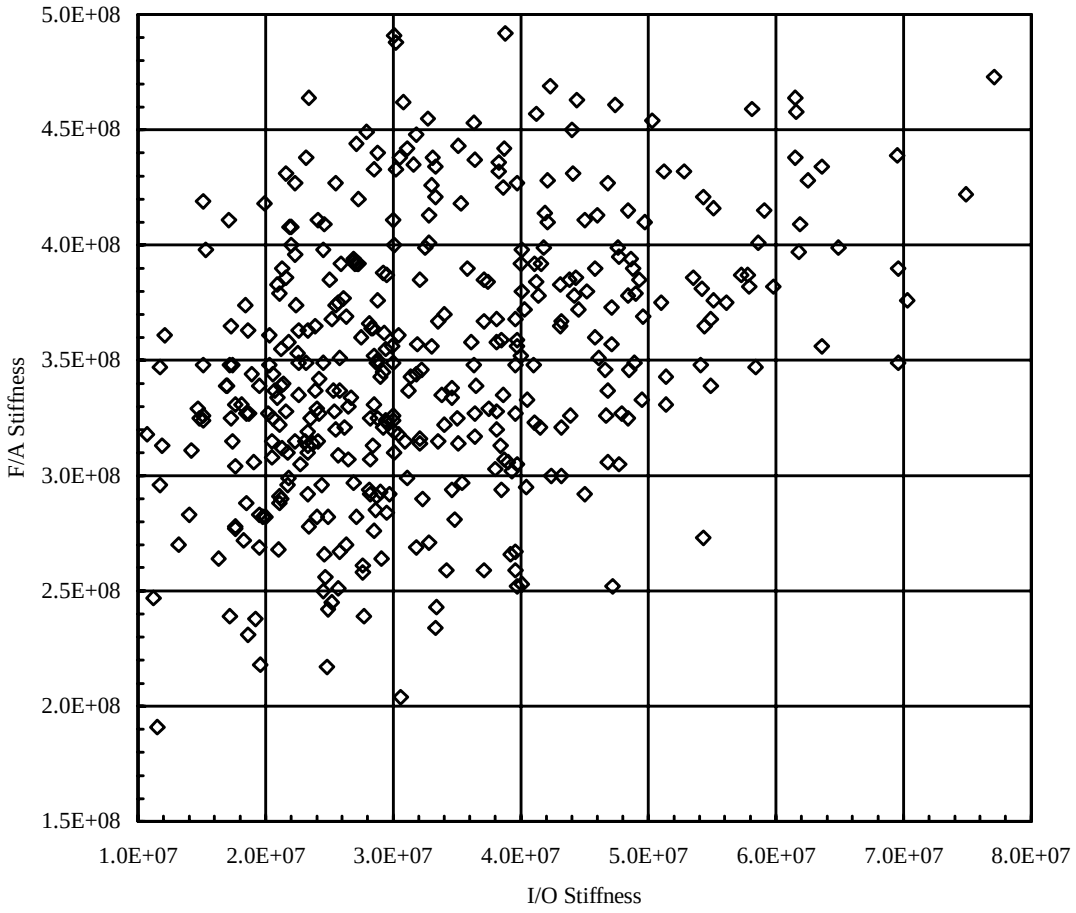

Figure 5.13a: Scatter Plots of I/O Stiffness vs. F/A Stiffness
for the Designs in the Database

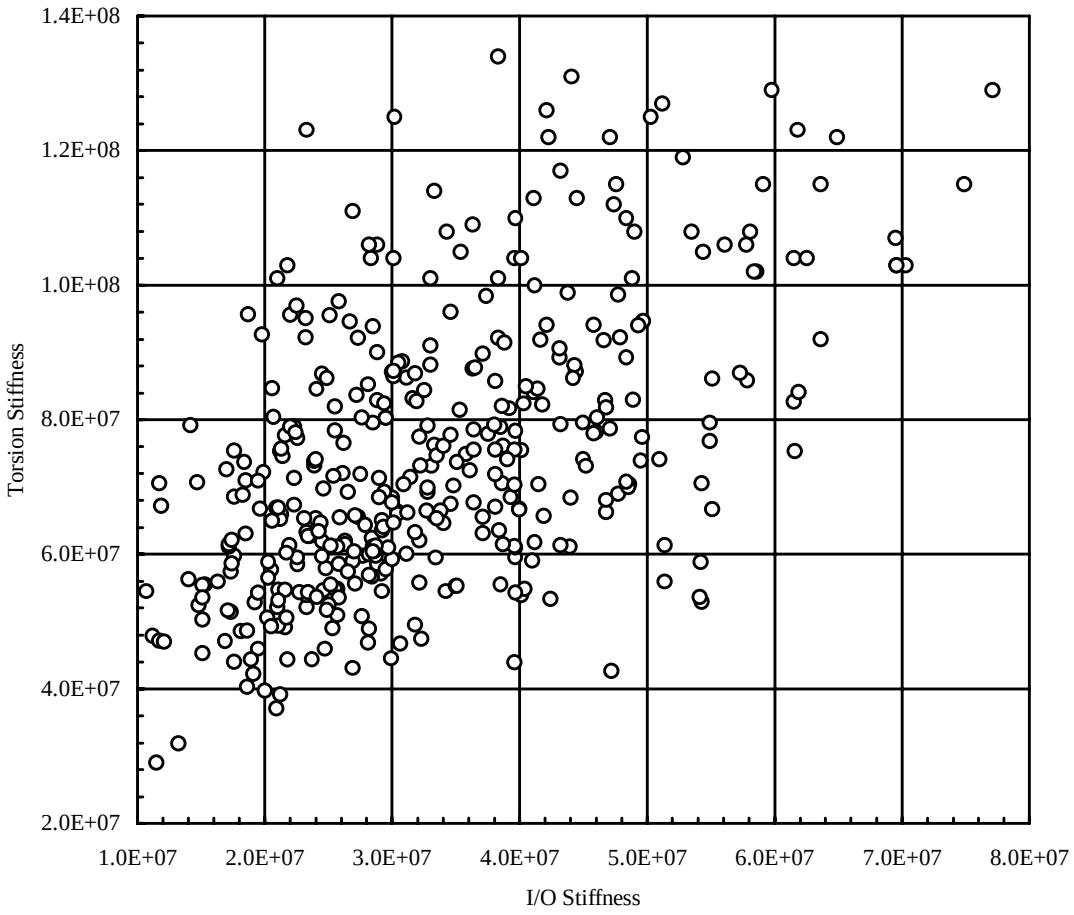

Figure 5.13b Scatter Plots of I/O Stiffness vs. Torsional Stiffness for the Designs in the Databse

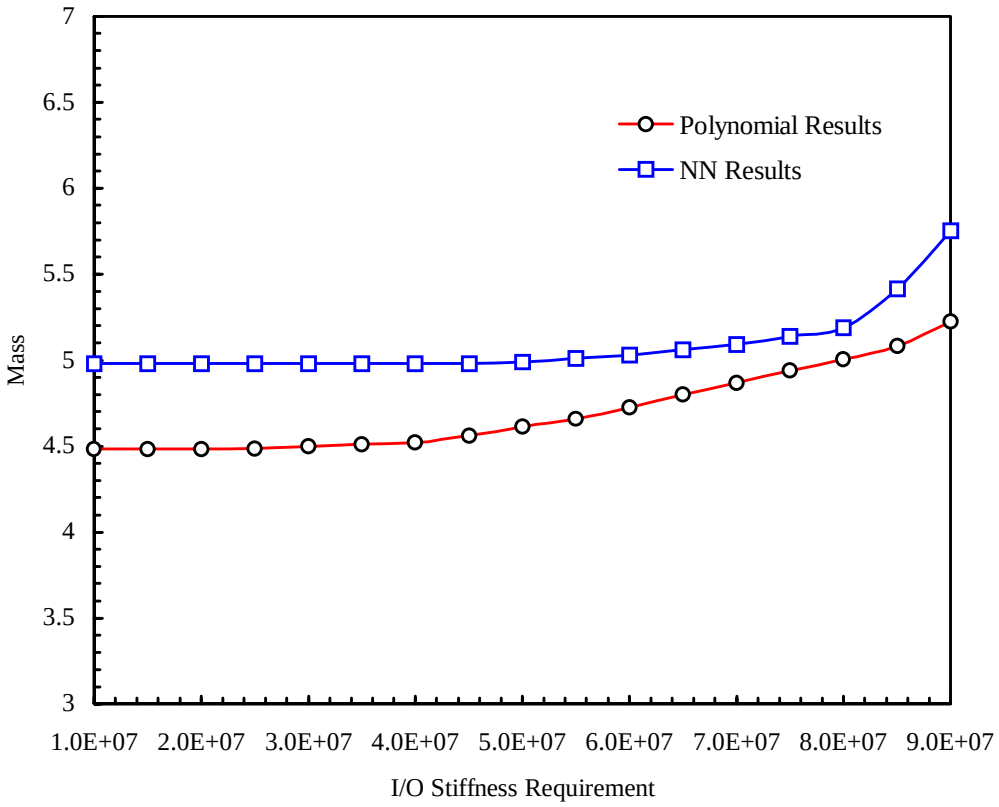

Figure 5.14a Relation between Mass and I/O Stiffness Requirement for the B-Pillar to Rocker Joint

($K_{F/A}$ >5.2297E8, K_{tor} >7.9788E7)

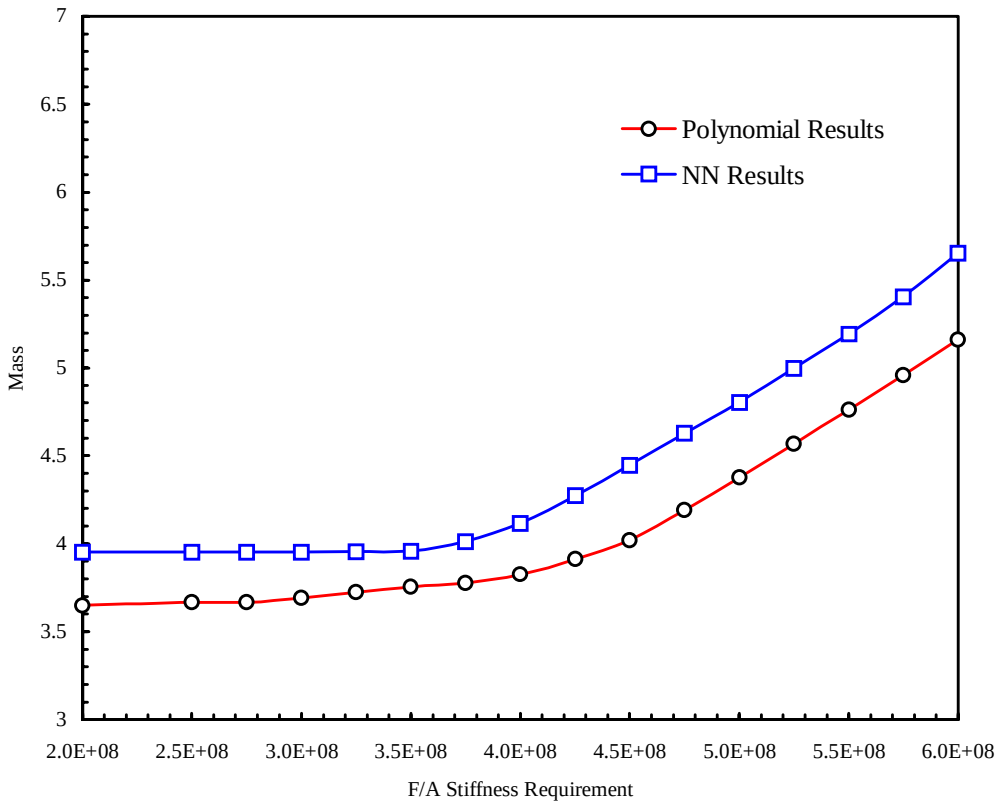

Figure 5.14b Relation between Mass and F/A Stiffness Requirement for the B-Pillar to Rocker Joint

($K_{I/O}$ >4.3899E7, K_{tor} >7.9788E7)

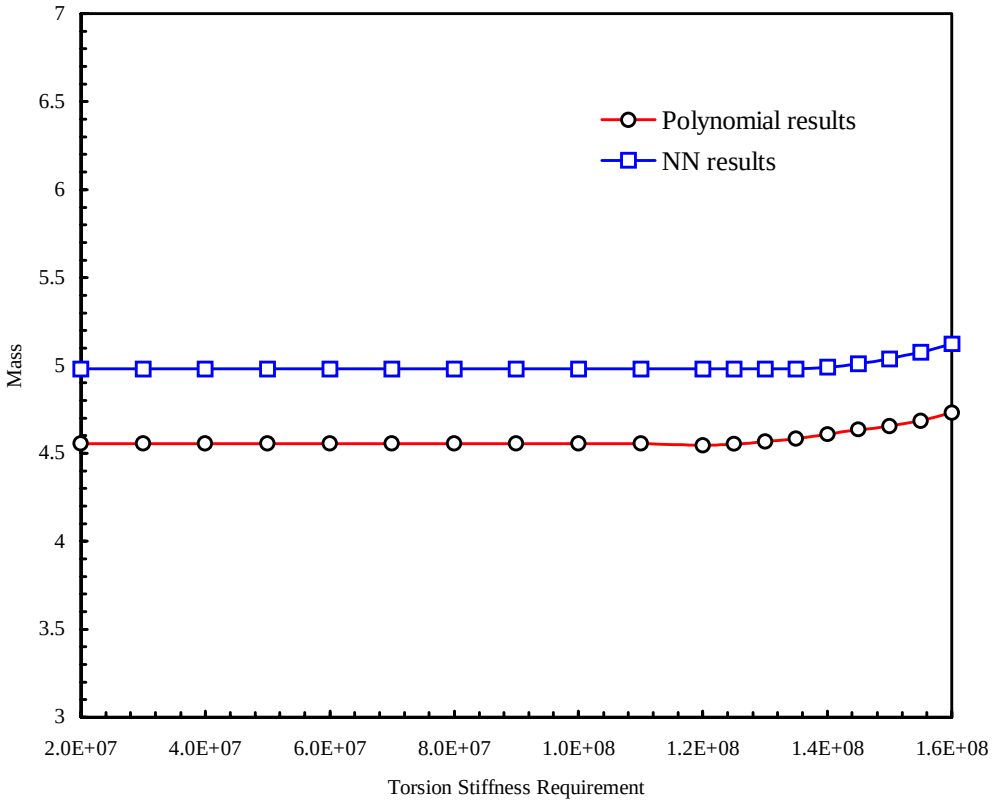

Figure 5.14c Relation between Mass and Torsional Stiffness Requirement for the B-Pillar to Rocker Joint

($K_{I/O}$>4.3899E7, $K_{F/A}$>5.2297E8)

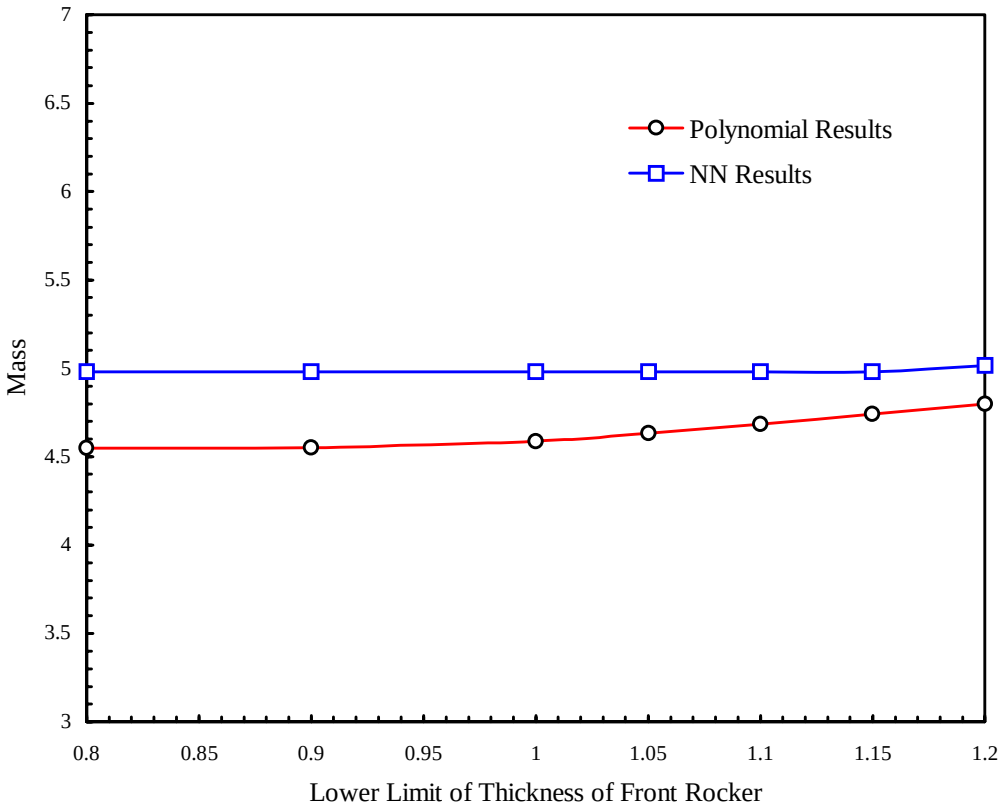

Figure 5.15a The Mass of Optimum Design of the B-pillar to Rocker Joint vs. the Lower Limit of the *Thickness of Rocker Outer Cell (Frontrock)*

($K_{I/O}$>4.3899E7, $K_{F/A}$>5.2297E8, K_{tor}>7.9788E7)

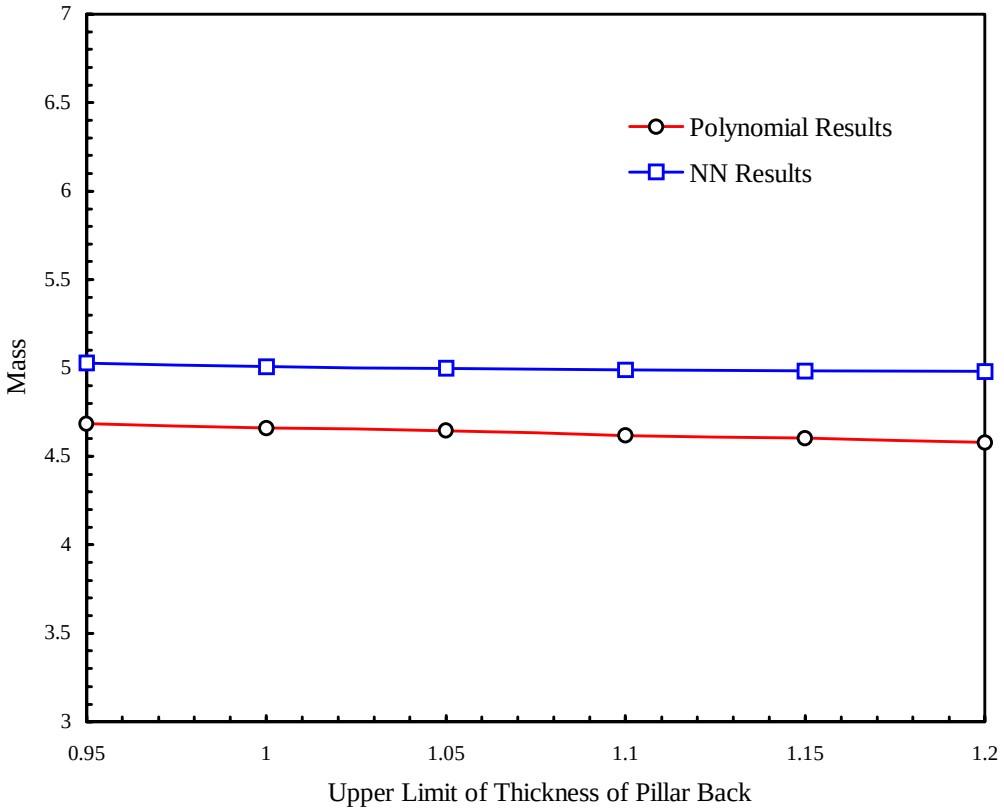

Figure 5.15b The Mass of Optimum Design of the B-pillar to Rocker Joint vs. the Upper Limit of *Thickness of Pillar Back*

($K_{I/O}$>4.3899E7, $K_{F/A}$>5.2297E8, K_{tor}>7.9788E7)

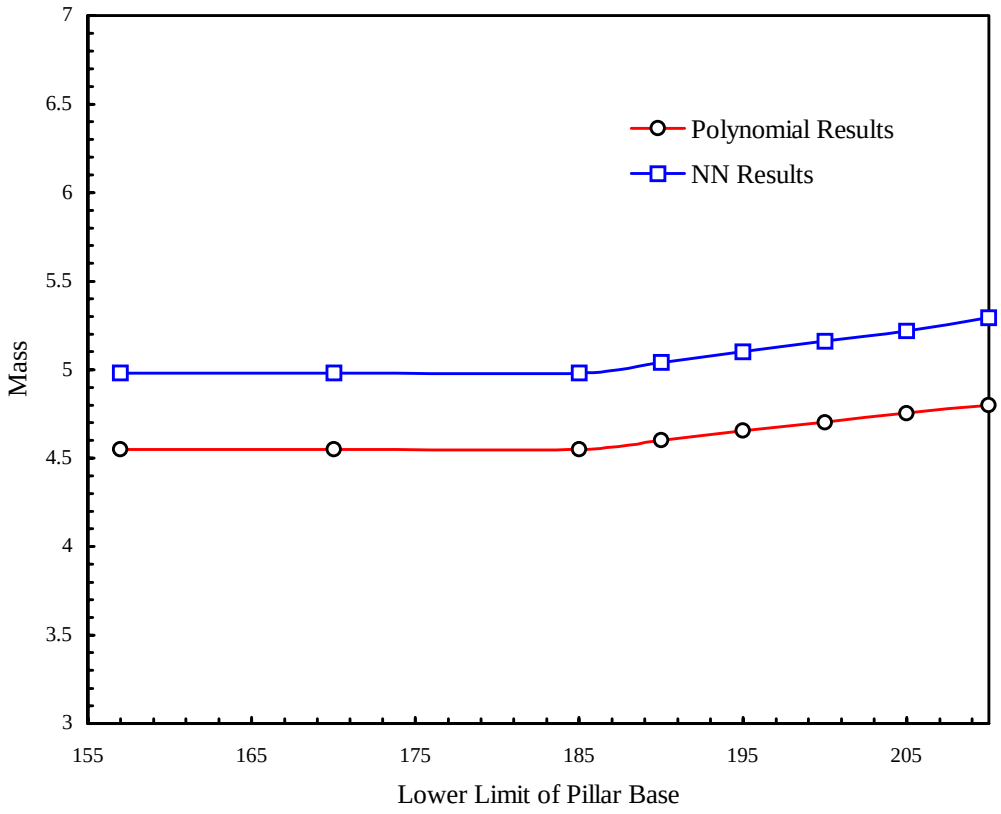

Figure 5.15c The Mass of Optimum Design of the B-pillar to Rocker Joint vs. the Lower Limit of *Pillar_Base*

($K_{I/O}$>4.3899E7, $K_{F/A}$>5.2297E8, K_{tor}>7.9788E7)

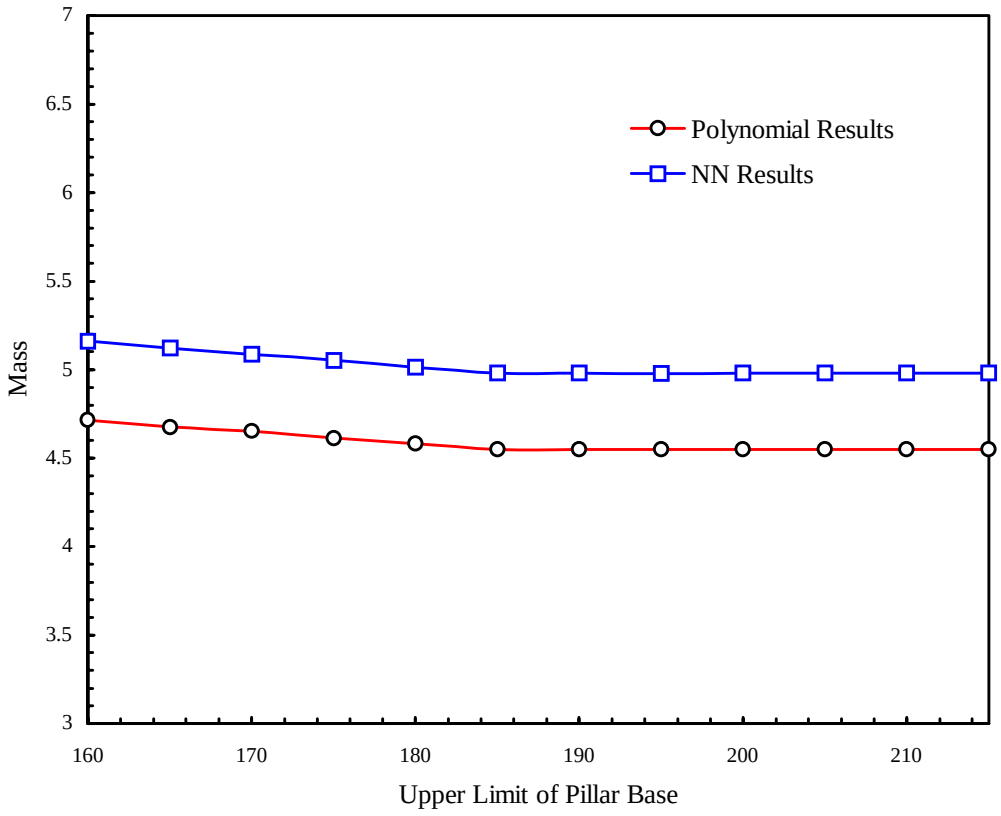

Figure 5.15d The Mass of Optimum Design of the B-pillar to Rocker Joint vs. the Upper Limit of *Pillar_Base*

($K_{I/O}$ >4.3899E7, $K_{F/A}$ >5.2297E8, K_{tor} >7.9788E7)

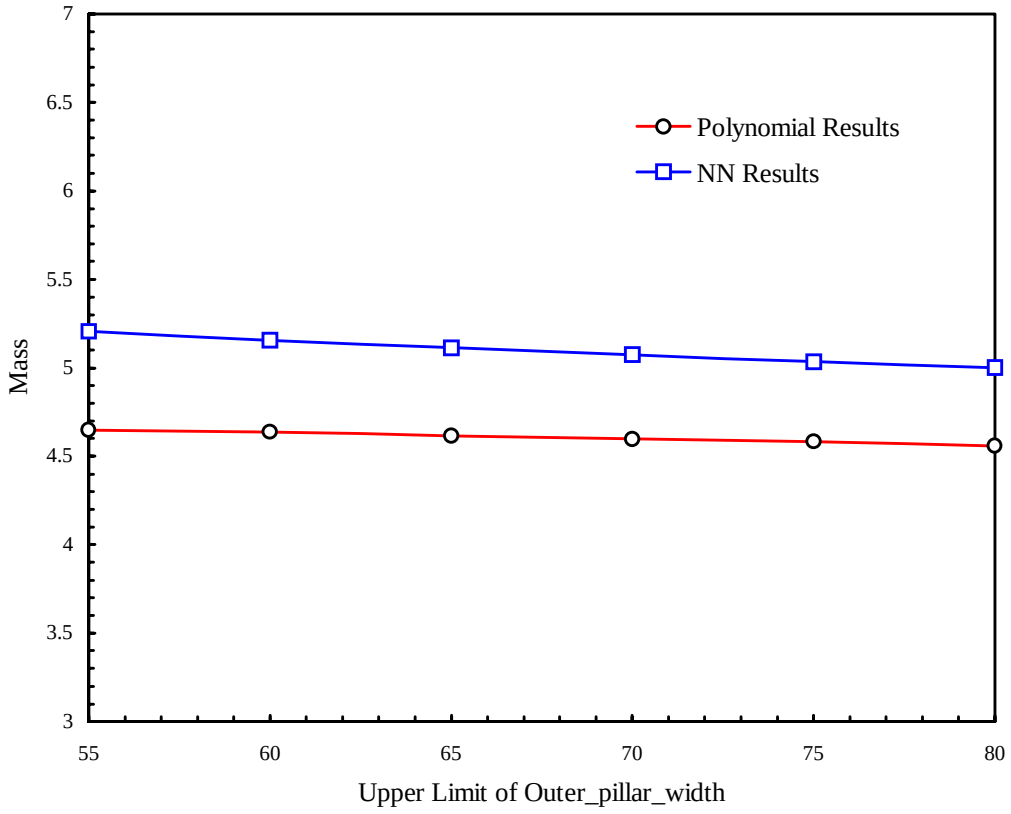

Figure 5.15e The Mass of Optimum Design of the B-pillar to Rocker Joint vs. the Upper Limit of *Outer_pillar_width*

($K_{I/O}$ >4.3899E7, $K_{F/A}$ >5.2297E8, K_{tor} >7.9788E7)

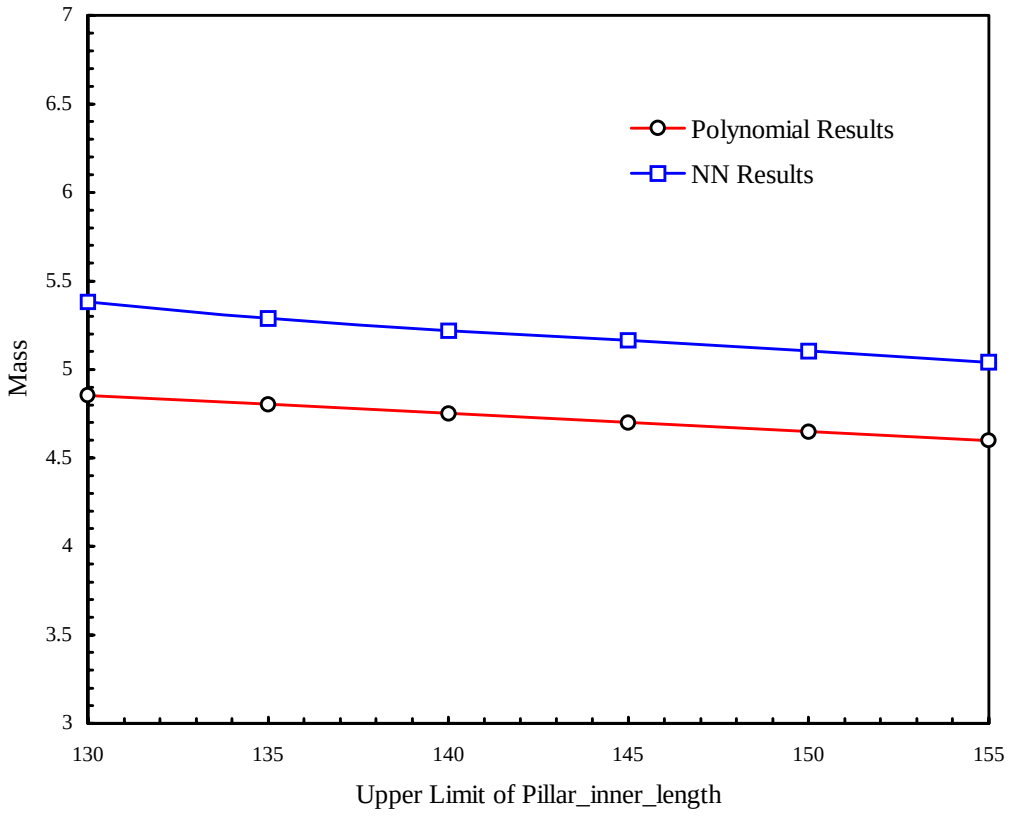

Figure 5.15f The Mass of Optimum Design of the B-pillar to Rocker Joint vs. the Upper Limit of *Pillar_inner_length*

($K_{I/O}$>4.3899E7, $K_{F/A}$>5.2297E8, K_{tor}>7.9788E7)

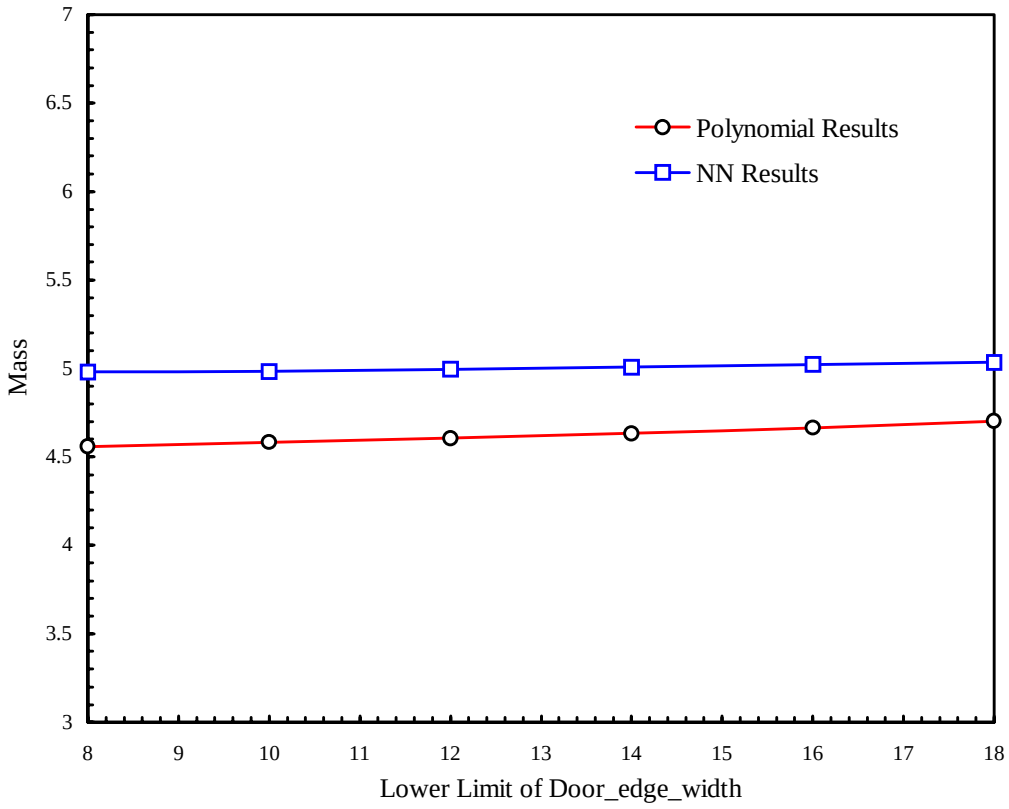

Figure 5.15g The Mass of Optimum Design of the B-pillar to Rocker Joint vs. the Lower Limit of *Door_edge_width*

($K_{I/O}$>4.3899E7, $K_{F/A}$>5.2297E8, K_{tor}>7.9788E7)

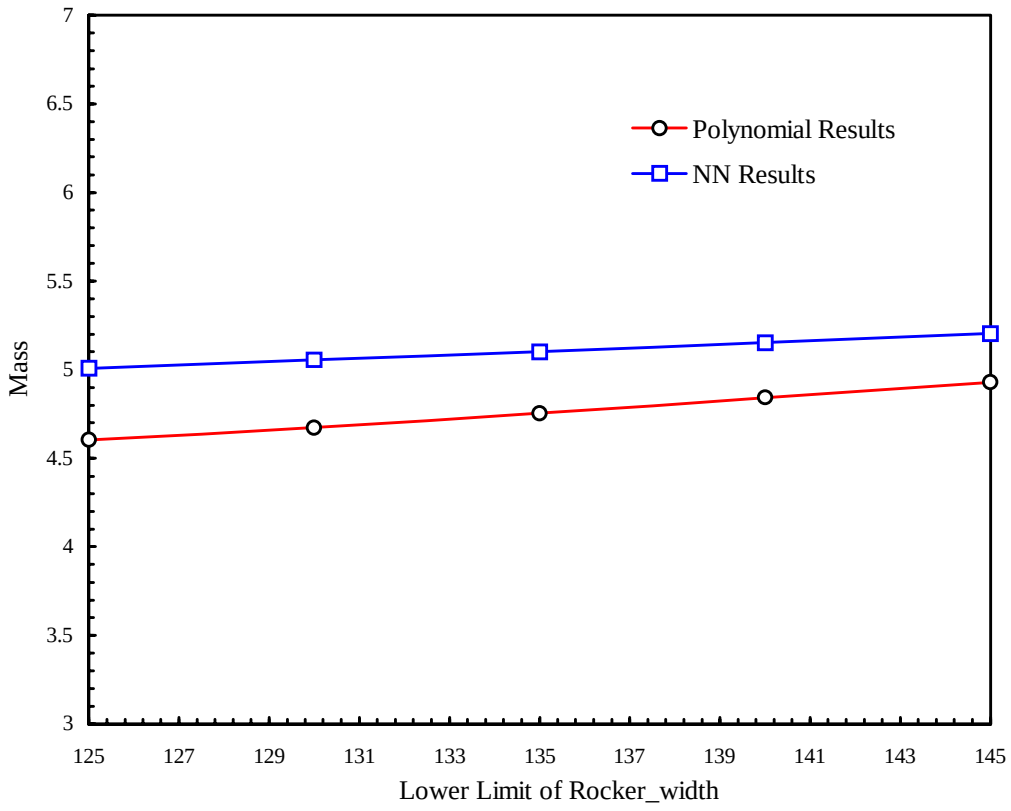

Figure 5.15h The Mass of Optimum Design of the B-pillar to Rocker Joint vs. the Lower Limit of *Rocker_width*

($K_{I/O}$>4.3899E7, $K_{F/A}$>5.2297E8, K_{tor}>7.9788E7)

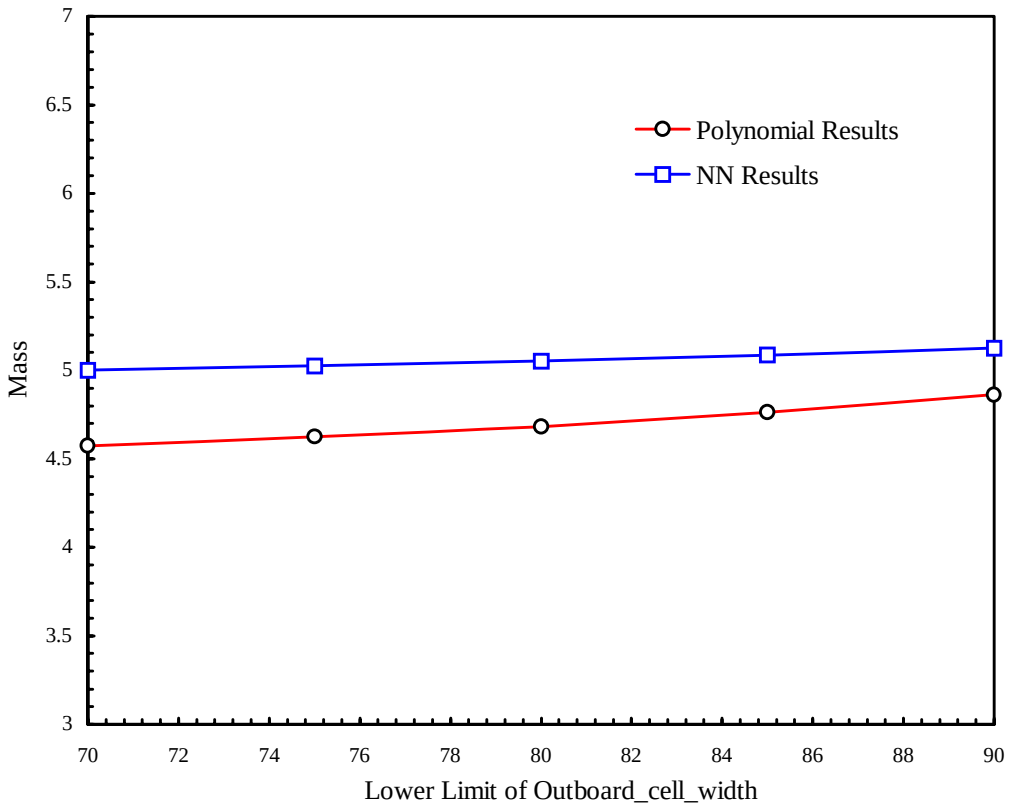

Figure 5.15i The Mass of Optimum Design of the B-pillar to Rocker Joint vs. the Lower Limit of *Outboard_cell_width*

($K_{I/O}$>4.3899E7, $K_{F/A}$>5.2297E8, K_{tor}>7.9788E7)

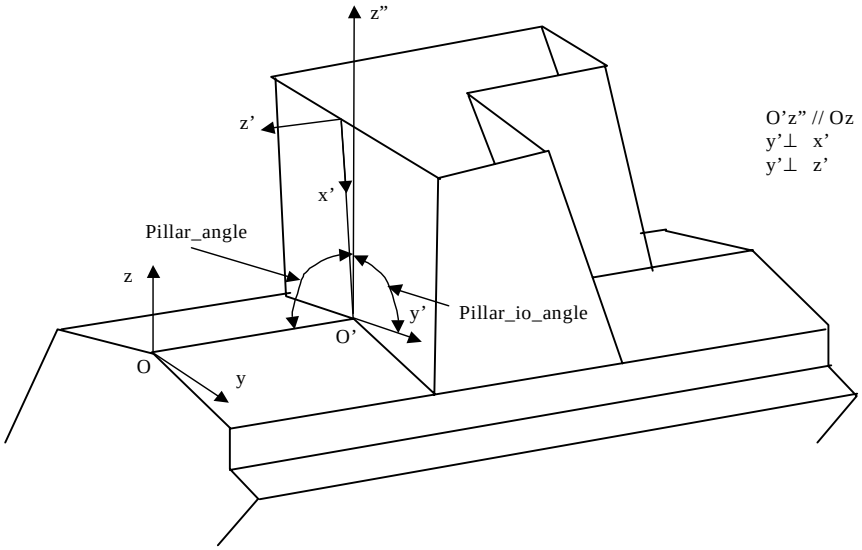

Figure 5.16 B-pillar Orientation

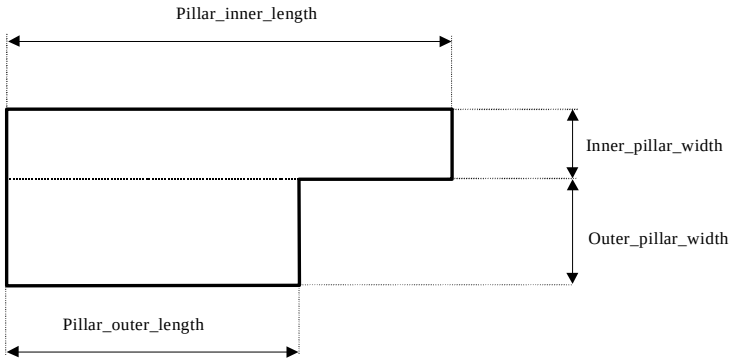

Figure 5.17 B-Pillar Dimensions

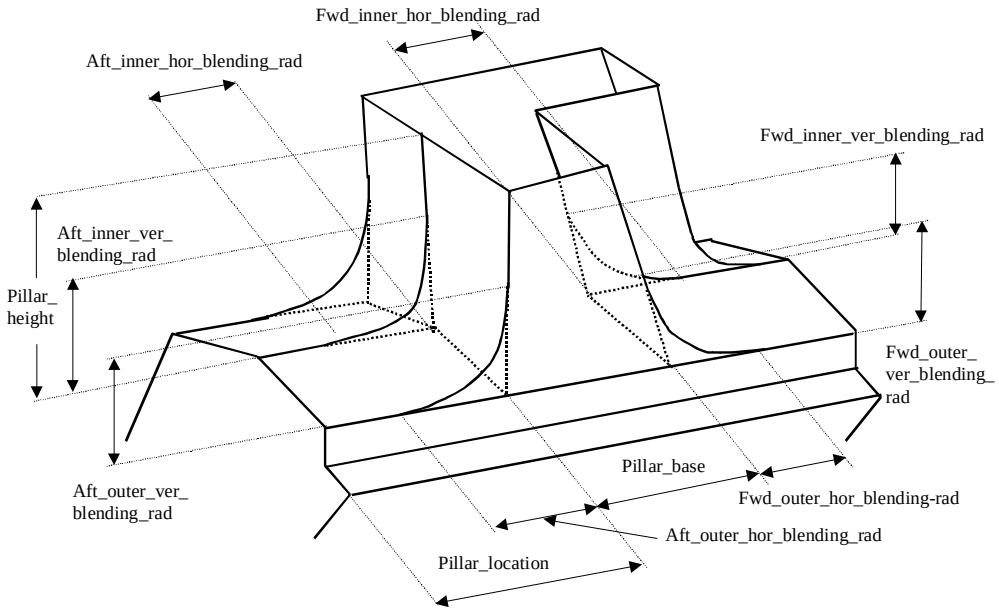

Figure 5.18 B-Pillar to Rocker Blending Radii

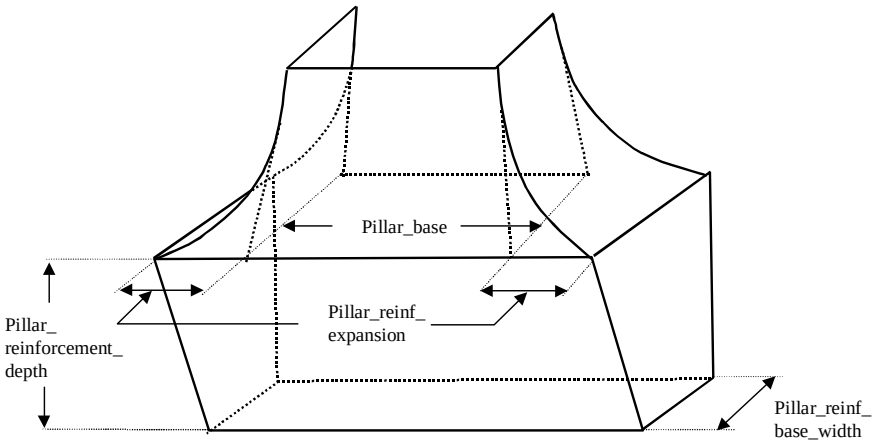

Figure 5.19 Pillar Reinforcement and Extended Pillar Reinforcement

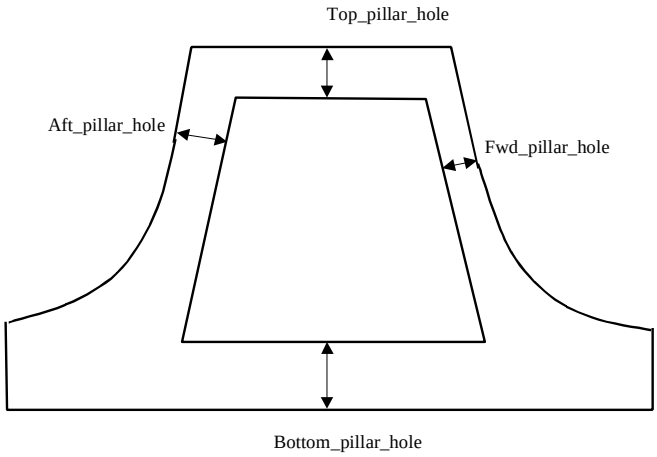

Figure 5.20 Opening in Back of Pillar

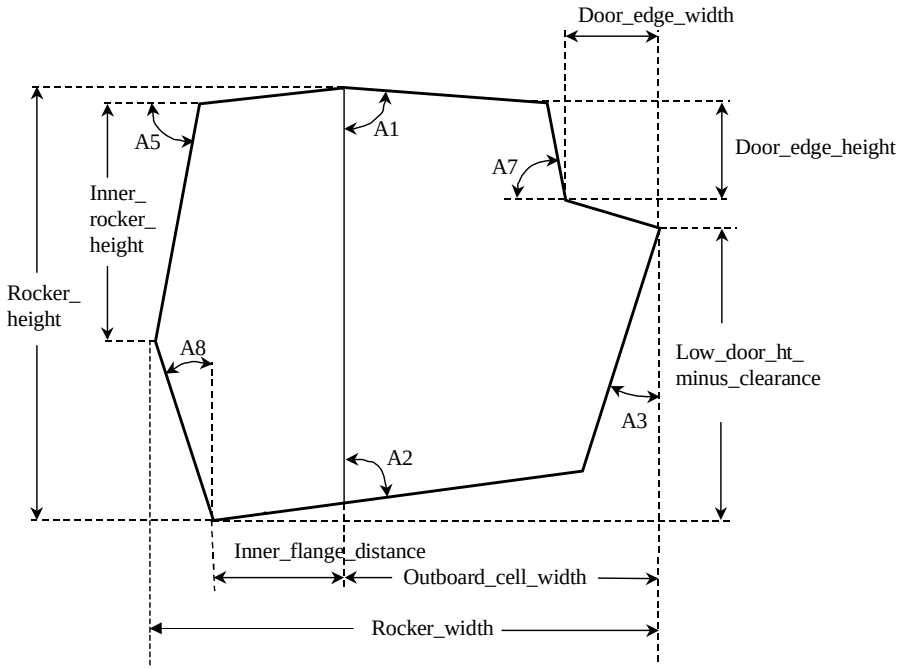

Figure 5.21 Rocker Cross Section

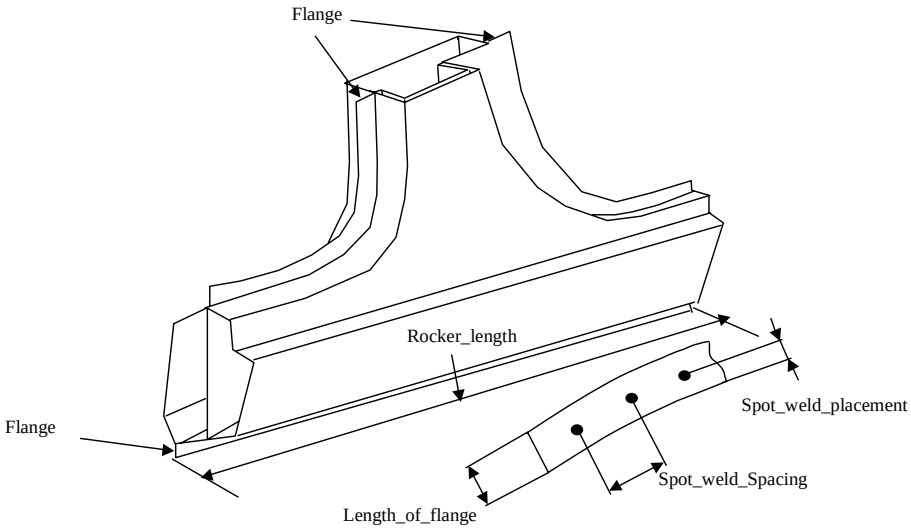

Figure 5.22 Flanges and Spot Welds

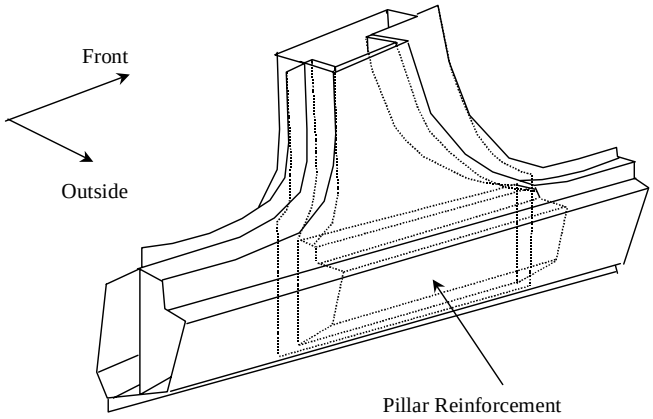

Figure 5.23 Extended Reinforcement for the B-pillar to Rocker Joint

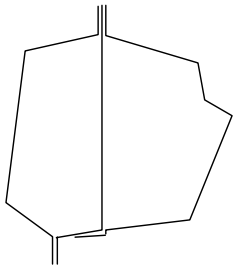

Type 1: Generic Type

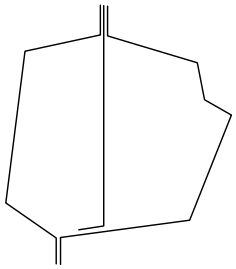

Type 2: Non Generic Type

Figure 5.24 Two Types of Rocker Cross Section

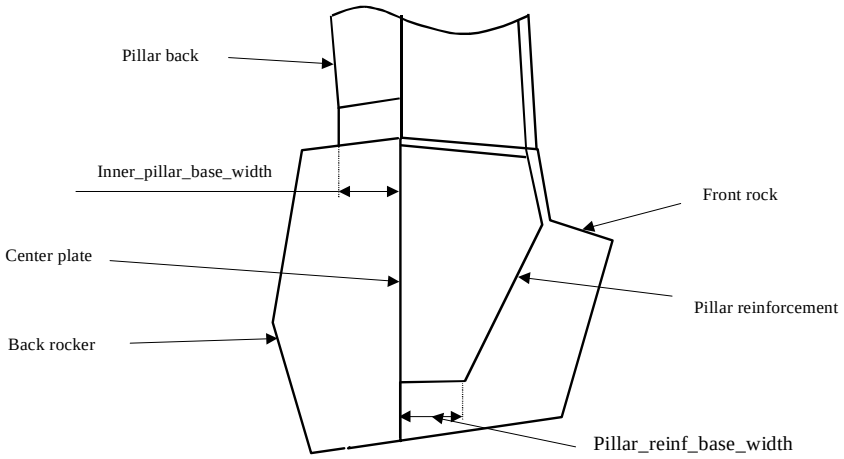

Figure 5.25 Pillar Reinforcement and Rocker Cross Section

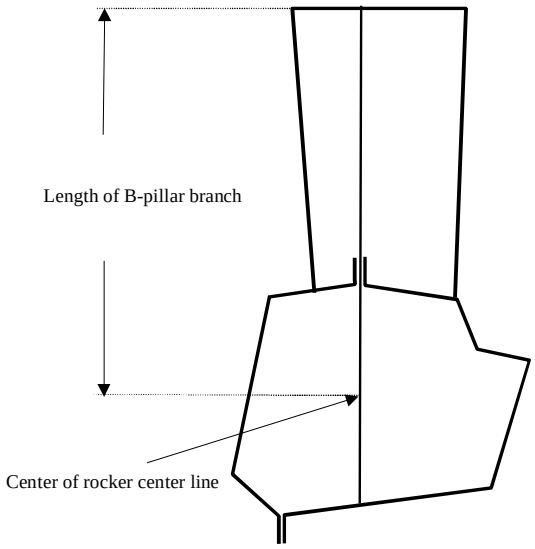

Figure 5.26 Definition of the Length of the B-pillar Branch

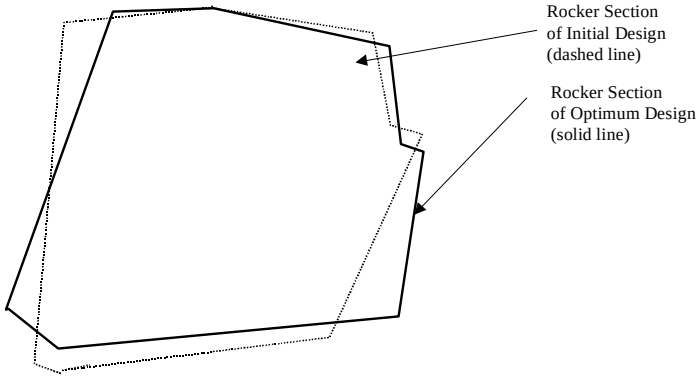

Figure 5.27 Rocker Cross Section of the Optimum Design

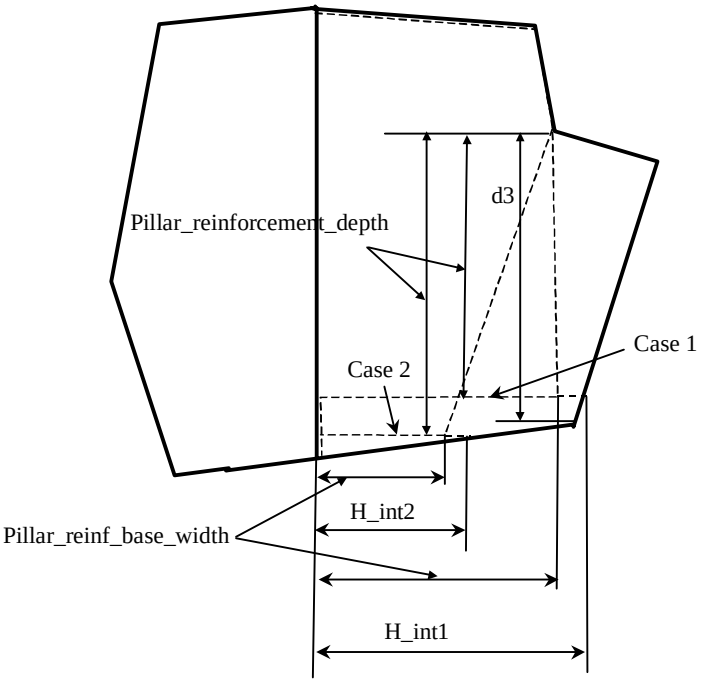

Figure 5.28 Constraints on the Extended Pillar Reinforcement

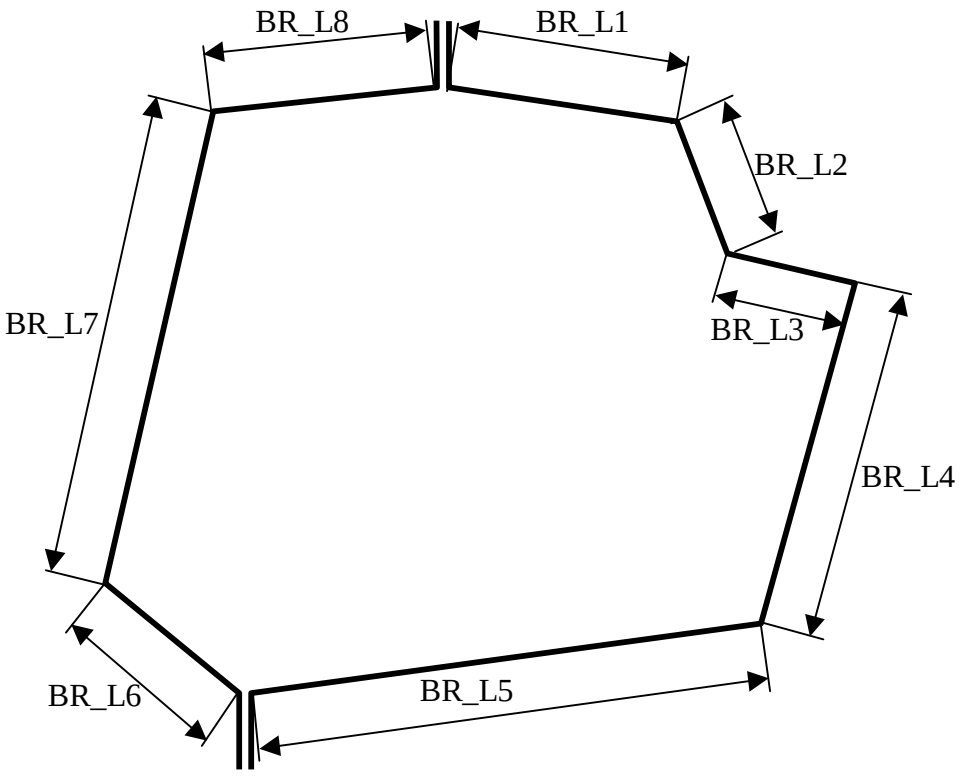

Figure 5.29 Manufacturing Constraints on Plate Lengths of Rocker Cross Section

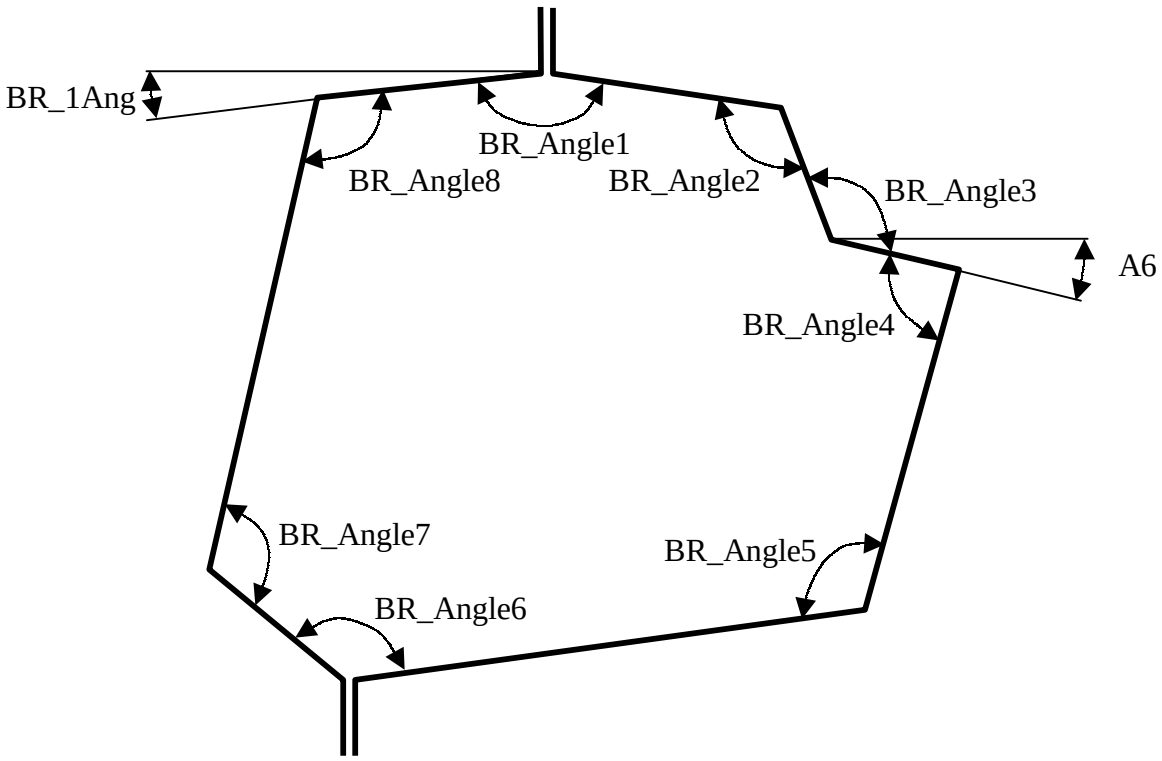

Figure 5.30 Manufacturing Constraints on Angles of Rocker Cross Section

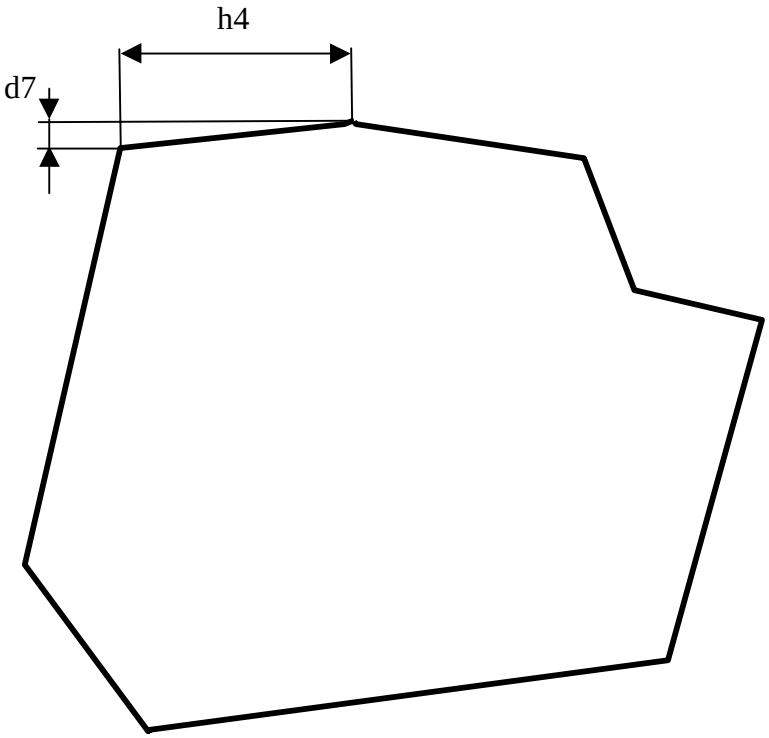

Figure 5.31 d7 and h4 of the Rocker Cross Section

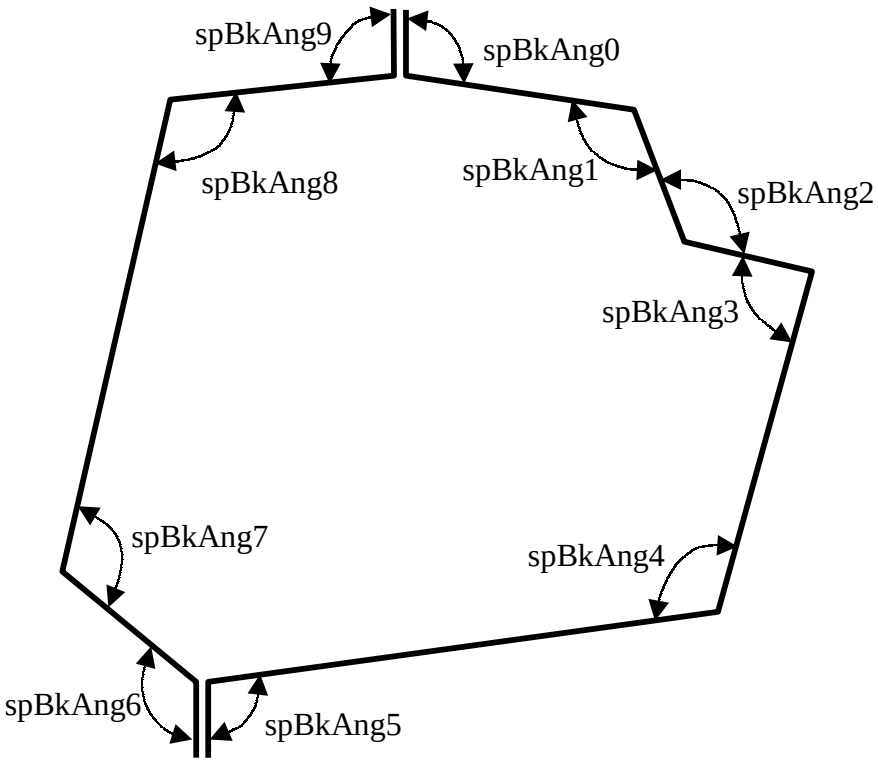

Figure 5.32 Spring Back Angles on Rocker Cross Section

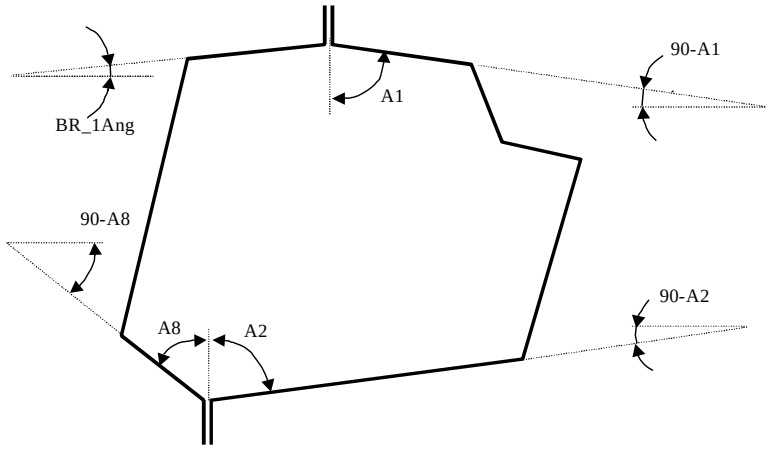

Figure 5.33 Die Lock Angles of the Rocker Cross Section

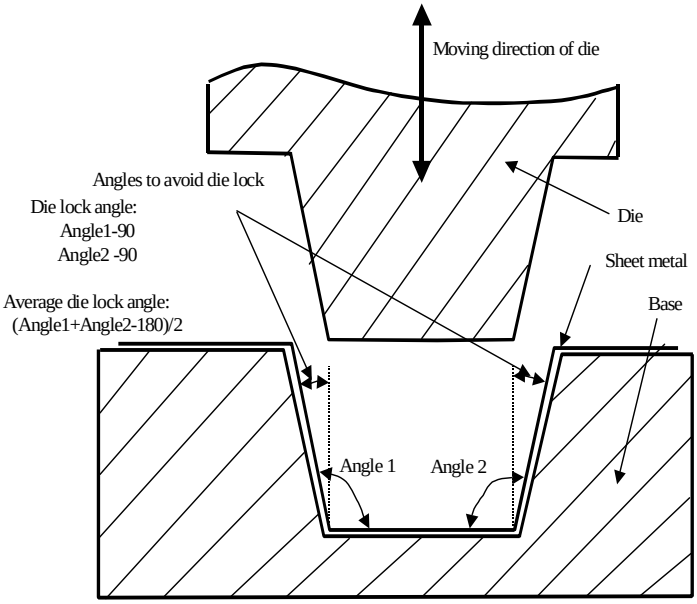

Figure 5.34 Explanation for Die Lock Angle

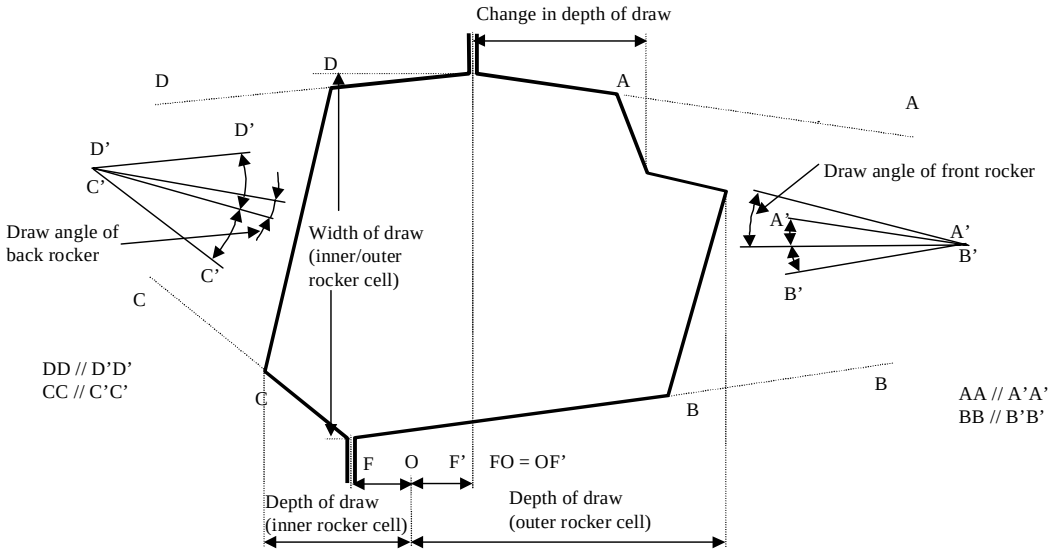

Figure 5.35 Manufacturing Constraints on Draw Angles and Draw Depth

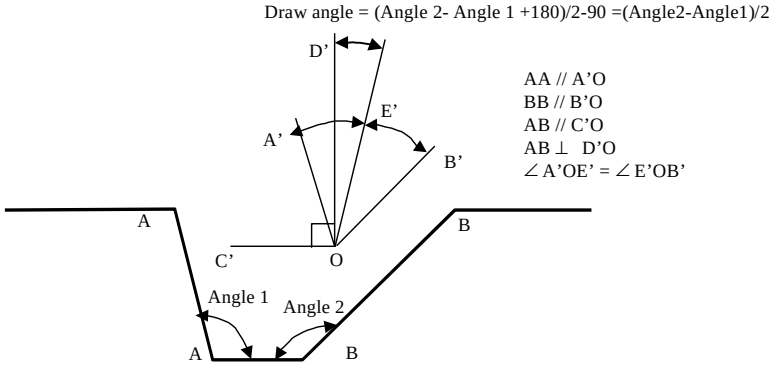

Figure 5.36 Explanation for Draw Angle

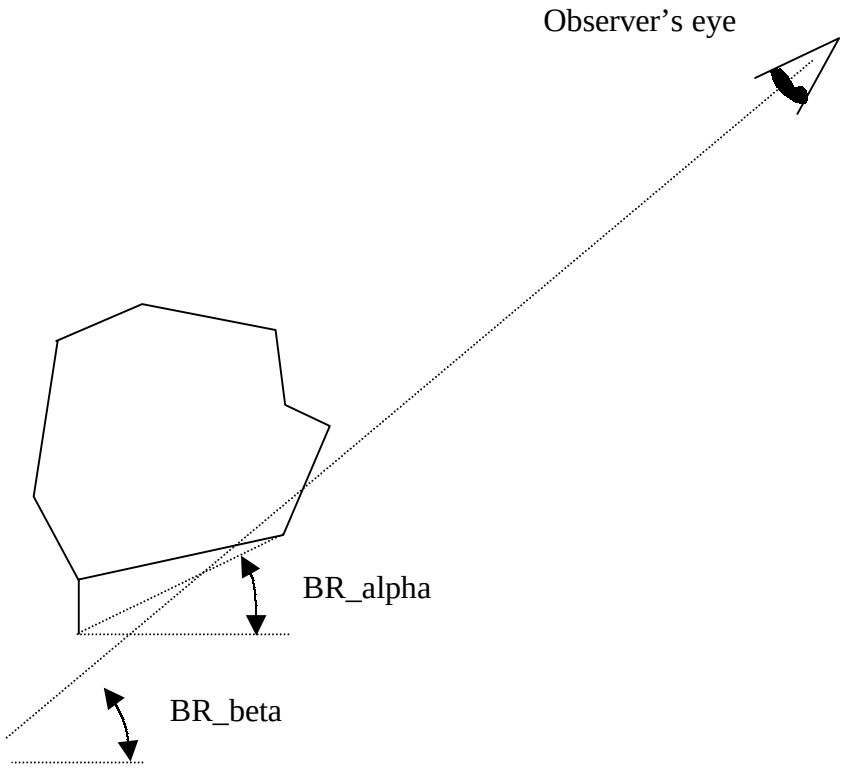

Figure 5.37 Styling Constraint on the Cross Section of Rocker

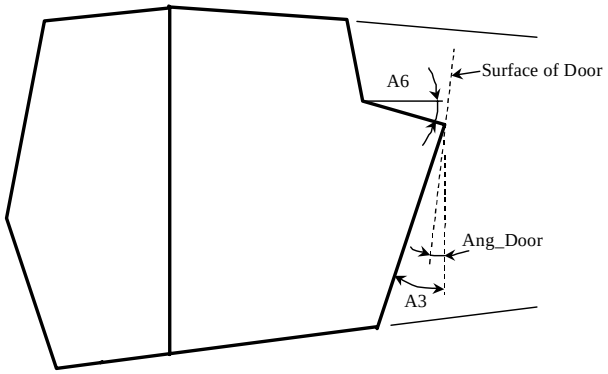

Figure 5.38 Angle A3 Should Meet Some Continuity Requirements

Qi Ling --- VITA

The author was born in Shanghai, China on September 25, 1964. He received his Bachelor of Science Degree in Naval Architecture and Ocean Engineering from Shanghai Jiao Tong University, Shanghai, China in July 1986. Then he entered Shanghai Port Machinery Factory for engineering practice and structural design. In 1991, he entered Shanghai Merchant Ship Design and Research Institute and worked as ship design engineer for six years. In August 1996, he entered Department of Aerospace and Ocean Engineering, Virginia Polytechnic Institute and State University for graduate Study in Ocean Engineering.